LAPPEENRANTA UNIVERSITY OF TECHNOLOGY
Faculty of Technology
LUT Mechanical Engineering
Master's Degree Program in Mechanical Engineering

John Bruzzo

A MULTIBODY DYNAMIC MODEL OF THE CROSS - COUNTRY SKI - SKATING TECHNIQUE

Examiners: Professor Aki Mikkola
Antti Valkeapää M.Sc. (Tech.)
Instructor: Professor Arend Schwab (TU Delft, The Netherlands)

ABSTRACT

Lappeenranta University of Technology
Faculty of Technology
LUT Mechanical Engineering
Degree Programme in Mechanical Engineering

John Bruzzo

A multibody dynamic model of the cross-country ski-skating technique

Master's Thesis

2012

100 pages, 47 figures, 10 tables and 3 appendices.

Examiners: Professor Aki Mikkola.
Antti Valkeapää M.Sc. (Tech.)
Instructor: Professor Arend Schwab (TU Delft, The Netherlands)

Keywords: multibody, cross-country skiing, skating model, Lagrange multipliers.

The objective of this thesis is the development of a multibody dynamic model matching the observed movements of the lower limb of a skier performing the skating technique in cross-country style. During the construction of this model, the formulation of the equation of motion was made using the Euler - Lagrange approach with multipliers applied to a multibody system in three dimensions.

The description of the lower limb of the skate skier and the ski was completed by employing three bodies, one representing the ski, and two representing the natural movements of the leg of the skier. The resultant system has 13 joint constraints due to the interconnection of the bodies, and four prescribed kinematic constraints to account for the movements of the leg, leaving the amount of degrees of freedom equal to one.

The push-off force exerted by the skate skier was taken directly from measurements made on-site in the ski tunnel at the Vuokatti facilities (Finland) and was input into the model as a continuous function. Then, the resultant velocities and movement of the ski, center of mass of the skier, and variation of the skating angle were studied to understand the response of the model to the variation of important parameters of the skate technique. This allowed a comparison of the model results with the real movement of the skier.

Further developments can be made to this model to better approximate the results to the real movement of the leg. One can achieve this by changing the constraints to include the behavior of the real leg joints and muscle actuation. As mentioned in the introduction of this thesis, a multibody dynamic model can be used to provide relevant information to ski designers and to obtain optimized results of the given variables, which athletes can use to improve their performance.

TABLE OF CONTENTS

Page

1 INTRODUCTION 1
1.1 Historical development of skiing as a sport activity 1
1.2 Objectives of the research 3

2 LITERATURE REVIEW IN CROSS COUNTRY SKI MODELING 6
2.1 Methodology for performing a systematic literature review 6
2.2 Results of the systematic literature review 8

3 CONSTRAINED MULTIBODY DYNAMICS THEORY 10
3.1 Definition of the Lagrange multipliers formulation 11
3.2 Vector of generalized coordinates and its derivatives 13
3.3 Constraints and Jacobian matrix of the system 18
3.4 Mass matrix of the system 20
3.5 Vector of Lagrange multipliers 26
3.6 Vector of generalized forces 31
3.7 Vector absorbing the terms that are quadratic in the velocities 34
3.8 Generation of an additional equation to convert DAEs into ODEs in the Lagrange formulation and its stabilization methods 36
3.9 Application of Fourier series to fit discrete data 38

4 FORMULATION OF EQUATION OF MOTION OF THE SKIER MODEL 40
4.1 Description of the phases and key variables of the skating technique . . . 40
4.2 Description of the model of the skier 41
4.3 Vector of generalized coordinates of the skier model 43
4.4 Constraints and Jacobian matrix of the skier model 45
4.5 Mass matrix of the skier model 60
4.6 Vector of Lagrange multipliers of the skier model 65
4.7 Vector of generalized forces of applied to the model 65
4.8 Vector absorbing the terms that are quadratic in the velocities. 69

5 MODELING RESULTS 70
5.1 Definition of the cases to be analyzed in terms of phase time and skating angle. 70
5.2 Leg retraction and extension versus time. 71
5.3 Push-off force function versus time, friction force, and air drag 72
5.4 Movement of the origin of the local reference system of the second body . 76
5.5 Set of simulation results 77
5.6 Simulation of a long ski run. 79

6 CONCLUSIONS 83

APPENDICES 87

ABBREVIATION AND SYMBOLS

Abbreviations

CM	center of mass
DAEs	differential algebraic equations
DOF	degrees of freedom
ISBS	International Society of Biomechanics in sport
Nelli	National electronic Library Interface
ODEs	ordinary differential equations
PRISMA	Systematic Reviews and Meta-Analyses
ZXZ	Euler angle rotation sequence

Symbols

a_0, a_k, b_k	Fourier series coefficients
$\boldsymbol{a}_0$	vector of the system generalized coordinates
$\boldsymbol{a}_v$	acceleration vector absorbing terms which are quadratic in the velocities
$\boldsymbol{A}$	rotation matrix
$\boldsymbol{c}$	vector of constant terms
$\boldsymbol{C}$	vector of kinematic constraints
$\boldsymbol{C_q}$	constraint Jacobian matrix
$\boldsymbol{C}_t$	vector of partial derivatives of the constraint equations with respect to time
$\boldsymbol{D}$	single rotation matrix
f	number of degrees of freedom
$\boldsymbol{F}$	vector of external forces
$\bar{\boldsymbol{G}}$	velocity transformation matrix between angular velocities and first time derivative of Euler parameters
$\boldsymbol{I}$	identity matrix
$\boldsymbol{I}_{\theta\theta}$	inertia tensor of the rigid body
m	number of constraints, number of Fourier coefficients
M	moment
$\boldsymbol{M}$	moment matrix
$\boldsymbol{M}^i$	mass matrix of the i-th body
n	number of bodies, number of generalized coordinates, number of half rotations, quantity of pairs of data
n_c	number of independent constraint equations
q	number of generalized coordinates
$\boldsymbol{q}$	vector of generalized coordinates

$\boldsymbol{Q}_e$	vector of generalized forces
$\boldsymbol{Q}_v$	vector of quadratic velocity inertia terms
$\boldsymbol{Q}_d$	vector absorbing terms that are the partial derivatives of the constraint equations
$\boldsymbol{r}_p$	position vector of particle P in a global coordinate system
r_{xy}	Pearson correlation coefficient
$\boldsymbol{R}$	position vector of the frame of reference
$\bar{\boldsymbol{u}}$	position vector within the body reference system
V	volume of the body
W^e	work of external forces
W_i	work of inertial forces
$\boldsymbol{X}_i$	coordinate system axis along the i-th direction

Greek Letters

α, β	parameters of the Baumgarte stabilization method
δ	partial differential operator of calculus
θ	generalized rotational coordinates planar case, step size in the Fourier fitting process
$\boldsymbol{\theta}$	vector of Euler angles, generalized rotational coordinates
$\boldsymbol{\lambda}$	vector of Lagrange multipliers
ρ	density of the body
φ, θ, ψ	Euler angles
$\boldsymbol{\xi}_i$	coordinate system axis along the i direction
$\bar{\boldsymbol{\omega}}$	vector of local angular velocities

Superscripts

b	number of bodies
i, j, 1, 2, 3	index of the body
T	transpose of a vector of a matrix

To the memory of my beloved mother Beatriz and to the love of my daughters Sarah and Saricer...

FOREWORDS

This master thesis work has been accomplished during the years 2011 - 2012, mainly in the Laboratory of Machine Design of the Department of Mechanical Engineering at Lappeenranta University of Technology as part of the requisites to be fulfilled to obtain the degree of Master of science.

Firstly, I thank God for the opportunity that has been given to me to be part of this world and at the same time to have met wonderful people that have been next to me to help me to overcome the moments of apparent difficulties.

Secondly, I am also grateful to my supervisor Professor Aki Mikkola for giving me the opportunity to develop myself in the academic world and for guiding and supporting me through the process of the elaboration of this work. I would also like to thank Antti Valkeapää for his full support during the whole process and to have participated actively as examiner of the work. Also, I would specially like to thank Professor Arend Schwab of TU Delft at Netherlands for being of unconditional support, and for showing me the first lights in the path to follow in this project.

Even though this work has been itself a magnificent experience, it would not be complete without mentioning my colleagues at work in the Laboratory of Machine Design for all their support, and good mood which allowed an even more pleasant stay during the long days at the office.

To Dr. Marko Matikainen I am grateful for his support in carrying out administrative tasks that allowed me being concentrated in my work.

To Saricer Mata I am grateful for her support at the moment of making the decision to come here. She has been an important influence in my life.

Finally, I would like to express my thankfulness to my daughters Sarah and Saricer. They have missed time and special moments in order to support me unconditionally. All this work and their results are for you both.

1 INTRODUCTION

The term skiing is defined by the Encyclopedia Britannica as the action of moving over the snow by the use of a pair of long skis (Allen, 2008). Skiing is considered to be one of the oldest activities still practiced nowadays, with only a few technological changes from its original concept. These changes mainly pertain to the fabrication materials and production of the skis. For example, in ancient times, skis were manufactured out of wooden flat pieces, while in modern times, the fabrication materials and technology comprise a sophisticated combination of wood and composites.

1.1 Historical development of skiing as a sport activity

Skiing can be traced back in time at least 6000 years, when its principal use was for hunting, gathering, transportation, and obtaining wood supplies. One well-known fact is that people from the Nordic countries used skiing to move from one place to another, mainly because their land was covered by snow most of the year. This can be seen in figure 1, which presents a pictograph from 2000 B.C. found in Rödöy, Norway, considered one of the most ancient graphical representations of the skiing culture of the Nordic tribes.

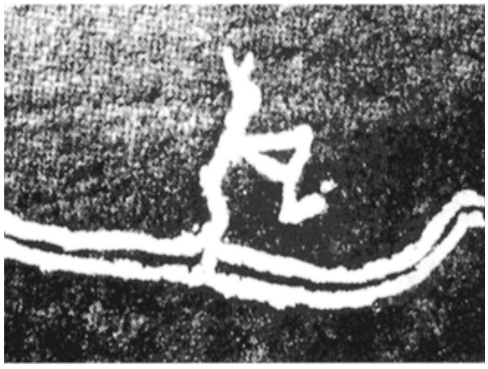

Figure 1. *Pictograph of ancient skiers in Rödöy, Norway, circa 2.000 B.C. (Lind et al., 2010, p. 2).*

Almost four thousand years later, since the year 1890, skiing has developed as a sport activity and assumed its current modern shape. Different techniques have evolved from the traditional Nordic style practiced between 1890 - 1940 by the aristocrats and wealthier middle classes. These techniques are currently known as alpine, ski jumping, free ride, free style and cross-country style (Allen, 2007, p. 1-6).

From the previous classification, the cross - country style may be considered as the original descendant of the Nordic style; in fact, nowadays the terms Nordic and cross - country are sometimes used synonymously when one makes reference to the ski style of the past.

At the time, cross - country skiing was preferred over all other types of skiing techniques that existed because people found it more suitable to traveling longer distances than the others (Hindman, 2005, p. 15). Presently, this activity has evolved into one of the most practiced sport and leisure activities around the world due to its low impact, short learning curve, and, above all, low cost (it requires neither specialized nor expensive gear to start practicing it).

If a basic comparison must be made, it can be said that one of the main differences between cross-country skiing and the other ski styles is that the binding between the foot and the ski attaches only at the toes, and the skis are more lightweight.

There are different variants of the cross-country style, among which are classical, Telemark, and skating. The classical technique, shown in figure 2, is the conventional technique of cross-country skiing, where the skier's movement is performed in diagonal strides while the skis remain parallel to each other.

Figure 2. *Classical cross country skiing practice (Hindman, 2005, p. 14).*

When the conditions of the path lead to a downhill, the skier applies the Telemark technique, as shown in figure 3. Sondre Norheim of Telemark, Norway pioneered this technique (Blikom, 2010).

The last (but not least important) technique found within the cross - country skiing styles is the skating technique. This technique is performed in a manner similar to ice skating. To perform the movement, the skier pushes outward with the cross - country ski in such a way that the inner edge of the ski pushes against the snow. Skiers mostly appropriate this technique for use on surfaces with firm and smooth snow. Figures 4(a), 4(b) and 4(c) show the execution of this technique by cross - country skiers so that it is possible to

Figure 3. *Telemark technique (Knightson, 2010).*

appreciate the range of movements required to accomplish the forward displacement.

(a) Propulsive phase (b) Gliding phase (c) Stride phase

Figure 4. *Different phases of the skating technique (Skating technique basics, 2011).*

One cannot deny the high impact of this sport discipline on its practitioners all over the world. Even athletes who are originally from countries where snow is not present are active in international competitions. This is because cross-country skiing is a highly attractive, developed sport receiving attention from the worldwide athletic community.

In regards to the performance side of the sport, one can read and study a great deal about the developments of cross-country skiing in terms of equipment manufactured by large companies and execution of the technique taught by personal trainers. However, in further sections of this research, the reader will find that not much work has been done toward a multibody simulation of the skating technique of cross-country skiing.

1.2 Objectives of the research

The main objective of this research is to formulate a simplified multibody dynamic model of a cross country skier that matches the observed behavior of the movements of the cross - country skating technique.

As previously mentioned, the skating technique has been studied extensively from physiological, medical, and training points of view (Rusko, 2033, p. 1-30). Nevertheless, as shown in the systematic literature review presented later, studies related to the modeling of the skier movement and skiing technique mechanics are in development in the field of multibody dynamics. The number of opportunities that the multibody dynamics field can offer and develop for athletes and teams participating in this discipline is vast.

Much can be done to achieve optimal performance in the training requirements of elite or high-level competitive skiers with a multibody dynamics model. It is possible to 1) determine in advance all the resultant kinematic parameters associated with the technique, such as velocities and accelerations of the skier or of different parts of the skier's body; 2) describe the complete geometry of the movements of skis, legs, and arms of the athlete; and 3) use these data to adjust the execution of the activity to obtain the maximum output with the least possible effort.

Moreover, with the multibody dynamics model, it is possible to model the influence of novel ski designs, products, and binding systems on the skiing itself. This might help a competitive skier to select the most optimal combination of gear components to maximize effectiveness during competition. It may also minimize field testing during the research and reduce the development phases and times of new prototypes.

The subsequent integration of this model with a more complex biomechanical model of the skating technique may lead to a deeper understanding in research on muscle actuation and energy consumption as well as on the stresses affecting bones. These findings could in turn be integrated into the bone strain formulation model that is currently implemented in the Laboratory of Machine Design of this University.

With the multibody dynamics model, new variants of the ski-skating technique can be proposed to make it more physiologically efficient. Also, the impact that the technique can have on the joints of the lower limbs of athletes can be assessed, and common injuries that top competitive athletes may develop with the continued practice of this sport discipline can be better studied.

This thesis presents a multibody dynamic formulation allowing for a broad set of configurations. It describes an explicitly formulated study of a three dimensional model of the technique on a leveled plane without the use of poles. However, the actual model might be used to study the different variants of the skating technique and even other similar techniques, as the prescribed parameters needed as an input to the model can simulate the natural movement of athletes.

The author of this research work considers that the use of multibody dynamics to simulate the skating technique will open new doors to a better understanding of the occurring phenomena in the execution of the technique. If developed consistently, the model can support athletes in obtaining maximum performance from individual capabilities.

2 LITERATURE REVIEW IN CROSS COUNTRY SKI MODELING

In this section, one main topic will be considered. The presentation of the current advances in the area of multibody modeling of cross-country skiing, which will be covered by means of a systematic literature review.

2.1 Methodology for performing a systematic literature review

Before one embarks on the development of a new model, it is important to know what has been previously done regarding the specific subject of interest in order to analyze and understand the different concepts and assumptions and to obtain a simplified version of a dynamic model that can be used in the present work.

To collect a relevant set of documents on the subject, a systematic literature review must be methodologically conducted, with the main objective of showing actual mathematical model proposals of the skier performing the cross-country ski skating technique. To the present knowledge of the author, it may be stated that this is one of the first reports of its kind summarizing what can be found in the scientific databases regarding this particular topic.

After the selection of the definitive studies to be reviewed, a comparison table was to be made with the following points:

- The multibody dynamics approach used to model the skier, including the preferred coordinate of systems, complexity of the formulation based on the number of bodies, final form of the equation of motion, numerical resolution method, and fitting of experimental coefficients, such as friction coefficients.

- The method or experimental procedure used to determine the value of the variables contained in the equation of motion, including the type of equipment and instrumentation used to gather this data.

To accomplish this systematic review, the Preferred Reporting Items for Systematic Reviews and Meta-Analyses (PRISMA) 2009 (Moher et al., 2009) was used, and its flow diagram for systematic reviews and check list were followed (see figure 5).

To identify the articles relevant to this study, the electronic review was carried out with the use of one report search engine and two databases. The first one of these resources used was the scientific report search engine Nelli (National Electronic Library Interface),

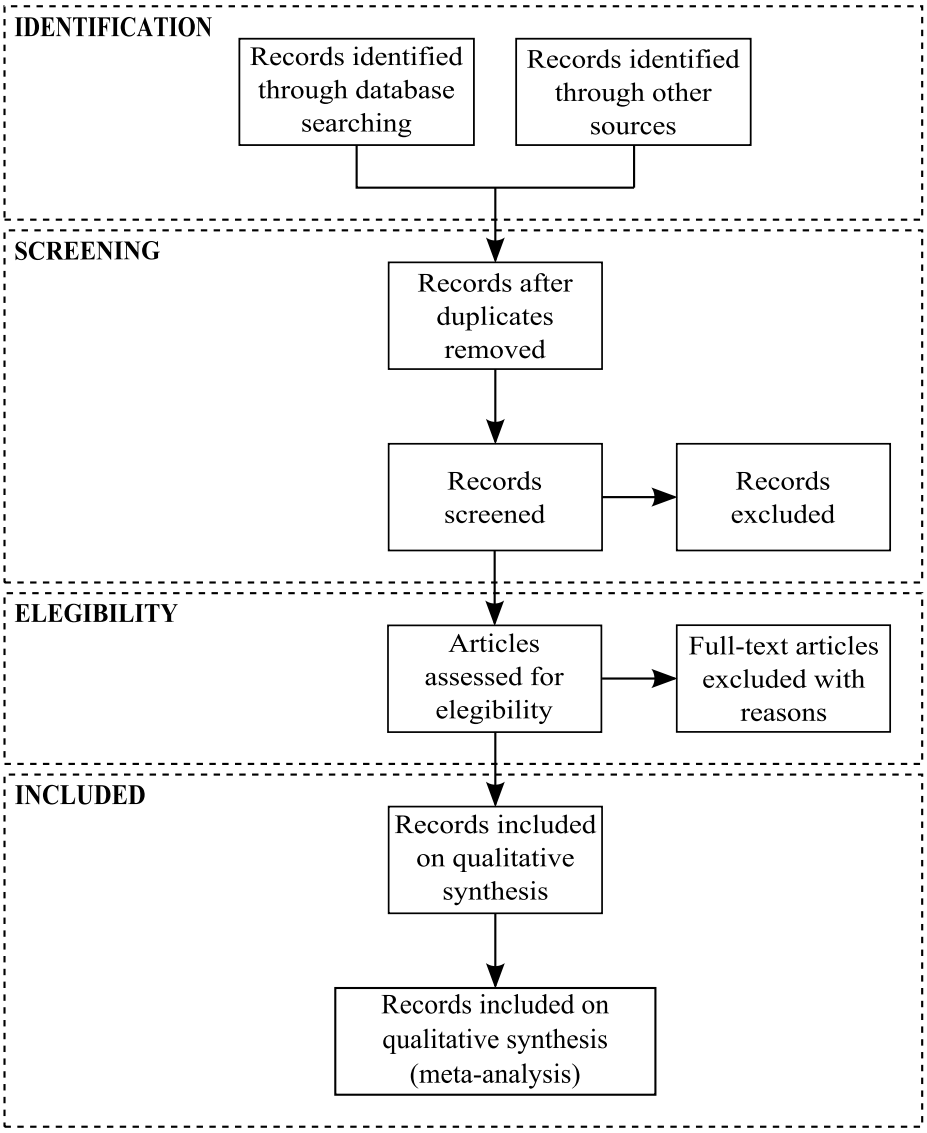

Figure 5. PRISMA 2009 Flow Diagram.

which is the national net library service used by all universities in Finland. This search engine executes a systematic search on databases such as EBSCO, Elsevier, Springer, and more than 21 others databases related to the scientific fields, and combines the possible duplicated articles bias titles and authors' recognition.

Secondly, the PubMed Database was used. This database contains studies related to the bio-medical field, including important studies concerning the behavior and modeling of the human body. Lastly, the International Society of Biomechanics in Sports (ISBS) database was used. This database contains the reports of ISBS proceedings related to the modeling of human body responses and the effect of diverse actions on the human body via simulation, modeling, or on-site experimentation.

The criteria for the literature review search were as follows:

- The language selected for the search of the scientific articles was English due to the extensive number of global references and organizations that primarily use English in their publications.
- The types of publications considered for the review were technical articles, conference papers, patents, or any other relevant documents resulting from the database searches.
- The period of time for performing the search had no imposed restrictions either in CPU time to accomplish the search or in the publication date of the retrieved reports.
- The key words used in the search engines were “cross-country” AND “ski” AND “skating” AND “model”.

For every result obtained, the abstract was preliminarily reviewed and then compared among the different database results to detect duplicated documents. The references included in the selected articles were also reviewed in order to take into account any missing article as a result of the systematic search process. In the appendices, the number of scientific articles by database at the time of the electronic review was populated in order to obtain an actual reference of the number of references screened.

The scientific articles retrieved from the databases were sorted and relevance to the study taken into account. Those articles with similar characteristics were carefully examined to determine if the field of application complied with the requirements of the literature review.

2.2 Results of the systematic literature review

The results of the electronic search carried out are shown schematically in figure 6. From the Nelli Database search engine and in accordance with the search characteristics, 1311 studies were retrieved; from the PubMed Database, two were retrieved; and from the ISBS Database, none was retrieved.

As can be seen in figure 6, no discussion or comparisons can be expressed from this systematic literature review because it was impossible to find any study concerned with the main topic of this thesis, at least from the databases consulted. This might mean that studies conducted in this field are not published yet, are located in a different database with special restrictions for the public audience, or are published in a language other than English.

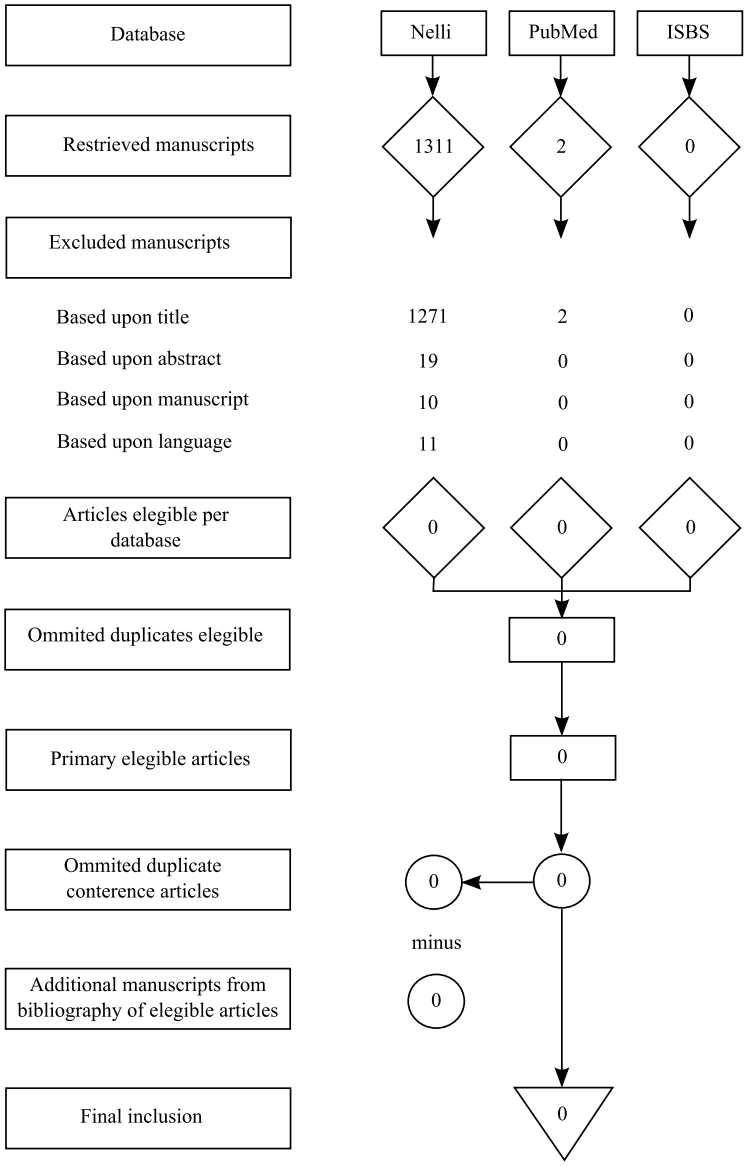

Figure 6. *Flow diagram of the literature selection process.*

This result provides valuable information to researchers of this field: there is a great opportunity to start developing models and validation methods to be applied to the skating technique of cross-country skiing to multiple ends. Such models and validation methods could create tools that can support further training methods, estimations of the impact of this technique on the human body (especially for injured skiers), and development of new equipment. This would allow a skate skier to take full advantage of all of the natural movements that the body performs during the execution of this activity.

3 CONSTRAINED MULTIBODY DYNAMICS THEORY

The definition of the type of formulation used to model a multibody system influences the steps taken to develop and to implement the system in a computerized manner.

The study of constrained multibody systems began with Euler (1707 - 1783) and D'Alembert (1717-1783). Their studies were based on earlier studies on linear motion carried out by Newton and on Euler's equations for rotational motion. A systematic analysis of constrained multibody systems was subsequently formulated and established by Lagrange (1736 - 1813). Lagrange was the first to perform the derivation of the generalized equations of motion for multibody systems (Chaudhary et al., 2009, p. 3).

Because of the focus on the automatic generation of the equation of motion via the implementation of specific and general computer codes, the most common lines of action or methodologies used to develop the dynamics of mechanical systems are presented in figure 7.

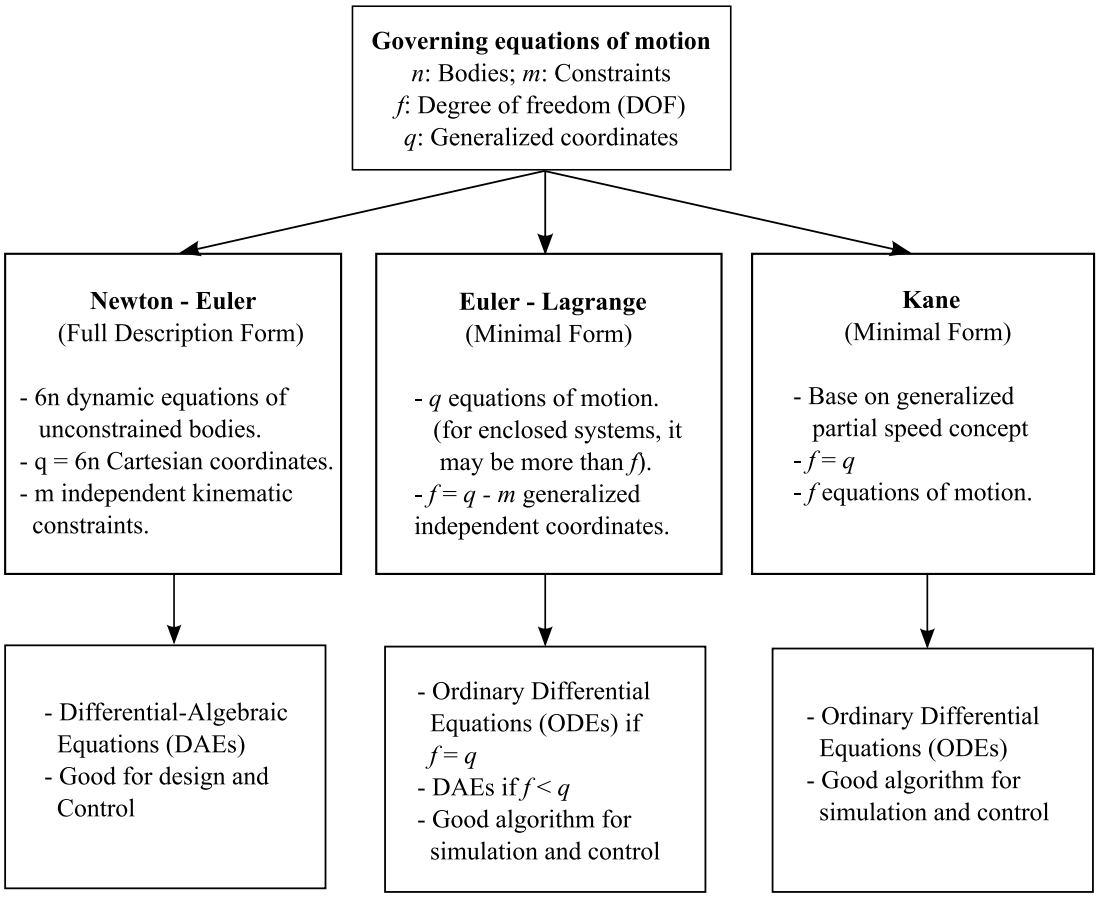

Figure 7. *Basic types of formulation of the equation of motion (Chaudhary et al., 2009, p. 4).*

Figure 7 shows that, depending on the purpose or information that the research team wants to retrieve, one formulation type might be more suitable than another. In the case of the development of the skate skier model, the information of interest for the team is the influence of the execution of the technique on variables such as the speed of the skier.

Further useful information acquired for purposes other than to know how fast the skier can travel is information related to the constraint forces of the ankle and knee of the skier. Knowledge of these forces makes it possible to analyze their impact from a physiological standpoint. This can be used as input for biomechanical studies related to the lower limb or to the development of improved gears.

This study could be considered the first stage of more complex research work dedicated to skiing as a high impact sport and to the improvement of the technique using multibody dynamics.

The formulation used in the research is based on the Euler - Lagrange equations. This was chosen because of its minimal form after proposing the model, its ease of implementation into a computer code such as Matlab and Maple, its significant amount of qualified bibliographic and electronic sources, and its application in the Laboratory of Machine Design of the Lappeenranta University of Technology.

These equations will be constructed using a spatial set of three bodies to represent the lower limb of the skier and the ski. The movement of the center of mass of the skier will have the capability of being described in any of the coordinate axes, meaning that the position and velocities of this point can be estimated and compared in a manner closer to reality.

3.1 Definition of the Lagrange multipliers formulation

One consideration when the Lagrange multipliers approach is applied is the use of absolute coordinates to describe the resultant different kinematic and dynamic vector quantities acting upon the bodies of the model supported by the use of local coordinate systems to simplify the location of important study points.

As mentioned in the previous section, one of the advantages of the implementation of the Lagrange multipliers approach is the simplicity of the method combined with the possibility of calculating accelerations simultaneously with the Lagrange multipliers terms. However, certain considerations have to be made during the integration steps of the equation of motion.

The first consideration to be made is related to the type of constraints that exist in the model. Usually, it is possible to have joint or driving constraints. Joint constraints define the connectivity between the bodies, and driving constraints describe specific motion patterns or trajectories that the point of the described body has to follow.

In the case of the present research, both types of constraints are present in the model, meaning that during the integration steps, continuous functions describing the trajectory of essential points and forces acting upon the body have to be fed. This transforms the problem into a partially inverse dynamics problem.

The aforementioned task becomes a key issue in every modeling process involving an inverse dynamics approach. Usually these data are taken from measurement instruments which perform a discrete capture of values of the monitored variable and store them in a specific way.

The discrete data have to be handled in such a way that a continuous function can be found to fit the imported values. In addition to that, the data have to be smooth up to the second derivative when the fitting refers to the position and orientation of objects. The fitting process might be accomplished in several ways; however, in this work, the data will be fitted by means of the use of Fourier series.

The second consideration to be taken into account is related to the way in which the differential algebraic equations (DAEs) are integrated. Because of the fact that the DAEs might be directly integrated without consideration of position and velocities constraints, there is the possibility of drifting and violating these constraints during each integration step. To avoid or minimize these deviations, some stabilization routines have been created and must be included in the computer code designed for the skier model.

One of the most widely and simply used methods adopted and implemented in this work is the Baumgarte stabilization method. Basically, the purpose of the Baumgarte stabilization method is to replace the acceleration equation with a combination of acceleration, velocity, and position constrain equations, creating a more stable set of ordinary differential equations (ODEs), (Cline, 2003, p. 4).

After including the stabilization method, this set of DAEs converted into ODEs can be integrated using the Runge-Kutta numerical algorithm. This popular algorithm is found as a built-in function in different symbolic and numerical mathematic software; therefore, there is no need to develop a customized mathematical solution for the model.

For constrained multibody systems, the equation of motion stated by the Lagrangian multipliers is based on equation (1).

$$\begin{aligned} \boldsymbol{M}\ddot{\boldsymbol{q}} + \boldsymbol{C}_{\boldsymbol{q}}^{\mathrm{T}}\boldsymbol{\lambda} &= \boldsymbol{Q}_{\boldsymbol{e}} + \boldsymbol{Q}_{\boldsymbol{v}} \\ \boldsymbol{C}_{\boldsymbol{q}}\ddot{\boldsymbol{q}} &= \boldsymbol{Q}_{\boldsymbol{d}} \end{aligned} \tag{1}$$

where $\boldsymbol{M}$ is the body mass matrix, $\boldsymbol{q} = [\boldsymbol{R}^{\boldsymbol{T}}\ \boldsymbol{\theta}^{\boldsymbol{T}}]$ is the vector of body generalized coordinates, $\boldsymbol{C}_{\boldsymbol{q}}$ is the constraint Jacobian matrix, $\boldsymbol{\lambda}$ is the vector of Lagrange multipliers, $\boldsymbol{Q}_{\boldsymbol{e}}$ is the vector of generalized forces, $\boldsymbol{Q}_{\boldsymbol{v}}$ is the quadratic velocity vector arising from differentiating the kinetic energy with respect to time and with respect to the generalized coordinates and $\boldsymbol{Q}_{\boldsymbol{d}}$ is the vector absorbing terms that are the partial derivatives of the constraint equations.

Equation (1), may also be presented in matrix form which is the way in which the final equation of motion of the model will be written. Refer to equation (2) for the matrix representation.

$$\begin{bmatrix} \boldsymbol{M} & \boldsymbol{C}_{\boldsymbol{q}}^{\mathrm{T}} \\ \boldsymbol{C}_{\boldsymbol{q}} & \boldsymbol{0} \end{bmatrix} \begin{bmatrix} \ddot{\boldsymbol{q}} \\ \boldsymbol{\lambda} \end{bmatrix} = \begin{bmatrix} \boldsymbol{Q}_{\boldsymbol{e}} + \boldsymbol{Q}_{\boldsymbol{v}} \\ \boldsymbol{Q}_{\boldsymbol{d}} \end{bmatrix} \tag{2}$$

Following the stated Lagrangian formulation for the constrained multibody system, the next chapter will be dedicated to defining each of the terms forming the equation of motion as specifically applied to the skier model. The first term is the vector of generalized coordinates.

3.2 Vector of generalized coordinates and its derivatives

As previously mentioned, the configuration of the multibody system in the Lagrangian multipliers formulation will be described using the absolute Cartesian and orientation coordinates. Therefore, the necessary information to define any point in the space is needed in the form of a vector to formulate the equations of motions of the model.

The vector containing the set of variables to completely define the location and orientation of a body is called the vector of generalized coordinates. Figure 8 shows the representation of a position vector of an arbitrary point of a body.

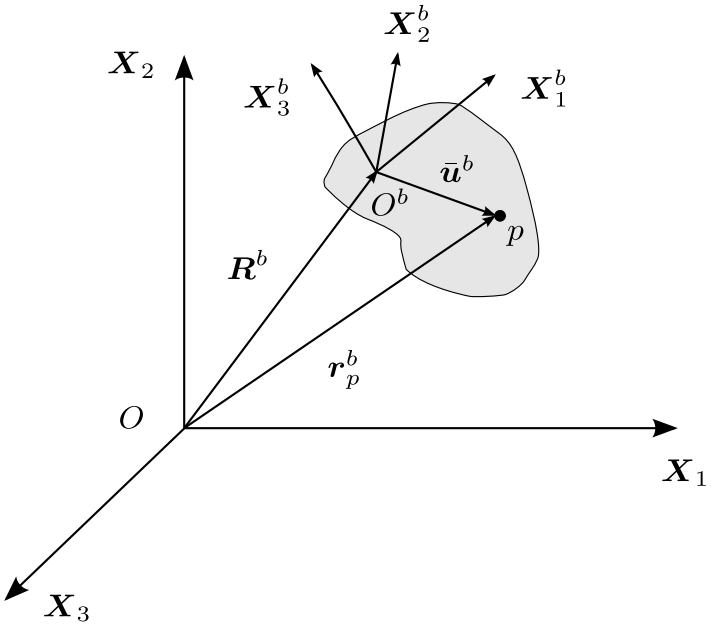

Figure 8. *Reference coordinates of the rigid body (Shabana, 1998, p. 11).*

The position of the point p of the body b is completely defined by equation (3)

$$\boldsymbol{r}_p^b = \boldsymbol{R}^b + \boldsymbol{A}^b\,\bar{\boldsymbol{u}}^b \tag{3}$$

where $\boldsymbol{r}_p^b$ is the position vector of the point P with respect to the inertial frame of reference, $\boldsymbol{R}^b$ is the position vector of the origin of the body reference system, $\boldsymbol{A}^b$ is the rotation matrix describing the orientation of the axes of the body reference system with respect to the absolute reference system and $\bar{\boldsymbol{u}}^b$ is the position vector of the point p with respect to the origin of the body reference system.

The vector representing the origin of the body reference system might be written as in equation (4)

$$\boldsymbol{R}^b = \left[R_1^b\ R_2^b\ R_3^b\right]^{\mathrm{T}} \tag{4}$$

Here, each one of the terms enclosed in the brackets represent the magnitud of the vectors oriented along the coordinate axes $\boldsymbol{X}_1$, $\boldsymbol{X}_2$ and $\boldsymbol{X}_3$, respectively. This representation is equivalent to the traditional X, Y and Z nomenclature, respectively.

The rotation matrix $\boldsymbol{A}^b$ deserves special attention; this stems from the fact that this matrix can be formulated employing different approaches which must be consistent during the whole model development.

Among the different approaches that might be used to specify the angular orientation of a rigid body, the following may be mentioned:

- Direction cosines
- Bryan angles
- Euler parameters
- Rodriguez parameters
- Quaternions

The selection of the method is related to the field of application of the model. For example, use of the direction cosines to describe the orientation of the body will lead to a matrix of nine elements and an additional set of six constraints between these coordinates. In complex models, it is often inconvenient to work with nine coordinates and six constraints (Wittenburg, 2008, p. 9). Each method entails advantages and disadvantages.

In the case of modeling of the skate skier, the system selected to describe the angular orientation of the body is the Euler angles. Its advantages and disadvantages will be discussed in the next paragraphs.

A Euler angle may be defined as a degree of freedom (DOF) representing a rotation about one of the coordinate axis (Grassia, 1998, p. 3). The angular orientation of the rigid body can then be said to be the result of three successive rotations. The three axes used to perform the rotations are not necessarily orthogonal (Shabana, 1998, p. 67), and these successive rotations are performed in a defined sequence maintained during the entire formulation of model.

In figure 9, two reference systems are presented. The first one is formed by the orthogonal vectors $\boldsymbol{X}_1\boldsymbol{X}_2\boldsymbol{X}_3$. The second system is formed by the orthogonal vectors $\boldsymbol{\xi}_1\boldsymbol{\xi}_2\boldsymbol{\xi}_3$, which initially coincide.

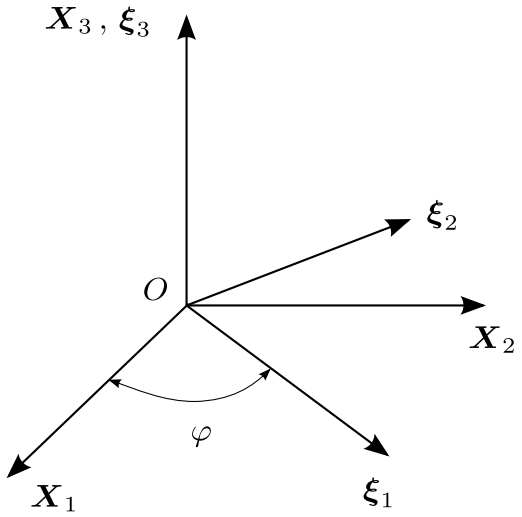

Figure 9. *Description of the rotation about the z axis. (Shabana, 1998, p. 67).*

If the system $\boldsymbol{\xi}_1\,\boldsymbol{\xi}_2\,\boldsymbol{\xi}_3$, is rotated by an angle φ located in the $\boldsymbol{\xi}_1\,\boldsymbol{\xi}_2$, about the $\boldsymbol{\xi}_3$ axis, then the result of this rotation can be written as in equation (5).

$$\boldsymbol{\xi} = \boldsymbol{D}_1 \boldsymbol{x} \tag{5}$$

where x represents the Cartesian coordinates on the plane of rotation and $\boldsymbol{D}_1$ is the transformation matrix to be applied to describe the magnitudes of any vector of the $\boldsymbol{\xi}_1\,\boldsymbol{\xi}_2\,\boldsymbol{\xi}_3$ system in $\boldsymbol{X}_1\,\boldsymbol{X}_2\,\boldsymbol{X}_3$ system.

The matrix $\boldsymbol{D}_1$, is presented in equation (6). This procedure is then performed on the other two remaining rotations to construct the final total rotation matrix (see equation (7)). For its compact and extended representation, refer to equation (8).

$$\boldsymbol{D}_1 = \begin{bmatrix} \cos\varphi & -\sin\varphi & 0 \\ \sin\varphi & \cos\varphi & 0 \\ 0 & 0 & 1 \end{bmatrix} \tag{6}$$

$$\boldsymbol{A} = \boldsymbol{D}_3 \boldsymbol{D}_2 \boldsymbol{D}_1 \tag{7}$$

$$\boldsymbol{A} = \begin{bmatrix} \cos\psi & -\sin\psi & 0 \\ \sin\psi & \cos\psi & 0 \\ 0 & 0 & 1 \end{bmatrix} \begin{bmatrix} 1 & 0 & 0 \\ 0 & \cos\theta & -\sin\theta \\ 0 & \sin\theta & \cos\theta \end{bmatrix} \begin{bmatrix} \cos\varphi & -\sin\varphi & 0 \\ \sin\varphi & \cos\varphi & 0 \\ 0 & 0 & 1 \end{bmatrix} \tag{8}$$

In equation (8), the angles φ, θ and ψ are the ones used to measure the rotations about the selected axes.

A special characteristic of the use of the Euler angles is the specific sequence of the successive rotations. The transformation matrix presented in equation (8) uses the sequence (ZXZ) that indicates about which axes of the local reference system the rotations are performed.

The advantages of the use of Euler angles are threefold: their reduced form of just three coordinates to describe the orientation; their suitability for integrating ODE; and the ease of computation of their derivatives, even though these functions are nonlinear.

The main disadvantage of the use of Euler angles is the possibility of "locking up the system". In the case of $\theta = n\pi(n = 0, \pm 1, \ldots)$, the axis of the third rotation coincides with the axis of the first rotation; thus, the angles ψ and φ cannot be distinguished. This phenomenon is known as Gimbal lock.

If Gimbal lock occurs, this physically means that "there is a direction in which the mechanism whose orientation is being controlled by the Euler rotation cannot respond to applied forces and torques" (Grassia, 1998, p. 3).

However, the suitability of the use of Euler angles remains when two physically significant directions exist and when the variations of the angle related to the second rotation keep within the limits, thus avoiding Gimbal lock.

During the modeling of the skate skier, special care must be taken to fulfill the limits related to the magnitude of the Euler angles in order to avoid any singularity during the simulation process. This also can be accounted for by observing the natural movements performed by the skier. It can be observed that in the skating technique, the amplitude of the rotations of the lower limb is limited to values that will not produce the locking of the system.

The next important parameter is the vector $\bar{\boldsymbol{u}}$, which defines the position of a point with respect to the absolute frame of reference. This vector represents the position vector in the local reference system. It can be written by employing the local coordinate axes (see equation (9)).

$$\bar{\boldsymbol{u}} = \begin{bmatrix} \bar{x}_p & \bar{y}_p & \bar{z}_p \end{bmatrix}^{\mathrm{T}} \tag{9}$$

As seen from the previous components of the position vector written for the absolute ref-

erence frame, some of those magnitudes are essential to defining positions, velocities,and accelerations of points of the bodies or the bodies themselves.

This set of important variables is included in a vector previously mentioned as the vector of generalized coordinates. It is presented in equation (10) along with its first and second derivatives, shown in equations (12) and (13), respectively.

$$\boldsymbol{q} = \begin{bmatrix} \boldsymbol{q}_1 & \boldsymbol{q}_2 & \dots & \boldsymbol{q}_i \end{bmatrix}^{\mathrm{T}} \tag{10}$$

in which,

$$\boldsymbol{q}_i = \begin{bmatrix} R_1^i & R_2^i & R_3^i & \varphi^i & \theta^i & \psi^i \end{bmatrix}^{\mathrm{T}} \tag{11}$$

where the terms R_j^i, with $i = 1 \dots 3$ (number of bodies in the model) and $j = 1 \dots 3$ (reference system axes x, y, z respectively) and the angles φ^i, θ^i and ψ^i are the Euler angles used to form the transformation matrices to define the orientation of the body reference systems, with respect the absolute reference system.

The derivatives of the vector of generalized coordinates are then presented in the next equations.

$$\dot{\boldsymbol{q}}_i = \begin{bmatrix} \dot{R}_1^i & \dot{R}_2^i & \dot{R}_3^i & \dot{\varphi}^i & \dot{\theta}^i & \dot{\psi}^i \end{bmatrix}^{\mathrm{T}} \tag{12}$$

$$\ddot{\boldsymbol{q}}_i = \begin{bmatrix} \ddot{R}_1^i & \ddot{R}_2^i & \ddot{R}_3^i & \ddot{\varphi}^i & \ddot{\theta}^i & \ddot{\psi}^i \end{bmatrix}^{\mathrm{T}} \tag{13}$$

The following section presents another term of the Lagrange multipliers equation of motion, the Jacobian matrix of the system.

3.3 Constraints and Jacobian matrix of the system

Before formulating the Jacobian matrix, it is necessary for one to define the constraint equations of the system. The constraint equations are the expressions that describe the connectivity between the bodies of a system as well as the specified motion trajectories that certain points follow (Shabana, 2001, p. 132).

Mathematically, one of the ways of formulating the constraint equations of a system is presented in equation (14).

$$\boldsymbol{C}(q_1, q_2, \ldots, q_n, t) = \boldsymbol{C}(\boldsymbol{q}, t) = \boldsymbol{0} \tag{14}$$

where $\boldsymbol{C} = [\ \boldsymbol{C}_1(\boldsymbol{q}, t)\ \boldsymbol{C}_2(\boldsymbol{q}, t)\ \ldots\ \boldsymbol{C}_n(\boldsymbol{q}, t)\ ]^T$ is the set of independent constraint equations, and n is the number of generalized coordinates.

The generalized coordinates and the constraint equations are related by the degrees of freedom (DOF) of the system. This relationship can be expressed as $DOF = n - n_c$, where n_c is the number of independent constraint equations.

From the previous relationship, other definitions may be derived for constrained multibody systems. If $n_c = n$, then the system is a kinematically driven system; however, if $n_c < n$, then the system is a dynamically driven system.

An additional important classification to be considered concerning the constraints is their dependency with time. If the constraint equations have the form presented in equation (14), they are called holonomic constraints. If these constraints do not change with time, they are called scleronomic constraints. Moreover, if the system is holonomic and time appears explicitly as in equation (14), then the system is called rheonomic (Shabana, 1998, p. 92). On the other hand, the constraints that cannot be written in the form of equation (14) are called nonholonomic constraints. These constraints might have the simple form presented in equation (15).

$$\boldsymbol{a}_0 + \boldsymbol{B}\dot{\boldsymbol{q}} = \boldsymbol{0} \tag{15}$$

where $\boldsymbol{a}_0 = \boldsymbol{a}_0(\boldsymbol{q}, t) = [\ \boldsymbol{a}_{01}\ \boldsymbol{a}_{02}\ \ldots\ \boldsymbol{a}_{nc}\ ]^T$, $\dot{\boldsymbol{q}} = [\ \dot{\boldsymbol{q}}_1\ \dot{\boldsymbol{q}}_2\ \ldots\ \dot{\boldsymbol{q}}_n\ ]^T$ is the vector of the system generalized velocities and $\boldsymbol{B}$ is a matrix having the form

$$\boldsymbol{B} = \begin{bmatrix} b_{11} & b_{12} & \cdots & b_{1n} \\ b_{21} & b_{22} & \cdots & b_{2n} \\ \vdots & \vdots & \ddots & \vdots \\ b_{n_c1} & b_{n_c2} & \cdots & b_{n_cn} \end{bmatrix} = \boldsymbol{B}\,(\boldsymbol{q}, t) \tag{16}$$

One important difference with respect to holonomic constraints is that nonholonomic constraints are unable to be integrated and written in terms of the generalized coordinates. In

this research, holonomic constraints are classified and referred to as geometric constraints, and nonoholonomic constraints are classified and referred to as kinematic constraints. The two types of representations are shown in equations (17) and (18).

$$\boldsymbol{C}\left(\boldsymbol{q}, t\right) = \boldsymbol{0} \qquad \text{Holonomic Constraint} \tag{17}$$

$$\boldsymbol{C}\left(\boldsymbol{q}, \dot{\boldsymbol{q}}, t\right) = \boldsymbol{0} \quad \text{Non-holonomic Constraint} \tag{18}$$

The identification of these two types of constraints during the definition phase of the Jacobian matrix of the system is essential due to the additional procedures to be applied when one integrates the equation of motion of the model.

If the vector of holonomic constraints if differentiated with respect to time, then the velocity kinematic equations can be obtained. See equation (19).

$$\frac{d}{dt}\boldsymbol{C}\left(\boldsymbol{q}, t\right) = \frac{\partial}{\partial \boldsymbol{q}}\boldsymbol{C}\frac{d}{dt}\boldsymbol{q} + \frac{d}{dt}\boldsymbol{C}$$

$$\boldsymbol{C}_{\boldsymbol{q}}\ddot{\boldsymbol{q}} = -\boldsymbol{C}_t \tag{19}$$

The term $\boldsymbol{C}_{\boldsymbol{q}}$ results from differentiating the constraint equations with respect to the generalized coordinates. It is called the Jacobian matrix of the system. $\boldsymbol{C}_t$ is the vector of partial derivatives of the constraint equations with respect to time (Garcia, 1994, 97). If scleronomic constraint equations are being modeled, the term $\boldsymbol{C}_t$ becomes zero vector.

To begin to define the constraint equations of the system, firstly one must do a detailed analysis of the body joints to determine the geometric constraints. Then, further analysis is needed to formulate the driving constraints. Because of the previous statements made in the initial assumptions, it may be foreseen that kinematic constraints will not appear in the development of the model, facilitating the implementation of well-known integration methods, such as the Runge - Kutta high-order integration routine.

3.4 Mass matrix of the system

In this section, the mass matrix of the model is formulated. To obtain its final form, it is necessary to refer to the study of the generalized inertia forces affecting the system. Generalized inertia forces are the forces derived from the effect of the linear and angular

accelerations acting on a body with specific mass properties.

One of the methods used to develop the generalized inertia forces is the application of the principle of virtual work to this type of acting forces. The first step is to determine the virtual change in the absolute position of an arbitrary point on the rigid body, as previously defined in equation (3). The virtual change of the position vector is provided in equation (20) (Shabana, 1998, p. 149-150).

$$\delta \boldsymbol{r}^i = \delta \boldsymbol{R}^i + \boldsymbol{A}^i \bar{\boldsymbol{u}}^i \delta \boldsymbol{\theta} \tag{20}$$

In the last equation, $\delta \boldsymbol{r}^i$ is the virtual change of the position vector of the point under study, and $\delta \boldsymbol{R}^i$ is the virtual change associated with the point origin of the body reference system. The term $\boldsymbol{A}^i \bar{\boldsymbol{u}}^i$ may be written as

$$\boldsymbol{A}^i \bar{\boldsymbol{u}}^i = \boldsymbol{A}^i \left(\bar{\boldsymbol{\omega}}^i \times \bar{\boldsymbol{u}}^i \right) = -\boldsymbol{A}^i \tilde{\bar{\boldsymbol{u}}}^i \bar{\boldsymbol{\omega}}^i \tag{21}$$

Here, $\bar{\boldsymbol{\omega}}^i$ is the body angular velocity vector, and $\tilde{\bar{\boldsymbol{u}}}^i$ is the skew symmetric matrix defined by

$$\tilde{\bar{\boldsymbol{u}}}^i = \begin{bmatrix} 0 & -x_3^i & x_2^i \\ x_3^i & 0 & -x_1^i \\ -x_2^i & x_1^i & 0 \end{bmatrix} \tag{22}$$

in which x_1^i, x_2^i and x_3^i are the components of the vector $\bar{\boldsymbol{u}}^i$.

Additionally, the angular velocity vector may be written as $\bar{\boldsymbol{\omega}}^i = \bar{\boldsymbol{G}}^i \dot{\boldsymbol{\theta}}^i$, where $\bar{\boldsymbol{G}}^i$ is a matrix that depends on the selected rotational coordinates of body i, and $\dot{\boldsymbol{\theta}}^i$ is the time derivatives of the rotational coordinates of the body reference system.

To define the matrix $\bar{\boldsymbol{G}}^i$, it is necessary to study the formulation of the angular velocity in the absolute and local reference system. Figure 10 shows a gyroscope which supports the formulation of these angular velocities.

Next, the angular velocity of the rotor can be expressed as $\boldsymbol{\omega} = \dot{\phi}\, \boldsymbol{k}^1 + \dot{\theta}\, \boldsymbol{i}^2 + \dot{\psi}\, \boldsymbol{k}^3$, where $\boldsymbol{k}^1$ is a unit vector along the $\boldsymbol{Z}^1$ axis, $\boldsymbol{i}^2$ is a vector along the $\boldsymbol{X}^2$ axis, and $\boldsymbol{k}^3$ is a unit vector along the $\boldsymbol{Z}^3$ axis. These vectors can be expressed in mathematical form as

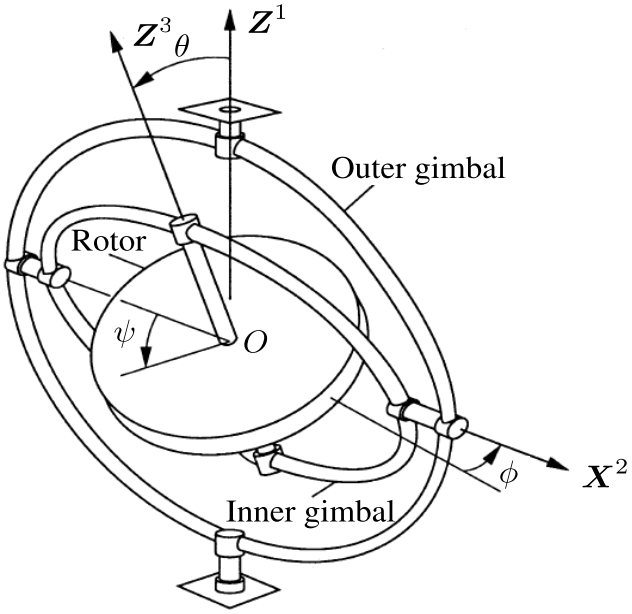

Figure 10. *Gyroscope (Shabana, 2001, p. 468).*

$$\boldsymbol{k}^1 = \begin{bmatrix} 0 & 0 & 1 \end{bmatrix}^T \tag{23}$$

$$\boldsymbol{i}^1 = \begin{bmatrix} \cos\phi & -\sin\phi & 0 \\ \sin\phi & \cos\phi & 0 \\ 0 & 0 & 1 \end{bmatrix} \begin{bmatrix} 1 \\ 0 \\ 0 \end{bmatrix} = \begin{bmatrix} \cos\phi \\ \sin\phi \\ 0 \end{bmatrix} \tag{24}$$

$$\boldsymbol{k}^3 = \begin{bmatrix} \cos\phi & -\sin\phi & 0 \\ \sin\phi & \cos\phi & 0 \\ 0 & 0 & 1 \end{bmatrix} \begin{bmatrix} 1 & 0 & 0 \\ 0 & \cos\theta & -\sin\theta \\ 0 & \sin\theta & \cos\theta \end{bmatrix} \begin{bmatrix} 0 \\ 0 \\ 1 \end{bmatrix} = \begin{bmatrix} \sin\phi\sin\theta \\ -\cos\phi\sin\theta \\ \cos\theta \end{bmatrix} \tag{25}$$

Then, the angular velocity vector can be written as

$$\boldsymbol{\omega} = \dot{\phi} \begin{bmatrix} 0 \\ 0 \\ 1 \end{bmatrix} + \dot{\theta} \begin{bmatrix} \cos\phi \\ \sin\phi \\ 0 \end{bmatrix} + \dot{\psi} \begin{bmatrix} \sin\phi\sin\theta \\ -\cos\phi\sin\theta \\ \cos\theta \end{bmatrix} \tag{26}$$

After operating, equation (26) can be written as

$$\boldsymbol{\omega} = \begin{bmatrix} \dot{\theta}\cos\phi + \dot{\psi}\sin\phi\sin\theta \\ \dot{\theta}\sin\phi - \dot{\psi}\cos\phi\sin\theta \\ \dot{\phi} + \dot{\psi}\cos\theta \end{bmatrix} = \begin{bmatrix} 0 & \cos\phi & \sin\phi\sin\theta \\ 0 & \sin\phi & -\cos\phi\sin\theta \\ 1 & 0 & \cos\theta \end{bmatrix} \begin{bmatrix} \dot{\phi} \\ \dot{\theta} \\ \dot{\psi} \end{bmatrix} \tag{27}$$

In its simplified form, equation (27) transforms into

$$\boldsymbol{\omega} = \boldsymbol{G}\,\dot{\boldsymbol{\theta}} \tag{28}$$

in which $\dot{\boldsymbol{\theta}}$ is the vector of the first derivatives of the Euler angles, and

$$\boldsymbol{G} = \begin{bmatrix} 0 & \cos\phi & \sin\phi\sin\theta \\ 0 & \sin\phi & -\cos\phi\sin\theta \\ 1 & 0 & \cos\theta \end{bmatrix} \tag{29}$$

To define this matrix in the local coordinate system of the body, the following transformation has to be applied:

$$\bar{\boldsymbol{G}} = \boldsymbol{A}^T\boldsymbol{G} \tag{30}$$

resulting in

$$\bar{\boldsymbol{G}} = \begin{bmatrix} \sin\theta\sin\psi & \cos\psi & 0 \\ \sin\theta\cos\psi & -\sin\psi & 0 \\ \cos\theta & 0 & 1 \end{bmatrix} \tag{31}$$

Substituting the definitions given in equation (21) and (31) into equation (20) makes it possible to obtain

$$\delta\boldsymbol{r}^i = \delta\boldsymbol{R}^i - \boldsymbol{A}^i\tilde{\bar{\boldsymbol{u}}}^i\bar{\boldsymbol{G}}^i\delta\boldsymbol{\theta}^i \tag{32}$$

This last expression may be written in a partitioned form as

$$\delta\boldsymbol{r}^i = \begin{bmatrix} \boldsymbol{I} & \boldsymbol{A}^i\tilde{\bar{\boldsymbol{u}}}^i\bar{\boldsymbol{G}}^i \end{bmatrix} \begin{bmatrix} \delta\boldsymbol{R}^i \\ \delta\boldsymbol{\theta}^i \end{bmatrix} \tag{33}$$

where $\boldsymbol{I}$ is a 3×3 identity matrix.

The virtual work of the inertia forces is

$$\delta W_i^i = \int_{V^i} \rho^i \ddot{\boldsymbol{r}}^{i\mathrm{T}} \delta \boldsymbol{r}^i dV^i \tag{34}$$

In equation (34), ρ^i and V^i are the mass density and volume of the rigid body i, respectively. The vector $\ddot{\boldsymbol{r}}^{i\mathrm{T}}$ represents the absolute linear acceleration of the point under observation, and it is defined in equation (35).

$$\ddot{\boldsymbol{r}}^i = \begin{bmatrix} \boldsymbol{I} & \boldsymbol{A}^i \tilde{\bar{\boldsymbol{u}}}^i \bar{\boldsymbol{G}}^i \end{bmatrix} \begin{bmatrix} \ddot{\boldsymbol{R}}^i \\ \ddot{\boldsymbol{\theta}}^i \end{bmatrix} + \boldsymbol{a}_v^i \tag{35}$$

in which $\ddot{\boldsymbol{R}}^i$ is the absolute acceleration of the origin of the body i reference system, $\ddot{\boldsymbol{\theta}}^i$ is the double derivative with respect to time of the rotational coordinates, and $\boldsymbol{a}_v^i$ is a vector absorbing terms which are quadratic in the velocities. This vector is defined as

$$\boldsymbol{a}_v^i = \left(\tilde{\boldsymbol{\omega}}^i\right)^2 \boldsymbol{u}^i - \tilde{\boldsymbol{u}}^i \dot{\boldsymbol{G}}^i \dot{\boldsymbol{\theta}}^i \tag{36}$$

The term $\tilde{\boldsymbol{\omega}}^i$ is the skew symmetric matrix of $\boldsymbol{\omega}^i$described by

$$\tilde{\boldsymbol{\omega}}^i = \begin{bmatrix} 0 & -\bar{\omega}_3^i & \bar{\omega}_2^i \\ \bar{\omega}_3^i & 0 & -\bar{\omega}_1^i \\ -\bar{\omega}_2^i & \bar{\omega}_1^i & 0 \end{bmatrix} \tag{37}$$

where $\bar{\omega}_1^i$, $\bar{\omega}_2^i$ and $\bar{\omega}_3^i$ are the components of the vector $\bar{\boldsymbol{\omega}}^i$.

The substitution of equations (35) and (33) into equation (34) yields

$$\delta W_i^i = \begin{bmatrix} \ddot{\boldsymbol{R}}^{i^T} & \ddot{\boldsymbol{\theta}}^{i^T} \end{bmatrix} \left\{ \int_{V^i} \rho^i \left\{ \begin{bmatrix} I \\ -\bar{\boldsymbol{G}}^{i^T} \tilde{\bar{\boldsymbol{u}}}^{i^T} \boldsymbol{A}^{i^T} \end{bmatrix} \begin{bmatrix} I & -\boldsymbol{A}^i \tilde{\bar{\boldsymbol{u}}}^i \bar{\boldsymbol{G}}^i \end{bmatrix} \right.\right.$$

$$\left.\left. + \boldsymbol{a}_v^{i^T} \begin{bmatrix} I & -\boldsymbol{A}^i \tilde{\bar{\boldsymbol{u}}}^i \bar{\boldsymbol{G}}^i \end{bmatrix} \right\} dV^i \right\} \begin{bmatrix} \delta \boldsymbol{R}^i \\ \delta \boldsymbol{\theta}^i \end{bmatrix} \tag{38}$$

which can be written as

$$\delta W_i^i = \left[\begin{array}{cc} \ddot{\boldsymbol{q}}^{i^{\mathrm{T}}} \boldsymbol{M}^i & -\boldsymbol{Q}_v^{i^{\mathrm{T}}} \end{array} \right] \delta \boldsymbol{q}^i \tag{39}$$

The term $\boldsymbol{M}^i$ is the symmetric stiffness mass matrix

$$\boldsymbol{M}^i = \int_{V^i} \rho^i \left[\begin{array}{cc} \boldsymbol{I} & -\boldsymbol{A}^i \tilde{\bar{\boldsymbol{u}}}^i \bar{\boldsymbol{G}}^i \\ symmetric & \bar{\boldsymbol{G}}^{i^{\mathrm{T}}} \tilde{\bar{\boldsymbol{u}}}^{i^{\mathrm{T}}} \tilde{\bar{\boldsymbol{u}}}^i \bar{\boldsymbol{G}}^i \end{array} \right] dV^i \tag{40}$$

and $\boldsymbol{Q}_v^{i^{\mathrm{T}}}$ is the vector of inertia forces that absorbs the terms that are quadratic in the velocities.

This symmetric mass matrix presented in equation (40) may be written in the form

$$\boldsymbol{M}^i = \left[\begin{array}{cc} \boldsymbol{m}_{RR}^i & \boldsymbol{m}_{R\theta}^i \\ \boldsymbol{m}_{\theta R}^i & \boldsymbol{m}_{\theta\theta}^i \end{array} \right] \tag{41}$$

where

$$\boldsymbol{m}_{RR}^i = m^i \boldsymbol{I} \tag{42}$$

$$\boldsymbol{m}_{R\theta}^i = \boldsymbol{m}_{\theta R}^{i^T} = -\boldsymbol{A}^i \left[\int_{V^i} \rho^i \tilde{\bar{\boldsymbol{u}}}^i dV^i \right] \bar{\boldsymbol{G}}^i \tag{43}$$

and

$$\boldsymbol{m}_{\theta\theta}^i = \bar{\boldsymbol{G}}^{i^{\mathrm{T}}} \bar{\boldsymbol{I}}_{\theta\theta}^i \bar{\boldsymbol{G}}^i \tag{44}$$

where m^i is the total mass of the rigid body i, and $\bar{\boldsymbol{I}}_{\theta\theta}^i$ is a 3×3 symmetric matrix called the inertia tensor of the rigid body.

The inertia tensor of the rigid body may be formulated as

$$\bar{\boldsymbol{I}}_{\theta\theta}^i = \int_{V^i} \rho^i \tilde{\bar{\boldsymbol{u}}}^{i^{\mathrm{T}}} \tilde{\bar{\boldsymbol{u}}}^i dV^i \tag{45}$$

$$\bar{\boldsymbol{I}}^i_{\theta\theta} = \begin{bmatrix} i^i_{xx} & i^i_{xy} & i^i_{xz} \\ & i^i_{yy} & i^i_{yz} \\ symmetric & & i^i_{zz} \end{bmatrix} \tag{46}$$

where the elements i^i_{xx}, i^i_{yy} and i^i_{zz} are called the moments of inertia and i^i_{xy}, i^i_{xz} and i^i_{yz} are called the products of inertia.

Constancy is an important characteristic of moments and products of inertia, because they are defined in the local coordinate system. However, the term $\boldsymbol{m}^i_{\theta\theta}$ changes with respect to time, as it depends on the orientation coordinates of the rigid body.

Further comments must be made regarding the term $\boldsymbol{m}^i_{R\theta}$. As this term is based on the skew symmetric matrix $\tilde{\bar{\boldsymbol{u}}}^i$, it can be concluded that if the origin of the body reference system is attached to the center of mass of the body, then the skew matrix is a null matrix.

3.5 Vector of Lagrange multipliers

In constrained multibody systems, one may make a dynamic analysis without isolating the bodies that form the system. This type of approach considering the system as a whole is usually referred to as the embedding technique in multibody dynamics.

This embedding technique keeps the constraint forces apparently hidden in the formulation of the equation of motion. However, to solve the vector of generalized accelerations with the Lagrangian formulation, a second set of equations has to be introduced to account for the constraint forces and to make the complete system of equations solvable.

The term Lagrange multipliers appears as a key factor in accounting for the constraint forces. Both vectors, Lagrange and generalized accelerations, are used then to define the vector of constraint forces.

To formulate the vector of Lagrange multipliers of the skate skier model, it is necessary to derive the general procedure defining their values. In figure 11, two rigidly attached bodies are presented as a system example. This would be restricted to the planar case that can be applicable to the three dimensional case.

The vector of constraint equations of this system is presented in equation (47).

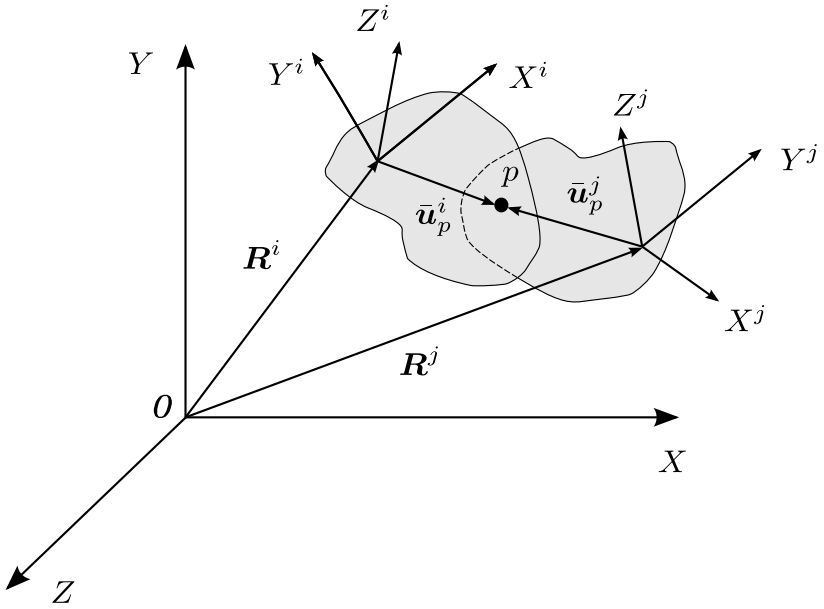

Figure 11. *System of two bodies rigidly attached to each other (Shabana, 2001, p. 324).*

$$\boldsymbol{C} = \begin{bmatrix} \boldsymbol{R}^i + \boldsymbol{A}^i \bar{\boldsymbol{u}}_p^i - \boldsymbol{R}^j - \boldsymbol{A}^j \bar{\boldsymbol{u}}_p^j \\ \theta^i - \theta^j \end{bmatrix} \tag{47}$$

The first row of the matrix accounts for the non-relative translation of the two bodies while the remaining one account for the non-relative rotation.

The Jacobian matrix of the two body system can be written in partitioned form as

$$\boldsymbol{C} = \begin{bmatrix} \boldsymbol{C}_q^i & \boldsymbol{C}_q^j \end{bmatrix} \tag{48}$$

$$\boldsymbol{C}_q^i = \begin{bmatrix} \boldsymbol{I} & \boldsymbol{A}_{\theta^i}^i \bar{\boldsymbol{u}}_p^i \\ \boldsymbol{0} & 1 \end{bmatrix} \tag{49}$$

$$\boldsymbol{C}_q^j = \begin{bmatrix} \boldsymbol{I} & \boldsymbol{A}_{\theta^j}^j \bar{\boldsymbol{u}}_p^j \\ \boldsymbol{0} & 1 \end{bmatrix} \tag{50}$$

where $\boldsymbol{I}$ is the 2 x 2 identity matrix, and $\boldsymbol{A}_{\theta^i}^i$ and $\boldsymbol{A}_{\theta^j}^j$ are the partial derivatives of the transformation matrices $\boldsymbol{A}^i$ and $\boldsymbol{A}^j$ with respect to the generalized rotational coordinates θ related to each body.

If a free-body diagram (FBD) is made for the bodies of the system, then the constraint

forces appear as part of the forces acting on the bodies. This FBD is depicted in figure 12.

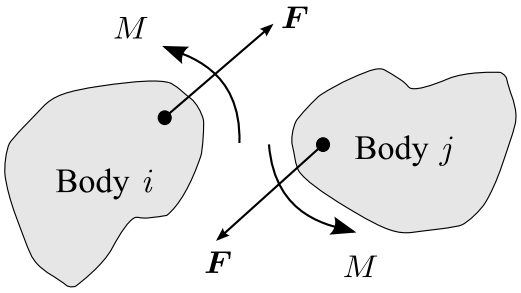

Figure 12. *Free-body diagram of the two-body system (Shabana, 2001, p. 325).*

The joint forces are $\boldsymbol{F} = \begin{bmatrix} \boldsymbol{F}_x & \boldsymbol{F}_y \end{bmatrix}^{\mathrm{T}}$ and M is the moment.

If the forces and moments are collected in a vector called $\boldsymbol{\lambda}$, the system may be defined as

$$\boldsymbol{\lambda} = -\begin{bmatrix} \boldsymbol{F} \\ M \end{bmatrix} \tag{51}$$

The reaction forces acting on bodies i and j are equal in magnitude and opposite in direction, and may be expressed in vector form as

$$\boldsymbol{F}^i = -\boldsymbol{\lambda} = \begin{bmatrix} \boldsymbol{F} \\ M \end{bmatrix} \tag{52}$$

$$\boldsymbol{F}^j = \boldsymbol{\lambda} = -\begin{bmatrix} \boldsymbol{F} \\ M \end{bmatrix} \tag{53}$$

These reaction forces are said to be equipollent to other systems of generalized reaction forces defined at the origin of the absolute coordinate system. The vector of generalized reaction forces is presented in the next equations.

$$\boldsymbol{Q}_c^i = \begin{bmatrix} \boldsymbol{F} \\ M + (\boldsymbol{A}^i \bar{\boldsymbol{u}}_P^i \times \boldsymbol{F}) \cdot \boldsymbol{k} \end{bmatrix} \tag{54}$$

$$\boldsymbol{Q}_c^j = \begin{bmatrix} \boldsymbol{F} \\ M + (\boldsymbol{A}^j \bar{\boldsymbol{u}}_P^j \times \boldsymbol{F}) \cdot \boldsymbol{k} \end{bmatrix} \tag{55}$$

where $\boldsymbol{k}$ is a unit vector along the z direction. Also, it can be demonstrated that the relationship $(\boldsymbol{A}^i \bar{\boldsymbol{u}}_P^i \times \boldsymbol{F}) \cdot \boldsymbol{k}$ is equal to $\bar{\boldsymbol{u}}_P^{i^{\mathrm{T}}} \boldsymbol{A}_\theta^{i^{\mathrm{T}}} \boldsymbol{F}$. In the following part, these identities will be developed.

$$(\boldsymbol{A}^i \bar{\boldsymbol{u}}_P^i \times \boldsymbol{F}) \cdot \boldsymbol{k} \tag{56}$$

$$\begin{aligned} \boldsymbol{A}^i \bar{\boldsymbol{u}}_P^i &= \begin{bmatrix} \cos\theta^i & -\sin\theta^i \\ \sin\theta^i & \cos\theta^i \end{bmatrix} \begin{bmatrix} \bar{u}_{px}^i \\ \bar{u}_{py}^i \end{bmatrix} \\ &= \begin{bmatrix} \bar{u}_{px}^i \cos\theta^i - \bar{u}_{py}^i \sin\theta^i & \bar{u}_{px}^i \sin\theta^i + \bar{u}_{py}^i \cos\theta^i \end{bmatrix} \end{aligned} \tag{57}$$

$$\begin{aligned} (\boldsymbol{A}^i \bar{\boldsymbol{u}}_P^i \times \boldsymbol{F}) \cdot \boldsymbol{k} &= \begin{vmatrix} \boldsymbol{i} & \boldsymbol{j} & \boldsymbol{k} \\ \bar{u}_{px}^i \cos\theta^i - \bar{u}_{py}^i \sin\theta^i & \bar{u}_{px}^i \sin\theta^i + \bar{u}_{py}^i \cos\theta^i & 0 \\ F_x^i & F_y^i & 0 \end{vmatrix} \cdot \boldsymbol{k} \\ &= F_y^i \left(\bar{u}_{px}^i \cos\theta^i - \bar{u}_{py}^i \sin\theta^i \right) - F_x^i \left(\bar{u}_{px}^i \sin\theta^i + \bar{u}_{py}^i \cos\theta^i \right) \end{aligned} \tag{58}$$

The second part of the identity is

$$\bar{\boldsymbol{u}}_P^{i^{\mathrm{T}}} \boldsymbol{A}_\theta^{i^{\mathrm{T}}} \boldsymbol{F} \tag{59}$$

$$\begin{aligned} \bar{\boldsymbol{u}}_P^{i^{\mathrm{T}}} \boldsymbol{A}_\theta^{i^{\mathrm{T}}} &= \begin{bmatrix} \bar{u}_{px}^i & \bar{u}_{py}^i \end{bmatrix} \begin{bmatrix} -\sin\theta^i & \cos\theta^i \\ -\cos\theta^i & -\sin\theta^i \end{bmatrix} \\ &= \begin{bmatrix} -\bar{u}_{px}^i \sin\theta^i - \bar{u}_{py}^i \cos\theta^i & \bar{u}_{px}^i \cos\theta^i - \bar{u}_{py}^i \sin\theta^i \end{bmatrix} \end{aligned} \tag{60}$$

$$\begin{aligned} \bar{\boldsymbol{u}}_P^{i^{\mathrm{T}}} \boldsymbol{A}_\theta^{i^{\mathrm{T}}} \boldsymbol{F} &= \begin{bmatrix} -\bar{u}_{px}^i \sin\theta^i - \bar{u}_{py}^i \cos\theta^i & \bar{u}_{px}^i \cos\theta^i - \bar{u}_{py}^i \sin\theta^i \end{bmatrix} \begin{bmatrix} F_x^i \\ F_y^i \end{bmatrix} \\ &= F_x^i \left(-\bar{u}_{px}^i \sin\theta^i - \bar{u}_{py}^i \cos\theta^i \right) + F_y^i \left(\bar{u}_{px}^i \cos\theta^i - \bar{u}_{py}^i \sin\theta^i \right) \end{aligned} \tag{61}$$

It can be seen in equations (58) and (61) that the result is the same. Furthermore,

$$\boldsymbol{Q}_c^i = \begin{bmatrix} \boldsymbol{F} \\ M + (\boldsymbol{A}^i \bar{\boldsymbol{u}}_P^i \times \boldsymbol{F}) \cdot \boldsymbol{k} \end{bmatrix} = \begin{bmatrix} \boldsymbol{I} & 0 \\ \bar{\boldsymbol{u}}_P^{i^T} \boldsymbol{A}_\theta^{i^T} & 1 \end{bmatrix} \begin{bmatrix} \boldsymbol{F} \\ M \end{bmatrix} \tag{62}$$

and

$$\boldsymbol{Q}_c^i = \begin{bmatrix} \boldsymbol{I} & 0 \\ \bar{\boldsymbol{u}}_P^{i^T} \boldsymbol{A}_\theta^{i^T} & 1 \end{bmatrix} \begin{bmatrix} \boldsymbol{F} \\ M \end{bmatrix} = -\boldsymbol{C}_{\boldsymbol{q}^i}^T \boldsymbol{\lambda} \tag{63}$$

$$\boldsymbol{Q}_c^j = \begin{bmatrix} \boldsymbol{I} & 0 \\ \bar{\boldsymbol{u}}_P^{j^T} \boldsymbol{A}_\theta^{j^T} & 1 \end{bmatrix} \begin{bmatrix} \boldsymbol{F} \\ M \end{bmatrix} = -\boldsymbol{C}_{\boldsymbol{q}^j}^T \boldsymbol{\lambda} \tag{64}$$

From the set of previous derivations of the generalized constraint forces, it can be seen that the dimension of the vector of Lagrange multipliers $\boldsymbol{\lambda}$ equals the number of constraints present in the system. In this case, the two bodies represented in the plane are rigidly attached and produce three constraint equations, two restricting the relative translation and one restraining the relative rotation, so the vector of Lagrange multipliers is a column vector of dimension three.

$$\boldsymbol{\lambda} = \begin{bmatrix} \lambda_1 \\ \lambda_2 \\ \lambda_3 \end{bmatrix} \tag{65}$$

where λ_1, λ_2 and λ_3 are the Lagrange multipliers associated with each one of the constraints of the system.

In the case of a multibody system formed by more than two bodies, the generalized reaction forces that appear due to the constraints imposed may be written as in equation (66).

$$\begin{aligned} \boldsymbol{Q}_1^i &= -\left(\boldsymbol{C}_1\right)_{\boldsymbol{q}^i}^T \boldsymbol{\lambda}_1 \\ \boldsymbol{Q}_2^i &= -\left(\boldsymbol{C}_2\right)_{\boldsymbol{q}^i}^T \boldsymbol{\lambda}_2 \\ &\vdots \\ \boldsymbol{Q}_{n_i}^i &= -\left(\boldsymbol{C}_{n_i}\right)_{\boldsymbol{q}^i}^T \boldsymbol{\lambda}_{n_i} \end{aligned} \tag{66}$$

in which $\boldsymbol{Q}_1^i$, $\boldsymbol{Q}_2^i$ and $\boldsymbol{Q}_{n_i}^i$ are the individual generalized constraint forces related to the constraints in body i. $\boldsymbol{C}_1$, $\boldsymbol{C}_2$ and $\boldsymbol{C}_n$ are the constraints of body i, and $\boldsymbol{\lambda}_1$, $\boldsymbol{\lambda}_2$ and $\boldsymbol{\lambda}_n$ are the corresponding Lagrange multipliers.

After the collection of the previous terms into one vector, the generalized constraint force affecting the body can be formulated. See equation (67).

$$\begin{aligned} \boldsymbol{Q}_C^i &= \boldsymbol{Q}_1^i + \boldsymbol{Q}_2^i + \ldots + \boldsymbol{Q}_2^i \\ \boldsymbol{Q}_C^i &= -\left(\boldsymbol{C}_1\right)_{\boldsymbol{q}^i}^T \boldsymbol{\lambda}_1 - \left(\boldsymbol{C}_2\right)_{\boldsymbol{q}^i}^T \boldsymbol{\lambda}_2 - \ldots - \left(\boldsymbol{C}_{n_i}\right)_{\boldsymbol{q}^i}^T \boldsymbol{\lambda}_{n_i} \\ \boldsymbol{Q}_C^i &= -\boldsymbol{C}_{\boldsymbol{q}^i}^T \boldsymbol{\lambda} \end{aligned} \tag{67}$$

As the reaction force of the whole system is the sum of the individual generalized constraint forces acting on each body, this force affecting the system may be written as in equation (68):

$$\boldsymbol{Q}_C = -\begin{bmatrix} \boldsymbol{C}_{\boldsymbol{q}^1}^T \boldsymbol{\lambda} \\ \boldsymbol{C}_{\boldsymbol{q}^2}^T \boldsymbol{\lambda} \\ \vdots \\ \boldsymbol{C}_{\boldsymbol{q}^{n_b}}^T \boldsymbol{\lambda} \end{bmatrix} = -\boldsymbol{C}_{\boldsymbol{q}}^T \boldsymbol{\lambda} \tag{68}$$

where the Lagrange multipliers vector contains one term per each constraint imposed on the system.

3.6 Vector of generalized forces

In order to introduce the concept of virtual forces associated with the generalized coordinates, the principle of virtual work must be applied. This is to extract the term formed during the formulation of this principle.

Figure 13 shows a force acting on the rigid body i.

Vector $\boldsymbol{F}^i$ represents the force acting on the body. When one applies the principle of virtual work to this vector, which is assumed to be defined in the global coordinate system, the virtual work of this vector can be written as

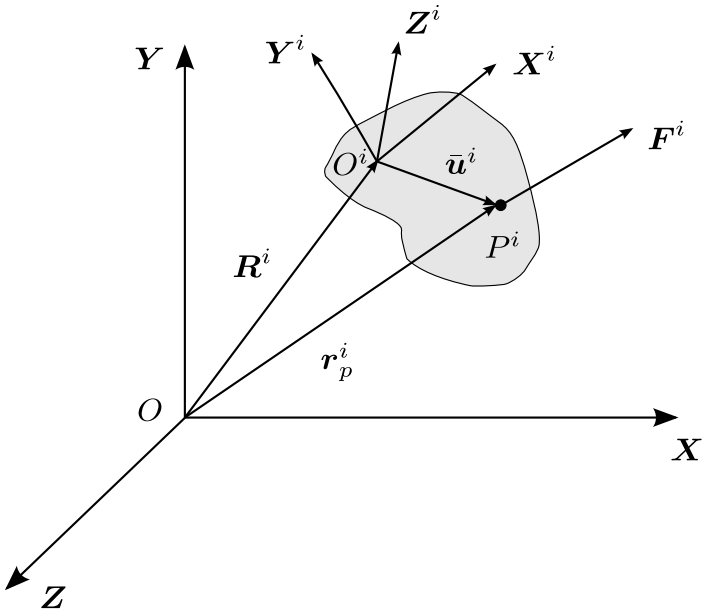

Figure 13. *Force vector on body i (Shabana, 2001, p. 414).*

$$\delta W_e^i = \boldsymbol{F}^{i^T} \delta \boldsymbol{r}_P^i \tag{69}$$

in which the vector $\boldsymbol{r}_P^i$, previously defined in equation (20), has the partitioned form

$$\delta \boldsymbol{r}^i = \begin{bmatrix} \boldsymbol{I} & -\boldsymbol{A}^i \tilde{\bar{\boldsymbol{u}}}^i \bar{\boldsymbol{G}}^i \end{bmatrix} \begin{bmatrix} \delta \boldsymbol{R}^i \\ \delta \boldsymbol{\theta}^i \end{bmatrix} \tag{70}$$

Recalling the identities $\tilde{\boldsymbol{u}}^i = \boldsymbol{A}^i \tilde{\bar{\boldsymbol{u}}}^i \boldsymbol{A}^{i^T}$ and $\bar{\boldsymbol{G}}^i = \boldsymbol{A}^{i^T} \boldsymbol{G}^i$, the virtual change in the position can be written as

$$\boldsymbol{A}^i \tilde{\bar{\boldsymbol{u}}}^i \left(\boldsymbol{A}^{i^T} \boldsymbol{G}^i \right) = \tilde{\boldsymbol{u}}^i \boldsymbol{G}^i \tag{71}$$

$$\delta \boldsymbol{r}^i = \begin{bmatrix} \boldsymbol{I} & -\tilde{\boldsymbol{u}}^i \boldsymbol{G}^i \end{bmatrix} \begin{bmatrix} \delta \boldsymbol{R}^i \\ \delta \boldsymbol{\theta}^i \end{bmatrix} \tag{72}$$

With the combination of equations (71) and (72), the virtual work can be written as

$$\delta W_e^i = \begin{bmatrix} \boldsymbol{F}^{i^T} & -\boldsymbol{F}^{i^T} \tilde{\boldsymbol{u}}^i \boldsymbol{G}^i \end{bmatrix} \begin{bmatrix} \delta \boldsymbol{R}^i \\ \delta \boldsymbol{\theta}^i \end{bmatrix} \tag{73}$$

or,

$$\delta W_e^i = \begin{bmatrix} \boldsymbol{F}_R^{i^T} & \boldsymbol{F}_\theta^{i^T} \end{bmatrix} \begin{bmatrix} \delta \boldsymbol{R}^i \\ \delta \boldsymbol{\theta}^i \end{bmatrix} \tag{74}$$

where $\boldsymbol{F}_R^{i^T} = \boldsymbol{F}^{i^T}$ and, $\boldsymbol{F}_\theta^{i^T} = -\boldsymbol{G}^{i^T} \tilde{\boldsymbol{u}}^{i^T} \boldsymbol{F}^i$. These terms are known as the generalized forces of the system, which in this specific example is formed by only one body.

Equation (74) may be physically interpreted in such a way that the force acting on an arbitrary point of the rigid body i is equipollent to another system located in the origin of the absolute reference system represented by the same force and the effect of that force associated with the orientation of the body reference system (Shabana, 2001, p. 415).

An additional presentation of the term $\boldsymbol{F}_\theta^{i^T}$ can be shown if the properties of the skew-symmetric matrices are considered. If $\tilde{\boldsymbol{u}}^i = -\tilde{\boldsymbol{u}}^{i^{\mathrm{T}}}$, then

$$\begin{aligned} \boldsymbol{F}_\theta^{i^T} &= \boldsymbol{G}^{i^T} \tilde{\boldsymbol{u}}^i \boldsymbol{F}^i \\ \boldsymbol{F}_\theta^{i^T} &= \boldsymbol{G}^{i^T} \left(\boldsymbol{u}^i \times \boldsymbol{F}^i \right) \end{aligned} \tag{75}$$

where the term $\boldsymbol{u}^i \times \boldsymbol{F}^i$ is the Cartesian moment resulting from the application of the force $\boldsymbol{F}^i$. If one calls this term $\boldsymbol{M}^i = \boldsymbol{u}^i \times \boldsymbol{F}^i$, equation (75) can be written as

$$\boldsymbol{F}_\theta^{i^T} = \boldsymbol{G}^{i^T} \boldsymbol{M}^i \tag{76}$$

It is important to expand the procedure previously used to include the effects of different forces acting on the different bodies of a multibody system. First, a case where several forces and moments act on a body will be discussed.

Let us consider that on the rigid body the forces $\boldsymbol{F}_1$, $\boldsymbol{F}_2$, ..., $\boldsymbol{F}_{nf}$ act respectively on the points whose position vectors are $\boldsymbol{r}_1$, $\boldsymbol{r}_2$, ..., $\boldsymbol{r}_{nf}$ and the set of moments $\boldsymbol{M}_1$, $\boldsymbol{M}_2$, ..., $\boldsymbol{M}_{n_m}$. The virtual work produced by these forces and moments is

$$\delta W_e = \boldsymbol{F}_1^T \delta \boldsymbol{r}_1 + \boldsymbol{F}_2^T \delta \boldsymbol{r}_2 + \cdots + \boldsymbol{F}_{nf}^T \delta \boldsymbol{r}_{nf} + (\boldsymbol{M}_1 + \boldsymbol{M}_2 + \cdots + \boldsymbol{M}_{n_m})^T \boldsymbol{G} \delta \boldsymbol{\theta} \tag{77}$$

Let us now consider the moment caused by the forces acting on a point different from the origin of the absolute reference system. The virtual work may be written as

$$\begin{aligned}\delta W_e = &\left(\boldsymbol{F}_1^T + \boldsymbol{F}_2^T + \cdots + \boldsymbol{F}_{nf}^T\right)\delta\boldsymbol{R} \\ &- \left(\boldsymbol{F}_1^T\tilde{\boldsymbol{u}}_1 + \boldsymbol{F}_2^T\tilde{\boldsymbol{u}}_2 + \cdots + \boldsymbol{F}_{nf}^T\tilde{\boldsymbol{u}}_{nf}\right)\boldsymbol{G}\delta\boldsymbol{\theta} \\ &+ \left(\boldsymbol{M}_1 + \boldsymbol{M}_2 + \cdots + \boldsymbol{M}_{n_m}\right)^T\boldsymbol{G}\delta\boldsymbol{\theta}\end{aligned} \tag{78}$$

The previous equation can be written as

$$\delta W_e = \left(\boldsymbol{Q}_e\right)_R^T\delta\boldsymbol{R} + \left(\boldsymbol{Q}_e\right)_\theta^T\delta\boldsymbol{\theta} \tag{79}$$

in which the terms $\left(\boldsymbol{Q}_e\right)_R$ and $\left(\boldsymbol{Q}_e\right)_\theta$ are

$$\left(\boldsymbol{Q}_e\right)_R = \sum_{j=1}^{nf}\boldsymbol{F}_j \tag{80}$$

$$\left(\boldsymbol{Q}_e\right)_\theta = \boldsymbol{G}^T\left[\sum_{k=1}^{n_m}\boldsymbol{M}_j + \sum_{j=1}^{nf}\left(\boldsymbol{u}_j\times\boldsymbol{F}_j\right)\right] \tag{81}$$

The vector of generalized forces for body i can be written as

$$\boldsymbol{Q}_e^i = \left[\begin{array}{cc}\left(\boldsymbol{Q}_e^i\right)_R & \left(\boldsymbol{Q}_e^i\right)_\theta\end{array}\right]^{\mathrm{T}} \tag{82}$$

The total vector of generalized forces can be formed by concatenating the vectors representing the generalized forces of each body:

$$\boldsymbol{Q}_e = \left[\begin{array}{cccc}\boldsymbol{Q}_e^1 & \boldsymbol{Q}_e^2 & \ldots & \boldsymbol{Q}_e^n\end{array}\right]^{\mathrm{T}} \tag{83}$$

3.7 Vector absorbing the terms that are quadratic in the velocities

The quadratic velocity vector appears as part of the formulation of the inertia forces generated by the rotation of the body. This vector was already introduced in equation (38),

and it can be written in a simplified form as

$$\boldsymbol{Q}_v^i = -\int_{V^i} \rho^i \begin{bmatrix} \boldsymbol{I} \\ -\bar{\boldsymbol{G}}^{i^T} \tilde{\bar{\boldsymbol{u}}}^{i^T} \boldsymbol{A}^{i^T} \end{bmatrix} \boldsymbol{a}_v^i dV^i \tag{84}$$

From the previous sections, it was also defined that the vector $\boldsymbol{a}_v^i$ is equal to $\left(\tilde{\boldsymbol{\omega}}^i\right)^2 \boldsymbol{u}^i - \tilde{\boldsymbol{u}}^i \dot{\boldsymbol{G}}^i \dot{\boldsymbol{\theta}}^i$. However, it can be also written that

$$\boldsymbol{a}_v^i = \boldsymbol{A}^i \left(\tilde{\bar{\boldsymbol{\omega}}}^i\right)^2 \bar{\boldsymbol{u}}^i - \boldsymbol{A}^i \tilde{\bar{\boldsymbol{u}}}^i \dot{\bar{\boldsymbol{G}}}^i \dot{\boldsymbol{\theta}}^i \tag{85}$$

Then, the quadratic velocity vector, can be expressed as a combination of two components,

$$\boldsymbol{Q}_v^i = \begin{bmatrix} \left(\boldsymbol{Q}_v^i\right)_R \\ \left(\boldsymbol{Q}_v^i\right)_\theta \end{bmatrix} \tag{86}$$

Where each one of the terms is

$$\left(\boldsymbol{Q}_v^i\right)_R = -\boldsymbol{A}^i \int_{V^i} \rho^i \left[\left(\tilde{\bar{\boldsymbol{\omega}}}^i\right)^2 \bar{\boldsymbol{u}}^i - \tilde{\bar{\boldsymbol{u}}}^i \dot{\bar{\boldsymbol{G}}}^i \dot{\boldsymbol{\theta}}^i \right] dV^i \tag{87}$$

$$\left(\boldsymbol{Q}_v^i\right)_\theta = \bar{\boldsymbol{G}}^{i^T} \int_{V^i} \rho^i \left[\tilde{\bar{\boldsymbol{u}}}^{i^T} \left(\tilde{\bar{\boldsymbol{\omega}}}^i\right)^2 \bar{\boldsymbol{u}}^i - \tilde{\bar{\boldsymbol{u}}}^{i^T} \tilde{\bar{\boldsymbol{u}}}^i \dot{\bar{\boldsymbol{G}}}^i \dot{\boldsymbol{\theta}}^i \right] dV^i \tag{88}$$

Furthermore, these vectors can be written as follows

$$\left(\boldsymbol{Q}_v^i\right)_R = -\boldsymbol{A}^i \left(\tilde{\bar{\boldsymbol{\omega}}}^i\right)^2 \left[\int_{V^i} \rho^i \bar{\boldsymbol{u}}^i dV^i \right] + \boldsymbol{A}^i \left[\int_{V^i} \rho^i \tilde{\bar{\boldsymbol{u}}}^i dV^i \right] \dot{\bar{\boldsymbol{G}}}^i \dot{\boldsymbol{\theta}}^i \tag{89}$$

$$\begin{aligned} \left(\boldsymbol{Q}_v^i\right)_\theta &= \bar{\boldsymbol{G}}^{i^T} \left[\int_{V^i} \rho^i \tilde{\bar{\boldsymbol{u}}}^{i^T} \left(\tilde{\bar{\boldsymbol{\omega}}}^i\right)^2 \bar{\boldsymbol{u}}^i dV^i \right] - \bar{\boldsymbol{G}}^{i^T} \bar{\boldsymbol{I}}_{\theta\theta}^i \dot{\bar{\boldsymbol{G}}}^i \dot{\boldsymbol{\theta}}^i \\ &= \bar{\boldsymbol{G}}^{i^T} \left[\bar{\boldsymbol{\omega}}^i \times \left(\bar{\boldsymbol{I}}_{\theta\theta}^i \bar{\boldsymbol{\omega}}^i \right) + \bar{\boldsymbol{I}}_{\theta\theta}^i \dot{\bar{\boldsymbol{G}}}^i \dot{\boldsymbol{\theta}}^i \right] \end{aligned} \tag{90}$$

It must be mentioned that in the case where the body coordinate system is attached to the center of mass of the body, an important simplification can be made. The terms

$\int_{V^i} \rho^i \bar{\boldsymbol{u}}^i dV^i$ and $\int_{V^i} \rho^i \tilde{\bar{\boldsymbol{u}}}^i dV^i$ are null, certifying a characteristic already mentioned in the formulation of the inertial forces:

$$\boldsymbol{m}^i_{R\theta} = \mathbf{0}, \quad \boldsymbol{m}^i_{\theta R} = \mathbf{0} \ \text{ and } \ \left(\boldsymbol{Q}^i_v\right)_R = \mathbf{0} \tag{91}$$

Similarly to the case of the generalized forces, the quadratic velocity vector for a multi-body system can be written as

$$\boldsymbol{Q}_v = \left[\begin{array}{cccc} \boldsymbol{Q}^1_v & \boldsymbol{Q}^2_v & \dots & \boldsymbol{Q}^n_v \end{array} \right]^{\mathrm{T}} \tag{92}$$

3.8 Generation of an additional equation to convert DAEs into ODEs in the Lagrange formulation and its stabilization methods

One of the techniques used to solve a set of differential algebraic equations is to convert them into a set of ordinary differential equations. This is accomplished by appending the second derivative with respect to time of the constraint equations (Flores et al., 2009, p. 306), to transform the equation of motion into an index-1 system of ODEs (Soellner, 2008, p. 53). During the process of integration of the equation of motion, it is possible to violate the geometrical constraints postulated for the model. This stems from the fact that during the derivation of the constraint equations, some magnitudes not dependent on time, such as length or angles, are lost, causing the bounds to be eliminated. The physical consequence of this effect is that the bodies ruled by these constraints might move away from or closer to each other without any control during the simulation process.

Several methods have been formulated in order to limit the violation of the constraints imposed. These methods include the following:

- Baumgarte stabilization method
- Integration of mixed systems of differential and algebraic equations
- Geometric projection stabilization approach
- Penalty-based stabilization techniques

The method used in the development of the model will be the Baumgarte stabilization method, which has been widely used and studied (Bauchau, 2010, p. 3).

To begin with the description of the transformation equation, it is necessary to recall the mathematical description of the constraint equations. This is shown in the next equation:

$$\boldsymbol{C}\left(\boldsymbol{q},t\right)=\boldsymbol{0} \tag{93}$$

When one derives equation (93) with respect to time twice, the following is obtained.

The first derivative is

$$\frac{d}{dt}\boldsymbol{C}\left(\boldsymbol{q},t\right)=\frac{\delta\boldsymbol{C}\left(\boldsymbol{q},t\right)}{\delta\boldsymbol{q}}\frac{d\boldsymbol{q}}{dt}+\frac{d\boldsymbol{C}\left(\boldsymbol{q},t\right)}{dt}=\boldsymbol{0} \tag{94}$$

$$\begin{aligned}\boldsymbol{C}_{\boldsymbol{q}}\dot{\boldsymbol{q}}+\boldsymbol{C}_{t}&=\boldsymbol{0}\\ \boldsymbol{C}_{\boldsymbol{q}}\dot{\boldsymbol{q}}&=-\boldsymbol{C}_{t}\end{aligned} \tag{95}$$

The second derivative is

$$\frac{d}{dt}\left(\boldsymbol{C}_{\boldsymbol{q}}\dot{\boldsymbol{q}}+\boldsymbol{C}_{t}\right)=\frac{d\boldsymbol{C}_{\boldsymbol{q}}\dot{\boldsymbol{q}}}{dt}+\frac{d\boldsymbol{C}_{t}}{dt} \tag{96}$$

$$\begin{aligned}\boldsymbol{C}_{\boldsymbol{q}}\ddot{\boldsymbol{q}}+\left(\boldsymbol{C}_{\boldsymbol{q}}\dot{\boldsymbol{q}}\right)_{\boldsymbol{q}}\dot{\boldsymbol{q}}+2\boldsymbol{C}_{\boldsymbol{q}t}\dot{\boldsymbol{q}}+\boldsymbol{C}_{tt}&=\boldsymbol{0}\\ \boldsymbol{C}_{\boldsymbol{q}}\ddot{\boldsymbol{q}}&=-\boldsymbol{C}_{tt}-\left(\boldsymbol{C}_{\boldsymbol{q}}\dot{\boldsymbol{q}}\right)_{\boldsymbol{q}}\dot{\boldsymbol{q}}-2\boldsymbol{C}_{\boldsymbol{q}t}\dot{\boldsymbol{q}}\end{aligned} \tag{97}$$

The last equation might be expressed in matrix form as a complement of the complete Lagrange equation:

$$\begin{bmatrix}\boldsymbol{C}_{\boldsymbol{q}} & \boldsymbol{0}\end{bmatrix}\begin{bmatrix}\ddot{\boldsymbol{q}}\\ \boldsymbol{\lambda}\end{bmatrix}=\boldsymbol{Q}_{d} \tag{98}$$

where $\boldsymbol{Q}_{d}$ is equal to $-\boldsymbol{C}_{tt}-\left(\boldsymbol{C}_{\boldsymbol{q}}\dot{\boldsymbol{q}}\right)_{\boldsymbol{q}}\dot{\boldsymbol{q}}-2\boldsymbol{C}_{\boldsymbol{q}t}\dot{\boldsymbol{q}}$.

The Baumgarte stabilization method proposes that the constraints be kept slightly violated before the correction actions can be effectively applied.

The application of the stabilization method consists of the substitution of equation (97) with the following relationship:

$$\begin{aligned} \ddot{\boldsymbol{C}} &= \boldsymbol{C_q}\ddot{\boldsymbol{q}} - \boldsymbol{Q}_d \\ \ddot{\boldsymbol{C}} + 2\alpha\dot{\boldsymbol{C}} + (\beta)^2\boldsymbol{C} &= \boldsymbol{0} \end{aligned} \tag{99}$$

where $\alpha > 0$ and $\beta \neq 0$ are the parameters of the stabilization method.

Equation (99) might be written in the form

$$\begin{aligned} \ddot{\boldsymbol{C}} &= \boldsymbol{C_q}\ddot{\boldsymbol{q}} - \boldsymbol{Q}_d \\ \boldsymbol{C_q}\ddot{\boldsymbol{q}} &= \boldsymbol{Q}_d - 2\alpha\left(\boldsymbol{C_q}\dot{\boldsymbol{q}} + \boldsymbol{C}_t\right) - (\beta)^2\boldsymbol{C} \end{aligned} \tag{100}$$

Then, the equation of motion that includes the Baumgarte stabilization method can be written in a general form:

$$\begin{bmatrix} \boldsymbol{M} & \boldsymbol{C}_{\boldsymbol{q}}^T \\ \boldsymbol{C_q} & \boldsymbol{0} \end{bmatrix} \begin{bmatrix} \ddot{\boldsymbol{q}} \\ \boldsymbol{\lambda} \end{bmatrix} = \begin{bmatrix} \boldsymbol{Q}_e + \boldsymbol{Q}_v \\ \boldsymbol{Q}_d - 2\alpha\left(\boldsymbol{C_q}\dot{\boldsymbol{q}} + \boldsymbol{C}_t\right) - (\beta)^2\boldsymbol{C} \end{bmatrix} \tag{101}$$

The selection methods of the values of the Baumgarte parameters have been studied widely, and there is no specific correct postulate to be used as a general guideline.

In this research, some experimental consideration will be made during the simulation of the skate skier. The following instructions will also be taken into account: both initial parameter values are positive and acquire the form

$$\alpha = \frac{1}{h} \text{ and } \beta = \frac{\sqrt{2}}{h}$$

where h is the time step chosen from the integration process (Flores et al., 2009, p. 306). Further variation to these values will be introduced to manually optimize the fulfillment of the constraint, but a large emphasis on the study of these parameters will not be made.

3.9 Application of Fourier series to fit discrete data

In the implementation of the ski-modeling process, forward dynamics will be used to obtain the response of the center of mass of the skier as a function of the forces exerted by the leg in each stride.

In order to use the discrete data generated from the measurement instruments, it is first

necessary to transform the data into continuous functions, with the purpose of making them smooth (up to the second derivative in the case of position data of body markers).

The procedure employed to achieve this is based on the use of the Fourier series, in which the set of data will be fitted by the application of equation (102).

$$y\left(\theta\right) = a_0 + \sum_{k=1}^{m} \left(a_k \sin\left(k\theta\right) + b_k \cos(k\theta)\right) \tag{102}$$

with

$$a_0 = \frac{\sum_{i=1}^{n} y_i}{n}$$

$$a_k = \frac{2\sum_{i=1}^{n} y_i \sin(k\theta_i)}{n}$$

$$b_k = \frac{2\sum_{i=1}^{n} y_i \cos(k\theta_i)}{n}$$

In the Fourier expansion, n is the quantity of pairs of data gathered; m is the total number of Fourier coefficients employed to perform the fitting; a_0, a_k and b_k are the Fourier series coefficients; y is the expected value of the unknown; and θ is the known variable usually referred to as the time step size of the capture process. These last two terms combine to form the set (y_1, θ_1), (y_2, θ_2), ..., (y_n, θ_n).

To have an idea of how good the fitted function is, the Pearson correlation coefficient r_{xy} is calculated in the way specified in equation (103). The closer the result of this coefficient is to the value of one indicates that the function used to calculate the expected values might be used to explain the behavior of the captured data.

$$r_{xy} = \frac{n\sum x_i y_i - \sum x_i \sum y_i}{\sqrt{n\sum x_i^2 - \left(\sum x_i\right)^2}\sqrt{n\sum y_i^2 - \left(\sum y_i\right)^2}} \tag{103}$$

4 FORMULATION OF EQUATION OF MOTION OF THE SKIER MODEL

In the development of a model of the skating technique, it is necessary to know and depict the coordination pattern of the characteristic movement that an athlete performs during the execution of the physical activity. One can make this description taking into account that this technique is similar to the one used in ice skating, in which the skater generates the forces by pushing in a sideward direction (Fintelman et al., 2011).

4.1 Description of the phases and key variables of the skating technique

The technique stroke may be divided into three basic phases: the glide, push-off and reposition phase (Fintelman et al., 2011) (see figure 14). During the glide phase, the whole body acquires translational movement while is supported over one leg. In the push-off phase, the ski moves sideward and, due to the grip and penetration of the ski in the snow, the skier generates the necessary force to produce translation movement of the whole body. In the reposition phase, the leg is retracted and prepares for the next cycle.

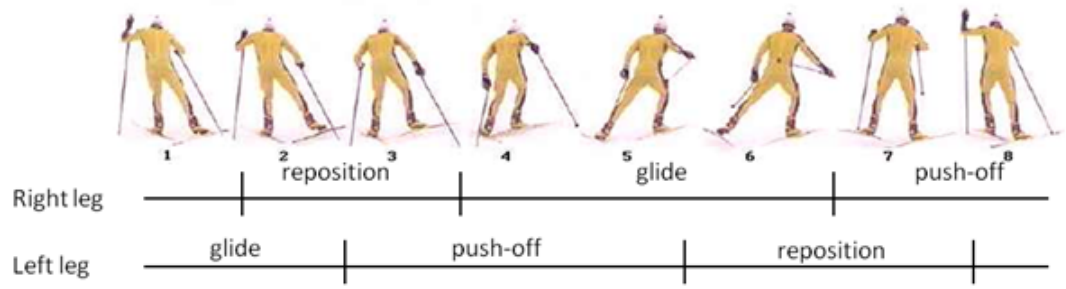

Figure 14. *Different phases of a stroke in skating technique of cross-country skiing (Rusko, 2003, p. 47).*

Moreover, some other physics variables have to be considered in addition to the ones applied to skating. These include friction, drag, gravity, force, mass, and velocity, and are further discussed below.

Friction: The cross-country style skier has a close relationship with the friction produced between the ski and the snow. Three cases of friction can be differentiated in cross-country skiing. When the skier is going downhill, the less the friction, the higher the speed and farther the distance achieved with less effort. However, when moving on a leveled plane or especially when making uphill progress, the skier needs the friction so that the skis can grip the snow, allowing the skier to push up and move the other ski forward.

Drag: Also called wind resistance, drag is produced by the rearrangement of the air

molecules located in front of the moving direction of the skier when the skier translates from one place to another. The effect of drag is basically seen in the speed of the skier. The higher the drag is, the more reduced the speed is.

Gravity: The effect of gravity is that of pulling bodies down to the ground. However, in skiing, gravity is not sufficient in itself to pull a skier downhill. This is due to the presence of friction in the ski - snow contact surface.

Force: The force generated in cross-country skiing may be produced in at least two ways. First, force is produced by the legs of the skier pushing the skis towards the snow; second, force is produced by the skier's use of poles.

Mass: The fact that the friction force generated by the skier is dependent on the mass of the person has introduced the use of external substances (such as waxes) into the sport to reduce the friction coefficient. Through the controlling of this coefficient, it is possible to level the playing field with regards to the influence of body weight in competitions.

Velocity: This parameter is affected by the frequency, length, and force of the stride (Duoos-Asche, 1984).

Next, some analysis of the key aspects of modeling is presented to reduce and constrain the complexity of the model. In table 1 below, a comparison of many points between a speed skating model (Fintelman et al., 2011) and a cross-country skate-skiing instructional video is presented.

Lastly, the selection of the methodology to formulate and find the solution for the equation of motion of the model will dictate its complexity, the relevant data needed as an input, and the results that can be acquired from it.

4.2 Description of the model of the skier

In order to begin the formulation of the model, it is necessary to postulate some assumptions which simplify the number of variables and phenomena to be taken into account.

Firstly, as observed in the instructional video and in the study made to model the speed skater, it can be seen that the consideration of the relative motions of the upper body with respect to the lower extremities in this first stage is irrelevant. It has been said that the upper body helps to balance the body of the athlete; however, its influence in the kinematical parameters of the movement is not yet clear. What is important to keep in mind is the effect of the position of the upper body when the air drag increases or when it

Table 1. Initial considerations for the development of the model

AREA	SKATING TECHNIQUES VIDEO (The Nordic Ski Project, 2006)	A SIMPLE 2-DIMENSIONAL MODEL OF SPEED SKATING WHICH MIMICS OBSERVED FORCES AND MOTIONS (Fintelman et al., 2011)
Ski-snow / skate-ice contact	There is no lateral slip. The ski edges are at the end of the glide to avoid slipping.	There is no lateral slip of the skate on the ice.
Level of the plane	The technique changes according to the steepness of the plane. Basically, the skating angles, the stride rate and the length of the glide are adjusted.	The travel is considered to be done on a leveled plane.
Direction of travel of the skies / skates	The skis travel in a straight line.	The skates travel in straight line.
Movement of the arms	The movement of the arms is neglected. They are used just to control the balance of the skier.	The movement of the arms is neglected.
Vertical motion of the center of mass of the skier	The vertical motion of the skier is not mentioned as an important parameter. It is mentioned that it is better to lower the center of gravity to gain a larger push-off force. The vertical movement follows the physiological pattern of the skier. During steep hills it is better to keep a constant height.	The vertical motion of the skater is neglected
Coefficient of friction		This value is found experimentally
Push-off force	This depends of the positioning of the body weight. The weight of the skier determines in part the push-off force.	The ground reaction force is due to the non- holonomic constraint of the skate.
Other remarks specifically mentioned in the reports	- The movement starts from the center line of the travel. - The normal skating angle should be about 45 degrees. In the video it is visible that the angle is not 45 degrees. - One should minimize body twisting. The body should face the direction of the travel. - It is important to maintain the symmetry of the movement in each side. - The glide and push off are combined.	

has to be considered as an opposing force to the movement of the skier.

An additional issue of the exclusion of the upper body from consideration is that the poles are not part of the model. This reduces the force-adding effect that the skier can use to increase velocity during the race.

Secondly, the model has to include the natural movement that the leg performs during the execution of the technique without modeling it exactly. To accomplish this, the lower body of the skier is modeled as a system formed by three bodies: one body that represents the ski, a second body that represents the lower part of the leg and the third body that represents the thigh.

Thirdly, the joint between the bodies is modeled as follows. The knee joint is modeled as a prismatic joint in order to reduce the input parameters needed to describe it without losing the generality of the movement. The joint between the lower leg and the ski is

modeled as a spherical joint resembling the movement of the human ankle. The joint between the ski and the ground will have five restrictions, allowing only the displacement of the ski on a straight path and on a leveled plane.

Lastly, instead of the use of a non-holonomic constraint to define the straight traveling of the ski, a simple holonomic constraint will be formulated to reduce the form in which the equation of motion is handled.

The model of the skier is depicted in figure 15 according to the previously mentioned assumptions.

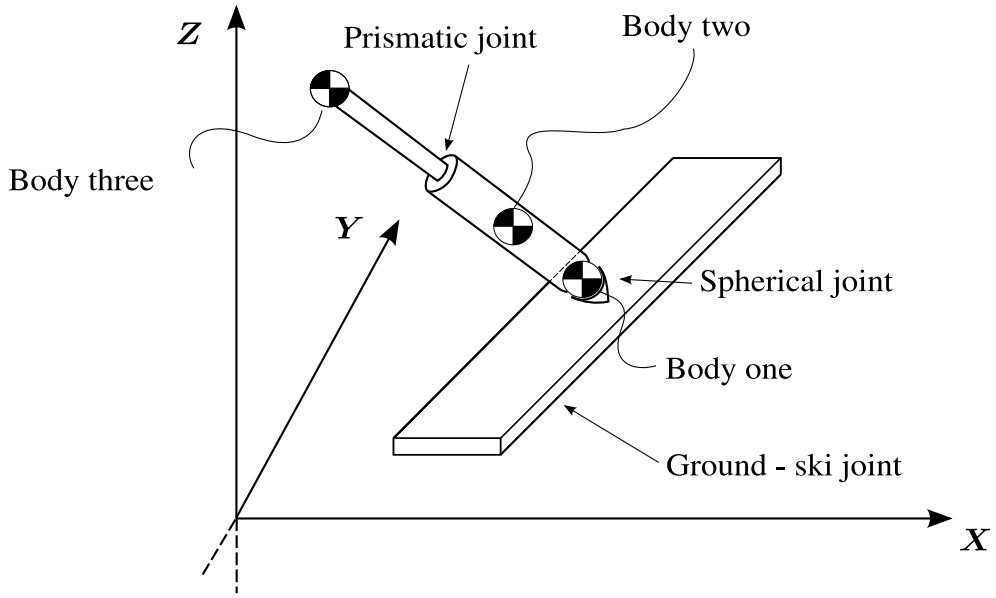

Figure 15. *Description of the multibody model of the skier.*

Now it is possible to start defining each one of the terms that conform to the equation of motion of the skier. These terms are formulated following the same order stated in chapter two. The first term formulated in the next section is the vector of generalized coordinates.

4.3 Vector of generalized coordinates of the skier model

In figure 16, the position and orientations of the body reference systems are indicated in order to formulate the position vector and their derived quantities.

As expressed in equation (10), the vector of generalized coordinates and its derivatives with respect to time of the skier model comprised of three bodies has the following form.

$$\boldsymbol{q} = \begin{bmatrix} \boldsymbol{q}_1 & \boldsymbol{q}_2 & \boldsymbol{q}_3 \end{bmatrix}^{\mathrm{T}} \tag{104}$$

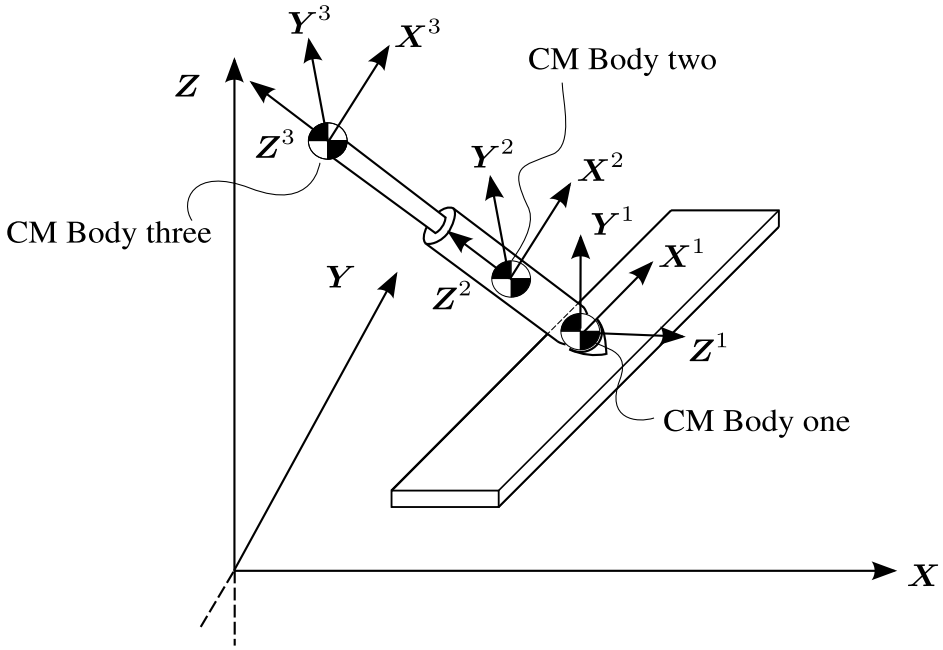

Figure 16. *Positioning and orientation of the body reference systems.*

$$\dot{\boldsymbol{q}} = \begin{bmatrix} \dot{\boldsymbol{q}}_1 & \dot{\boldsymbol{q}}_2 & \dot{\boldsymbol{q}}_3 \end{bmatrix}^{\mathrm{T}} \tag{105}$$

$$\ddot{\boldsymbol{q}} = \begin{bmatrix} \ddot{\boldsymbol{q}}_1 & \ddot{\boldsymbol{q}}_2 & \ddot{\boldsymbol{q}}_3 \end{bmatrix}^{\mathrm{T}} \tag{106}$$

Equation (104) and its first and second derivative with respect to time are shown next in expanded form.

$$\begin{aligned} \boldsymbol{q}_1 &= \begin{bmatrix} R_1^1 & R_2^1 & R_3^1 & \varphi^1 & \theta^1 & \psi^1 \end{bmatrix}^{\mathrm{T}} \\ \boldsymbol{q}_2 &= \begin{bmatrix} R_1^2 & R_2^2 & R_3^2 & \varphi^2 & \theta^2 & \psi^2 \end{bmatrix}^{\mathrm{T}} \\ \boldsymbol{q}_3 &= \begin{bmatrix} R_1^3 & R_2^3 & R_3^3 & \varphi^3 & \theta^3 & \psi^3 \end{bmatrix}^{\mathrm{T}} \end{aligned} \tag{107}$$

Here are the first derivatives with respect to time:

$$\begin{aligned} \dot{\boldsymbol{q}}_1 &= \begin{bmatrix} \dot{R}_1^1 & \dot{R}_2^1 & \dot{R}_3^1 & \dot{\varphi}^1 & \dot{\theta}^1 & \dot{\psi}^1 \end{bmatrix}^{\mathrm{T}} \\ \dot{\boldsymbol{q}}_2 &= \begin{bmatrix} \dot{R}_1^2 & \dot{R}_2^2 & \dot{R}_3^2 & \dot{\varphi}^2 & \dot{\theta}^2 & \dot{\psi}^2 \end{bmatrix}^{\mathrm{T}} \end{aligned} \tag{108}$$

$$\dot{\boldsymbol{q}}_3 = \begin{bmatrix} \dot{R}_1^3 & \dot{R}_2^3 & \dot{R}_3^3 & \dot{\varphi}^3 & \dot{\theta}^3 & \dot{\psi}^3 \end{bmatrix}^{\mathrm{T}}$$

And finally, here are the second derivatives with respect to time.

$$\begin{aligned} \ddot{\boldsymbol{q}}_1 &= \begin{bmatrix} \ddot{R}_1^1 & \ddot{R}_2^1 & \ddot{R}_3^1 & \ddot{\varphi}^1 & \ddot{\theta}^1 & \ddot{\psi}^1 \end{bmatrix}^{\mathrm{T}} \\ \ddot{\boldsymbol{q}}_2 &= \begin{bmatrix} \ddot{R}_1^2 & \ddot{R}_2^2 & \ddot{R}_3^2 & \ddot{\varphi}^2 & \ddot{\theta}^2 & \ddot{\psi}^2 \end{bmatrix}^{\mathrm{T}} \\ \ddot{\boldsymbol{q}}_3 &= \begin{bmatrix} \ddot{R}_1^3 & \ddot{R}_2^3 & \ddot{R}_3^3 & \ddot{\varphi}^3 & \ddot{\theta}^3 & \ddot{\psi}^3 \end{bmatrix}^{\mathrm{T}} \end{aligned} \tag{109}$$

4.4 Constraints and Jacobian matrix of the skier model

The constraint equations of the multibody system must be defined. First, a detailed analysis of the body joints is made to determine the geometric constraints. Then, further analysis is needed to formulate the driving constraints. Because of the previous statements made in the initial assumptions, it may be foreseen that kinematic constraints will not appear in the development of the model, facilitating the implementation of well-known integration methods, such as the Runge - Kutta high-order integration routine.

The first joint to be analyzed will be the ski - ground joint. The ski is considered as the first body of the system. The following facts will be taken into account during the formulation of the geometric restrictions:

- The ski travels on a leveled plane.
- The direction of the travel of the ski does not change with respect to time.
- The orientation of the body reference system does not change during the active phase of the ski.

For use as a reference, the definition of the ground constraints is expressed in equation (110) (Shabana, 2001, p. 136).

$$\boldsymbol{q}^{Ground} - \boldsymbol{c} = \boldsymbol{0} \tag{110}$$

Equation (110) might be interpreted as the invariance of the body reference system with respect to a set of constant initial values. The first resultant constraint equation representing the constant position level of the ski on the z axis is written in equation (111).

$$C1 = R_3^1 - c_3^1 = 0 \tag{111}$$

where c_3^1, is the initial value of the body reference system origin on the z axis.

The assumed fact that the ski travels following a line orientated φ^1 degrees from the global $\boldsymbol{X}$ axis, provides the necessary information to formulate the second constraint. Figure 17 shows a graphical representation of the previous statement.

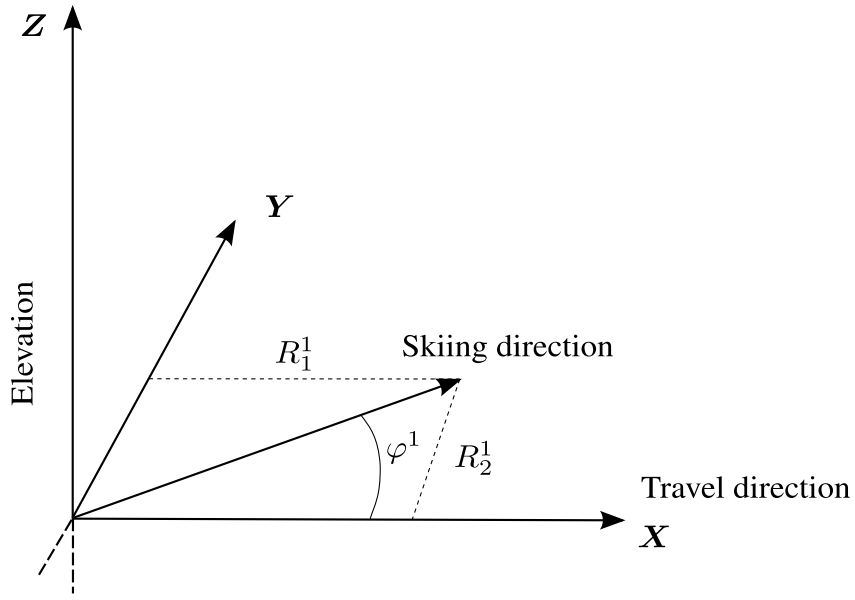

Figure 17. *Geometry of the active phase of the ski.*

The relationship between the x and y components of the origin of the body reference system may be completely described by the tangent trigonometric function.

$$\tan\varphi^1 = \frac{R_2^1}{R_1^1}$$

$$C2 = R_1^1 \sin\varphi^1 - R_2^1 \cos\varphi^1 = 0 \tag{112}$$

To represent the constant orientation of the body one reference system, the approach used to formulate the constraint equation $C1$ is used.

As the Euler angles representing the orientation at any moment of the body reference system do not change during the active phase of the ski, it may be said that the difference of the value of these angles with respect to a set of constant values $(c_{\varphi^1},\, c_{\theta^1},\, c_{\psi^1})$ does not change. These constraints are presented in equations (113) to (115).

$$C3 = \varphi^1 - c_{\varphi^1} = 0 \tag{113}$$

$$C4 = \theta^1 - c_{\theta^1} = 0 \tag{114}$$

$$C5 = \psi^1 - c_{\psi^1} = 0 \tag{115}$$

In constraint equations $C4$ and $C5$, the value of the constants used for this model is zero due to the condition of traveling on a leveled plane. In the remaining $C3$ equation, the angle ϕ^1 describes one of the most important parameters in the execution of the technique.

The values that this angle may acquire range from 0 to approximately 70 degrees. These values are mainly influenced by the steepness of the plane and the stride rate that the skier would need to apply to gain more velocity. For example, in steeper planes, the use of angles near 70 degrees would help the skier to overcome the lack of friction in pushing forward.

The second joint to be described is the spherical joint formed by the ski and second body. To define the constraint equations of this joint, figure 18 will be used as a visual aid in the development of the restrictions.

When one analyzes the relative degrees of freedom that the spherical constraint allows between the two bodies, it can be concluded that because of the configuration of the joint, only the relative translation is constrained, leaving only three degrees of freedom of relative rotation (Korkealaakso, 2009, p. 33,39).

The necessary condition to be fulfilled in the spherical joint is that two points, P^1 and P^2 on bodies 1 and 2 respectively, coincide throughout the whole motion. This condition may be written as

$$\boldsymbol{C}(\boldsymbol{q}^1, \boldsymbol{q}^2) = \boldsymbol{r}_P^1 - \boldsymbol{r}_P^2 = \boldsymbol{0} \tag{116}$$

When one applies equation (116) to the present case, then the constraint equation may be re-written as

$$\boldsymbol{C}(\boldsymbol{q}^1, \boldsymbol{q}^2) = \boldsymbol{R}^1 + \boldsymbol{A}^1 \bar{\boldsymbol{u}}_P^1 - \boldsymbol{R}^2 - \boldsymbol{A}^2 \bar{\boldsymbol{u}}_P^2 = \boldsymbol{0} \tag{117}$$

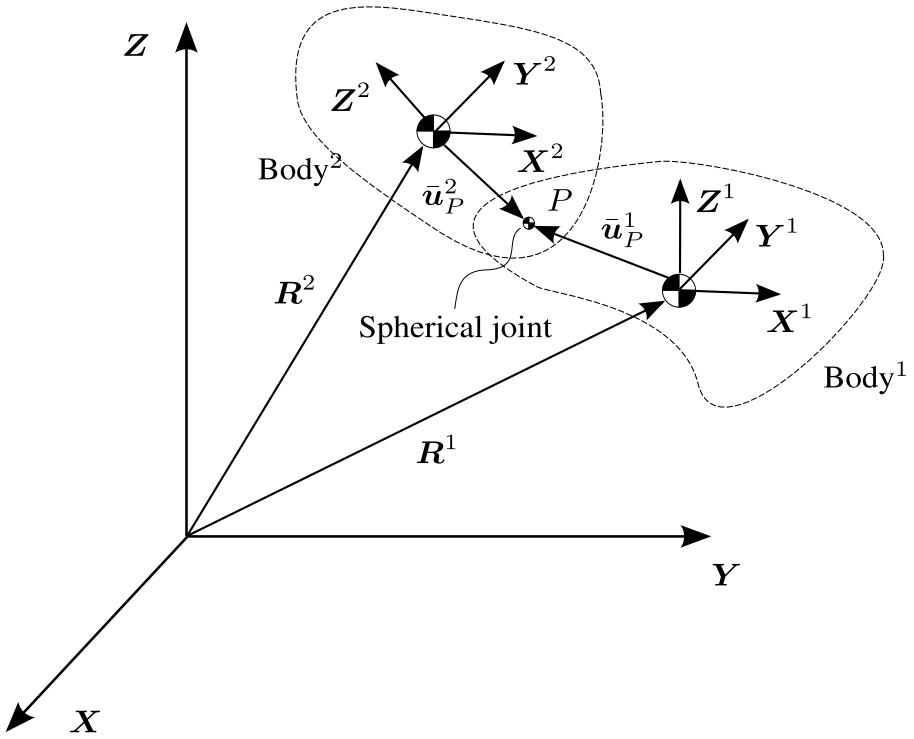

Figure 18. *Geometry of a spherical joint in three-dimensions.*

As equation (117) is a vector equation based on the generalized coordinates referring to the position of the point P, it leads to a set of three scalar equations related to the restriction of relative translation in three dimensions.

Substituting each one of the terms in equation (117) with their respective symbolic value related to the skier model, it is possible to formulate the constraint equations that will completely define this joint. In equation (118), a matrix representation of the constraint equations of the spherical joint is presented followed by the formulation of the scalar equations derived from it.

$$\begin{aligned}\begin{bmatrix} C6 \\ C7 \\ C8 \end{bmatrix} = &\begin{bmatrix} R_1^1 \\ R_2^1 \\ R_3^1 \end{bmatrix} + \begin{bmatrix} A_{11}^1 & A_{12}^1 & A_{13}^1 \\ A_{21}^1 & A_{22}^1 & A_{23}^1 \\ A_{31}^1 & A_{32}^1 & A_{33}^1 \end{bmatrix} \begin{bmatrix} \bar{r}_{P1}^1 \\ \bar{r}_{P2}^1 \\ \bar{r}_{P3}^1 \end{bmatrix} \\ &- \begin{bmatrix} R_1^2 \\ R_2^2 \\ R_3^2 \end{bmatrix} - \begin{bmatrix} A_{11}^2 & A_{12}^2 & A_{13}^2 \\ A_{21}^2 & A_{22}^2 & A_{23}^2 \\ A_{31}^2 & A_{32}^2 & A_{33}^2 \end{bmatrix} \begin{bmatrix} \bar{r}_{P1}^2 \\ \bar{r}_{P2}^2 \\ \bar{r}_{P3}^2 \end{bmatrix}\end{aligned} \tag{118}$$

The terms inside the transformation matrices are abbreviated according to their positions on the matrix. This simplification is made in order to limit the size of the formulas to the

workspace of the report and to facilitate the interpretation and reading of them.

The transformation matrix and the position vector of the point in the local coordinate system are calculated as presented previously in equations (8) and (3). Then, in order to fully describe the constraint equations for the spherical joint of the model, it is necessary to determine the specific data related to the origins of the body reference systems and the location of the spherical joint.

The origin of the body reference system of body 1 is located in the center of the ski, and it coincides with the position of the joint. The origin of the body reference system of the second body is located in the middle of the segment representing this body. In accordance with this, the following relationships may be established:

$$\boldsymbol{r}_P^1 = \begin{bmatrix} R_1^1 \\ R_2^1 \\ R_3^1 \end{bmatrix} + \begin{bmatrix} A_{11}^1 & A_{12}^1 & A_{13}^1 \\ A_{21}^1 & A_{22}^1 & A_{23}^1 \\ A_{31}^1 & A_{32}^1 & A_{33}^1 \end{bmatrix} \begin{bmatrix} 0 \\ 0 \\ 0 \end{bmatrix} = \begin{bmatrix} R_1^1 \\ R_2^1 \\ R_3^1 \end{bmatrix} \tag{119}$$

$$\boldsymbol{r}_P^2 = \begin{bmatrix} R_1^2 \\ R_2^2 \\ R_3^2 \end{bmatrix} + \begin{bmatrix} A_{11}^2 & A_{12}^2 & A_{13}^2 \\ A_{21}^2 & A_{22}^2 & A_{23}^2 \\ A_{31}^2 & A_{32}^2 & A_{33}^2 \end{bmatrix} \begin{bmatrix} 0 \\ 0 \\ l_1 \end{bmatrix} = \begin{bmatrix} R_1^2 \\ R_2^2 \\ R_3^2 \end{bmatrix} + \begin{bmatrix} l_1 A_{13}^2 \\ l_1 A_{23}^2 \\ l_1 A_{33}^2 \end{bmatrix} \tag{120}$$

where l_1 is the distance from the origin of the reference system of the second body to the joint measured about the $\boldsymbol{Z}^2$ local axis. Equation (121) shows the construction of the constraint equations.

$$\begin{bmatrix} C6 \\ C7 \\ C8 \end{bmatrix} = \begin{bmatrix} R_1^1 \\ R_2^1 \\ R_3^1 \end{bmatrix} - \begin{bmatrix} R_1^2 \\ R_2^2 \\ R_3^2 \end{bmatrix} - \begin{bmatrix} l_1 A_{13}^2 \\ l_1 A_{23}^2 \\ l_1 A_{33}^2 \end{bmatrix} \tag{121}$$

$$C6 = R_1^1 - R_1^2 - l_1 A_{13}^2 \tag{122}$$

$$C7 = R_2^1 - R_2^2 - l_1 A_{23}^2 \tag{123}$$

$$C8 = R_3^1 - R_3^2 - l_1 A_{33}^2 \tag{124}$$

The last joint to be described is the prismatic joint present between the second and third body. Figure 19 shows the configuration used to formulate the constraint equations.

A prismatic joint in three dimensions has one DOF and five relative movement restrictions

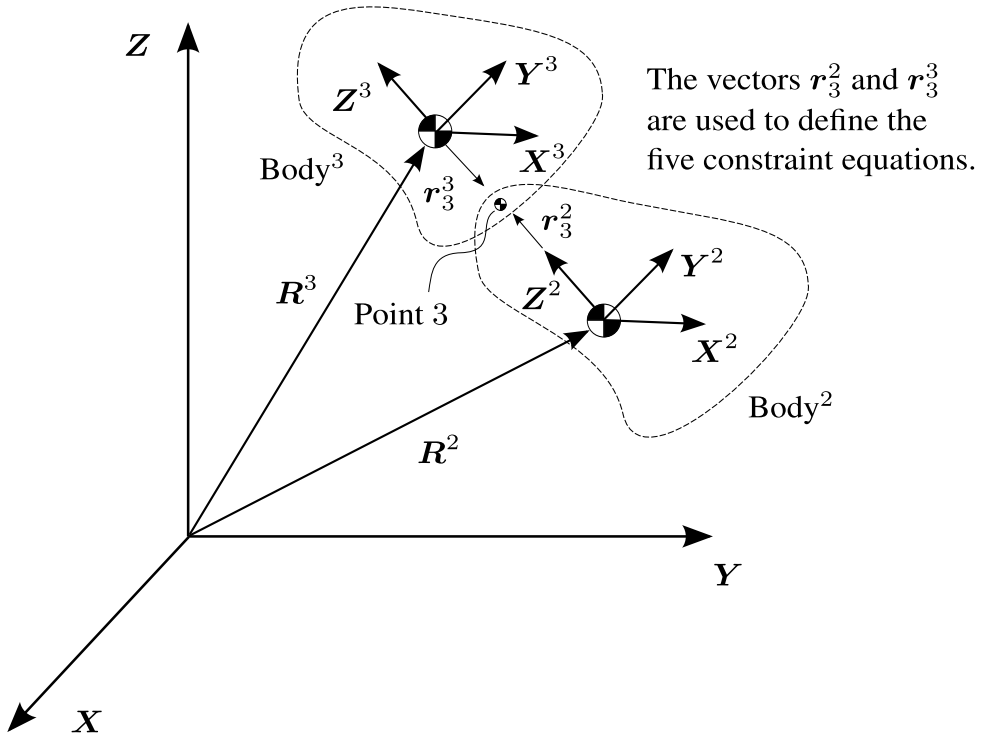

Figure 19. *Considerations in the development of the constraint equations of the prismatic joint.*

comprised of two translations and three rotations. The use of this joint in the model is convenient for describing the vertical motion of the center of mass of the skier. Indeed, this effect has not been considered in an analogous research project carried out for the speed skater, but it is a very important consideration because of the close relationship with the force exerted by the skier during the push off phase.

The five constraint equations that arise from this joint are based on the following assumptions:

- The vectors $\boldsymbol{r}_3^2$ and $\boldsymbol{r}_3^3$ are parallel and they are aligned.
- There is no relative orientation change between the two bodies.

To express these considerations in a mathematical form, the properties of the cross and scalar product of the vector will be used.

To specify the parallelism of these two vectors, let us refer to figure 20 to formulate this condition.

Two vectors are said to be parallel if the result of their cross product is the zero vector. This is written in equation (125) in its traditional representation.

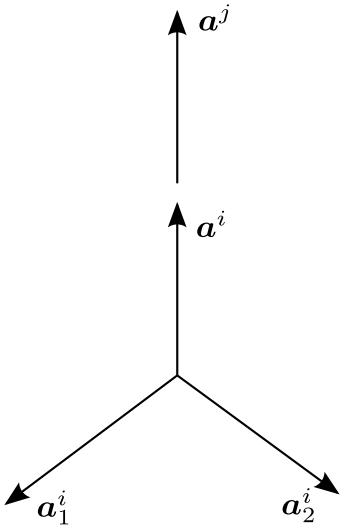

Figure 20. *Perpendiculars and parallel vectors (Shabana, 2001, p.51).*

$$\boldsymbol{a}^i \times \boldsymbol{a}^j = \mathbf{0} \tag{125}$$

When this vector equation is calculated, three scalar equations appear. Two of these equations are dependent, but the identification of these is a task requiring some additional steps that will not be introduced in this work. In order to avoid the additional process, another approach to set the condition of parallelism is used.

The new approach leads to two scalar equations which automatically neglect the third dependent equation, thus resulting in no need for further analysis. Equation (126) shows the parallelism of two vectors using the dot product.

When one applies the dot product to demonstrate the parallelism condition, it is necessary to make use of additional construction vectors. These vectors are constructed perpendicular to the vectors to be proven in the mentioned condition. Refer to vectors $\boldsymbol{a}_1^i$ and $\boldsymbol{a}_2^i$ in figure 20.

$$\begin{aligned} \boldsymbol{a}_1^{iT}\boldsymbol{a}^j &= 0 \\ \boldsymbol{a}_2^{iT}\boldsymbol{a}^j &= 0 \end{aligned} \tag{126}$$

Given that vectors $\boldsymbol{a}_1^i$ and $\boldsymbol{a}_2^i$ are by definition constructed perpendicular to the body vector $\boldsymbol{a}^i$, the fulfillment of the conditions presented in equation (126) is enough to guarantee the parallelism condition between $\boldsymbol{a}^i$ and $\boldsymbol{a}^j$.

As mentioned in the assumptions to formulate the prismatic joint in three dimensions, the vectors to be proven parallels in the model are $\boldsymbol{r}_3^2$ and $\boldsymbol{r}_3^3$. These vectors are defined in bodies two and three respectively and are aligned with the local $\boldsymbol{Z}$ axis of each body.

The perpendicular construction vectors will be taken from the unit vectors aligned with the second body local axis $\boldsymbol{X}^2$ and $\boldsymbol{Y}^2$.

The definition of the first two constraint equations related to this joint starts with the formulation of the body and construction vectors. Equation (127) shows the vector related to the second body.

$$\boldsymbol{r}_3^2 = \boldsymbol{R}^2 + \boldsymbol{A}^2\bar{\boldsymbol{r}}_z^2 - \boldsymbol{R}^2$$

$$\boldsymbol{r}_3^2 = \begin{bmatrix} A_{11}^2 & A_{12}^2 & A_{13}^2 \\ A_{21}^2 & A_{22}^2 & A_{23}^2 \\ A_{31}^2 & A_{32}^2 & A_{33}^2 \end{bmatrix} \begin{bmatrix} 0 \\ 0 \\ 1 \end{bmatrix}$$

$$\boldsymbol{r}_3^2 = \begin{bmatrix} A_{13}^2 \\ A_{23}^2 \\ A_{33}^2 \end{bmatrix} \tag{127}$$

where $\boldsymbol{r}_3^2$ is the vector related to the second body, $\boldsymbol{A}^2$ is the transformation matrix of the second body coordinate system, and $\boldsymbol{r}_z^2$ is the unit local vector aligned with the local $\boldsymbol{Z}^2$ axis.

In a similar form, equation (128) shows the vector related to the third body.

$$\boldsymbol{r}_3^3 = \boldsymbol{R}^3 + \boldsymbol{A}^3\bar{\boldsymbol{r}}_z^3 - \boldsymbol{R}^3$$

$$\boldsymbol{r}_3^3 = \begin{bmatrix} A_{11}^3 & A_{12}^3 & A_{13}^3 \\ A_{21}^3 & A_{22}^3 & A_{23}^3 \\ A_{31}^3 & A_{32}^3 & A_{33}^3 \end{bmatrix} \begin{bmatrix} 0 \\ 0 \\ 1 \end{bmatrix}$$

$$\boldsymbol{r}_3^3 = \begin{bmatrix} A_{13}^3 \\ A_{23}^3 \\ A_{33}^3 \end{bmatrix} \tag{128}$$

where $\boldsymbol{r}_3^3$ is the vector related to the second body, $\boldsymbol{A}^3$ is the transformation matrix of the third body coordinate system, and $\boldsymbol{r}_z^3$ is the unit local vector aligned with the local $\boldsymbol{Z}^3$ axis.

In equations (129) and (131), the perpendicular vectors are used to apply the second approach to demonstrate the parallelism condition. One can do this by using the properties of the scalar product of two vectors.

$$\boldsymbol{r}_1^2 = \boldsymbol{R}^2 + \boldsymbol{A}^2\bar{\boldsymbol{r}}_x^2 - \boldsymbol{R}^2$$

$$\boldsymbol{r}_1^2 = \begin{bmatrix} A_{11}^2 & A_{12}^2 & A_{13}^2 \\ A_{21}^2 & A_{22}^2 & A_{23}^2 \\ A_{31}^2 & A_{32}^2 & A_{33}^2 \end{bmatrix} \begin{bmatrix} 1 \\ 0 \\ 0 \end{bmatrix}$$

$$\boldsymbol{r}_1^2 = \begin{bmatrix} A_{11}^2 \\ A_{21}^2 \\ A_{31}^2 \end{bmatrix} \tag{129}$$

where $\boldsymbol{r}_1^2$ is a perpendicular construction vector related to the second body and $\bar{\boldsymbol{r}}_x^2$ is the unit local vector aligned with the local $\boldsymbol{X}^2$ axis.

$$\boldsymbol{r}_2^2 = \boldsymbol{R}^2 + \boldsymbol{A}^2\bar{\boldsymbol{r}}_y^2 - \boldsymbol{R}^2 \tag{130}$$

$$\boldsymbol{r}_2^2 = \begin{bmatrix} A_{11}^2 & A_{12}^2 & A_{13}^2 \\ A_{21}^2 & A_{22}^2 & A_{23}^2 \\ A_{31}^2 & A_{32}^2 & A_{33}^2 \end{bmatrix} \begin{bmatrix} 0 \\ 1 \\ 0 \end{bmatrix}$$

$$\boldsymbol{r}_2^2 = \begin{bmatrix} A_{12}^2 \\ A_{22}^2 \\ A_{32}^2 \end{bmatrix} \tag{131}$$

in which $\boldsymbol{r}_2^2$ is a perpendicular construction vector related to the second body and $\bar{\boldsymbol{r}}_y^2$ is the unit local vector aligned with the local $\boldsymbol{Y}^2$ axis.

With the application of equation (126) to the specific conditions of the model, the follow-

ing relationships may be written.

$$\boldsymbol{r}_1^{2T}\boldsymbol{r}_3^3 = \begin{bmatrix} A_{11}^2 & A_{21}^2 & A_{31}^2 \end{bmatrix} \begin{bmatrix} A_{13}^3 \\ A_{23}^3 \\ A_{33}^3 \end{bmatrix} = \mathbf{0} \tag{132}$$

$$\boldsymbol{r}_2^{2T}\boldsymbol{r}_3^3 = \begin{bmatrix} A_{12}^2 & A_{22}^2 & A_{32}^2 \end{bmatrix} \begin{bmatrix} A_{13}^3 \\ A_{23}^3 \\ A_{33}^3 \end{bmatrix} = \mathbf{0} \tag{133}$$

In equations (132) and (133), the results of the matrix multiplication for each case are presented. These equations become constraint equations $C9$ and $C10$, representing the parallelism condition of the two body vectors positioned in the second and third body.

$$\begin{aligned} C9 &= \boldsymbol{r}_1^{2T}\boldsymbol{r}_3^3 \\ C9 &= A_{11}^2A_{13}^3 + A_{21}^2A_{23}^3 + A_{31}^2A_{33}^3 = 0 \end{aligned} \tag{134}$$

$$\begin{aligned} C10 &= \boldsymbol{r}_2^{2T}\boldsymbol{r}_3^3 \\ C10 &= A_{12}^2A_{13}^3 + A_{22}^2A_{23}^3 + A_{32}^2A_{33}^3 = 0 \end{aligned} \tag{135}$$

The second condition to be considered when one formulates the geometric constraints of this joint is the expression related to the alignment of the vectors $\boldsymbol{r}_3^2$ and $\boldsymbol{r}_3^3$. In order to achieve this, the conditions of parallelism are inspected on a vector formed by two points, one from each body vector. If the conditions of parallelism are fulfilled, it means that the two body vectors are aligned. Figure 21 depicts the construction of the vectors to prove the alignment of the body vectors.

Because the origins of the local reference systems are used to formulate the body vectors to describe the joint, these two points are employed to form the vector to support the inspection of the alignment between $\boldsymbol{r}_3^2$ and $\boldsymbol{r}_3^3$.

$$\boldsymbol{r}_{Alig} = \boldsymbol{R}^2 - \boldsymbol{R}^3$$

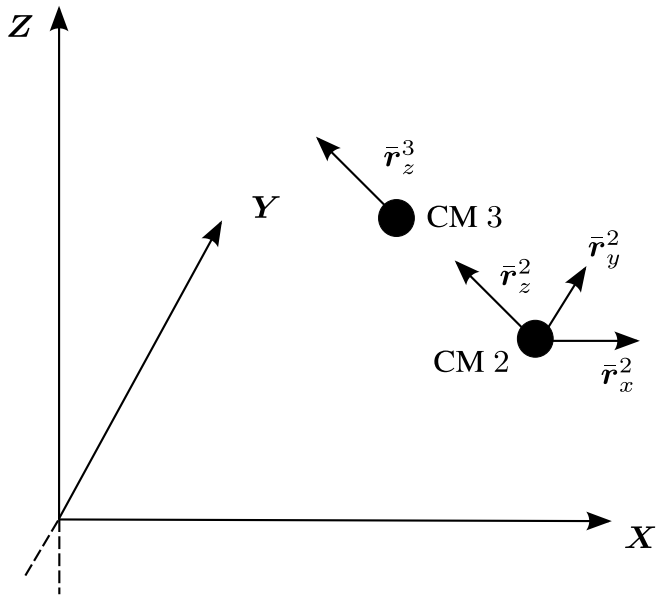

Figure 21. *Visual representation of the vectors used to prove the alignment of the body vectors.*

$$\boldsymbol{r}_{Alig} = \begin{bmatrix} R_1^2 \\ R_2^2 \\ R_3^2 \end{bmatrix} - \begin{bmatrix} R_1^3 \\ R_2^3 \\ R_3^3 \end{bmatrix} = \begin{bmatrix} R_1^2 - R_1^3 \\ R_2^2 - R_2^3 \\ R_3^2 - R_3^3 \end{bmatrix} \tag{136}$$

With the application of the conditions of parallelism to vector $\boldsymbol{r}_{Alig}$, the following expressions and equations are presented.

$$C11 = \boldsymbol{r}_1^{2T}\boldsymbol{r}_{Alig} = \begin{bmatrix} A_{11}^2 & A_{21}^2 & A_{31}^2 \end{bmatrix} \begin{bmatrix} R_1^2 - R_1^3 \\ R_2^2 - R_2^3 \\ R_3^2 - R_3^3 \end{bmatrix} \tag{137}$$

$$C11 = A_{11}^2\left(R_1^2 - R_1^3\right) + A_{21}^2\left(R_2^2 - R_2^3\right) + A_{31}^2\left(R_3^2 - R_3^3\right) = 0 \tag{138}$$

$$C12 = \boldsymbol{r}_2^{2T}\boldsymbol{r}_{Alig} = \begin{bmatrix} A_{12}^2 & A_{22}^2 & A_{32}^2 \end{bmatrix} \begin{bmatrix} R_1^2 - R_1^3 \\ R_2^2 - R_2^3 \\ R_3^2 - R_3^3 \end{bmatrix} \tag{139}$$

$$C12 = A_{12}^2\left(R_1^2 - R_1^3\right) + A_{22}^2\left(R_2^2 - R_2^3\right) + A_{32}^2\left(R_3^2 - R_3^3\right) = 0 \tag{140}$$

The condition of no relative rotation between the bodies is the last condition to finally define the constraints that this joint generates. To postulate this condition, an additional vector $\boldsymbol{r}_1^3$ has to be constructed perpendicular to the body vector on the third body. This vector is shown previously in figure 21.

$$\boldsymbol{r}_1^3 = \boldsymbol{R}^3 + \boldsymbol{A}^3 \bar{\boldsymbol{r}}_x^3 - \boldsymbol{R}^3$$

In the last expression, $\bar{\boldsymbol{r}}_x^3$ is the unit local vector aligned with the local x axis.

$$\boldsymbol{r}_1^3 = \begin{bmatrix} A_{11}^3 & A_{12}^3 & A_{13}^3 \\ A_{21}^3 & A_{22}^3 & A_{23}^3 \\ A_{31}^3 & A_{32}^3 & A_{33}^3 \end{bmatrix} \begin{bmatrix} 1 \\ 0 \\ 0 \end{bmatrix}$$

$$\boldsymbol{r}_1^3 = \begin{bmatrix} A_{11}^3 \\ A_{21}^3 \\ A_{31}^3 \end{bmatrix} \tag{141}$$

The non-relative rotation condition is guaranteed if the previous vector stays perpendicular to the vector $\boldsymbol{r}_2^2$ of the second body. In mathematical notation, this condition may be written in the form presented in equation (142).

$$C13 = \boldsymbol{r}_2^{2T} \boldsymbol{r}_1^3 = \begin{bmatrix} A_{12}^2 & A_{22}^2 & A_{32}^2 \end{bmatrix} \begin{bmatrix} A_{11}^3 \\ A_{21}^3 \\ A_{31}^3 \end{bmatrix} \tag{142}$$

$$C13 = A_{12}^2 A_{11}^3 + A_{22}^2 A_{21}^3 + A_{32}^2 A_{31}^3 = 0$$

Up to this point, the model contains 18 (generalized coordinates) -13 (constraints) $=$ 5 degrees of freedom. It is necessary to specify additional constraints controlling the physiological parameters of leg extension and range of angles.

To restrict the extension of the leg during the active phase, the following length constraint is imposed. See figure 22 for an adequate interpretation of this constraint.

This geometric constraint may be written in terms of the position of the origin of the local reference system located in the third and first bodies (see figure 23).

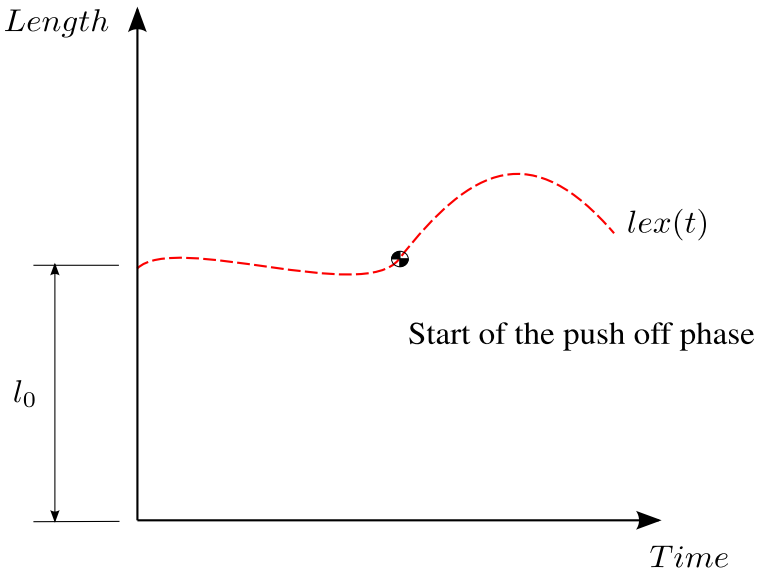

Figure 22. *Constraint of the leg extension imposed in the model.*

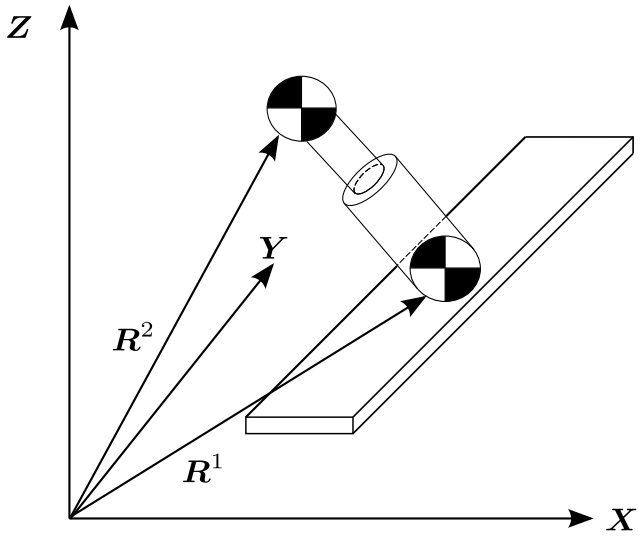

Figure 23. *Formulation of the leg extension.*

$$lex\left(t\right) = \left|\boldsymbol{R}_3 - \boldsymbol{R}_1\right|$$

$$lex\left(t\right) = \left\| \begin{bmatrix} R_1^3 \\ R_2^3 \\ R_3^3 \end{bmatrix} - \begin{bmatrix} R_1^1 \\ R_2^1 \\ R_3^1 \end{bmatrix} \right\| = \sqrt{\left(R_1^3 - R_1^1\right)^2 + \left(R_2^3 - R_2^1\right)^2 + \left(R_3^3 - R_3^1\right)^2} \tag{143}$$

Then, the constraint equation that represents the desire leg extension may be written as

$$C14 = \sqrt{\left(R_1^3 - R_1^1\right)^2 + \left(R_2^3 - R_2^1\right)^2 + \left(R_3^3 - R_3^1\right)^2} - lex\left(t\right) = 0 \qquad (144)$$

The next constraints to be imposed are those related to the angles that the leg covers while performing the movement during the active phase. This task can be achieved by using different approaches, one of which is constraint of the relative orientation of the second and first body with respect to each other.

In this particular case, one can impose the constraints by formulating the trajectory of the origin of the local reference system of the second body. Figure 24 shows the description of this constraint.

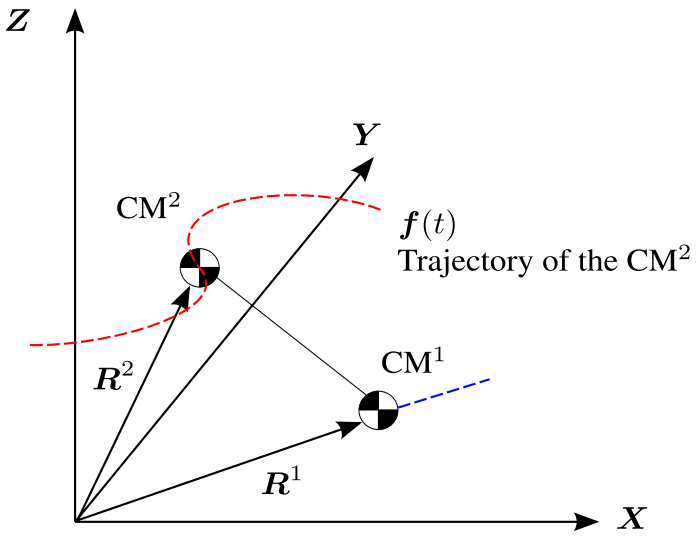

Figure 24. *Constraint movement of the origin of the local reference system of the second body.*

This condition imposes three additional constraints to the model. These are shown in the next equations.

$$\begin{aligned} C15 &= R_1^2 - f_1\left(t\right) \\ C16 &= R_2^2 - f_2\left(t\right) \\ C17 &= R_3^2 - f_3\left(t\right) \end{aligned} \qquad (145)$$

in which $f_1\left(t\right)$, $f_2\left(t\right)$ and $f_3\left(t\right)$ are respectively the $X(t)$, $Y(t)$ and $Z(t)$ components of the trajectory $\boldsymbol{f}\left(t\right)$ that follows this point.

The previously defined constraints of the model can be summarized as presented in tables 2, 3, 4, and 5 Along with this summary, a physical interpretation of each constraint is added to provide a realistic meaning to the mathematical formulations employed.

Table 2. Ski-ground constraints

CONSTRAINT EQUATION	PHYSICAL INTERPRETATION
$C1 = R_3^1 - c_3^1 = 0$	Movement of the ski on a leveled plane
$C2 = R_1^1 \sin\phi^1 - R_2^1 \cos\phi^1 = 0$	Movement of the ski on a line orientated φ^1 with respect to the global Y axis of the absolute X-Y plane
$C3 = \phi^1 - c_{\phi^1} = 0$	Constant orientation of the body reference system referred to the φ^1 Euler angle
$C4 = \theta^1 - c_{\theta^1} = 0$	Constant orientation of the body reference system referred to the θ^1 Euler angle
$C5 = \psi^1 - c_{\psi^1} = 0$	Constant orientation of the body reference system referred to the ψ^1 Euler angle .

Table 3. Ski-lower leg constraints

CONSTRAINT EQUATION	PHYSICAL INTERPRETATION
$C6 = R_1^1 - R_1^2 - l_1 A_{13}^2$	Restriction of relative translation along the X global axis
$C7 = R_2^1 - R_2^2 - l_1 A_{23}^2$	Restriction of relative translation along the Y global axis
$C8 = R_3^1 - R_3^2 - l_1 A_{33}^2$	Restriction of relative translation along the Z global axis

After one finds the constraint equations of the system, the next step is to formulate the Jacobian matrix as previously depicted in equation (19).

The constraint equations of the system are collected in the vector of constraint equations. See equation (146). After the differentiation of this vector with respect to the generalized coordinates is performed, the resulting final form is presented in appendix B.

$$\boldsymbol{C} = \begin{bmatrix} C_1 & C_2 & C_3 & C_4 & C_5 & C_6 & C_7 & C_8 & C_9 & C_{10} \\ C_{11} & C_{12} & C_{13} & C_{14} & C_{15} & C_{16} & C_{17} & & & \end{bmatrix}^{\mathrm{T}} \tag{146}$$

Table 4. Lower - upper leg constraints

CONSTRAINT EQUATION	PHYSICAL INTERPRETATION
$C9 = A^2_{11}A^3_{13} + A^2_{21}A^3_{23} + A^2_{31}A^3_{33} = 0$	Condition of parallelism of the two body vectors
$C10 = A^2_{12}A^3_{13} + A^2_{22}A^3_{23} + A^2_{32}A^3_{33} = 0$	Condition of parallelism of the two body vectors
$C11 = A^2_{11}\left(R^2_1 - R^3_1\right) + A^2_{21}\left(R^2_2 - R^3_2\right) + A^2_{31}\left(R^2_3 - R^3_3\right) = 0$	Condition of alignment of the axes of the bodies
$C12 = A^2_{12}\left(R^2_1 - R^3_1\right) + A^2_{22}\left(R^2_2 - R^3_2\right) + A^2_{32}\left(R^2_3 - R^3_3\right) = 0$	Condition of alignment of the axes of the bodies
$C13 = A^2_{12}A^3_{11} + A^2_{22}A^3_{21} + A^2_{32}A^3_{31} = 0$	Restriction of relative rotation between the two bodies affected by the joint

Table 5. Kinematic rheonomic constraints

CONSTRAINT EQUATION	PHYSICAL INTERPRETATION
$C14 = \sqrt{\left(R^3_1 - R^1_1\right)^2 + \left(R^3_2 - R^1_2\right)^2 + \left(R^3_3 - R^1_3\right)^2} - lex\left(t\right) = 0$	Restriction of the leg extension during the active phase
$C15 = R^2_1 - f_1\left(t\right)$	Restriction of the movement of the second body with respect to the ski X global direction
$C16 = R^2_2 - f_2\left(t\right)$	Restriction of the movement of the second body with respect to the ski Y global direction
$C17 = R^2_3 - f_3\left(t\right)$	Restriction of the movement of the second body with respect to the ski Z global direction

4.5 Mass matrix of the skier model

The complete mass stiffness matrix of the multibody system is constructed out of three individual body matrices, one for each body present in the model.

In the following steps, the individual mass matrices of the bodies are formulated using equations (31), (41), (42), (44), and (45).

Mass matrix of body 1:

The first body corresponds to the ski itself and is modeled as a parallelepiped volume. The moments and products of inertia of this common shape can be found ready tabulated and are collected into the next equations (Huston, 1990, p. 204). Figure 25 shows how

the inertia moments are described according to the local orientation axes.

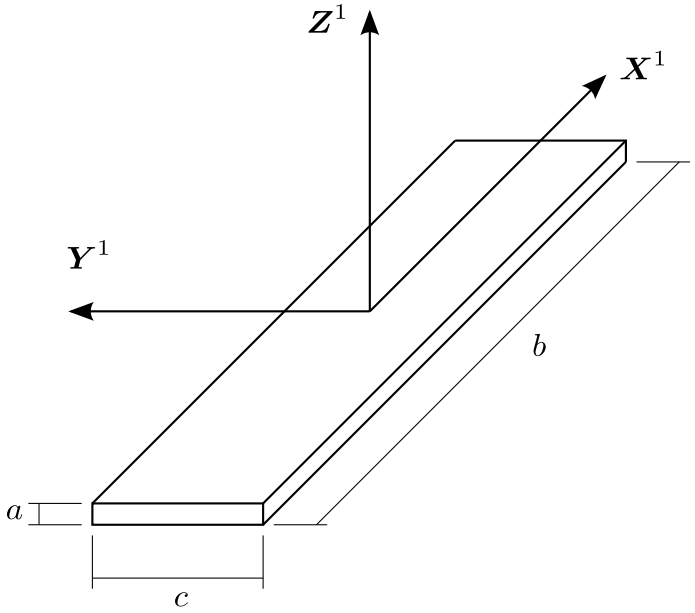

Figure 25. *Assumed geometry of the ski.*

$$i_{xx}^1 = \frac{m^1}{12}\left(a^2 + c^2\right) \tag{147}$$

$$i_{yy}^1 = \frac{m^1}{12}\left(a^2 + b^2\right) \tag{148}$$

$$i_{zz}^1 = \frac{m^1}{12}\left(b^2 + c^2\right) \tag{149}$$

The substitution of equations (147), (148) and (149) into equation (45) yields

$$\bar{\boldsymbol{I}}_{\theta\theta}^1 = \begin{bmatrix} \frac{m^1}{12}\left(a^2 + c^2\right) & & \\ & \frac{m^1}{12}\left(a^2 + b^2\right) & \\ & & \frac{m^1}{12}\left(b^2 + c^2\right) \end{bmatrix} \tag{150}$$

The products of inertia are zero for in case due to the specific alignments of the body reference axis.

For the first body, equation (31) takes the following form:

$$\bar{\boldsymbol{G}}^1 = \begin{bmatrix} \sin\theta^1 \sin\psi^1 & \cos\psi^1 & 0 \\ \sin\theta^1 \cos\psi^1 & -\sin\psi^1 & 0 \\ \cos\theta^1 & 0 & 1 \end{bmatrix} \tag{151}$$

With the substitution of the results of equations (150) and (151) into equation (44), the value of $\boldsymbol{m}^1_{\theta\theta}$ it is found. The values of the moments of inertia will remain denoted as I^1_{xx}, I^1_{yy} and I^1_{zz} to facilitate the handling of the matrices.

$$\boldsymbol{m}^1_{\theta\theta} = \begin{bmatrix} \sin\theta^1 \sin\psi^1 & \sin\theta^1 \cos\psi^1 & \cos\theta^1 \\ \cos\psi^1 & -\sin\psi^1 & 0 \\ 0 & 0 & 1 \end{bmatrix} \begin{bmatrix} I^1_{xx} & & \\ & I^1_{yy} & \\ & & I^1_{zz} \end{bmatrix} \begin{bmatrix} \sin\theta^1 \sin\psi^1 & \cos\psi^1 & 0 \\ \sin\theta^1 \cos\psi^1 & -\sin\psi^1 & 0 \\ \cos\theta^1 & 0 & 1 \end{bmatrix} \tag{152}$$

$$\boldsymbol{m}^1_{\theta\theta} = \begin{bmatrix} m^1_{\theta\theta_{1,1}} & m^1_{\theta\theta_{1,2}} & m^1_{\theta\theta_{1,3}} \\ & m^1_{\theta\theta_{2,2}} & 0 \\ symmetric & & m^1_{\theta\theta_{3,3}} \end{bmatrix} \tag{153}$$

The remaining term for the final formulation of the mass matrix of the first body is a diagonal 3×3 matrix with the mass of the ski as the diagonal term.

$$\boldsymbol{m}^1_{RR} = \begin{bmatrix} m^1 & & \\ & m^1 & \\ & & m^1 \end{bmatrix} \tag{154}$$

Then, the final reduced form of the mass matrix of the first body can be presented such as in the following equation. For a more detailed presentation of these mass matrices and those related to the second and third body, please refer to appendix B.

$$\boldsymbol{M}^1 = \begin{bmatrix} \boldsymbol{m}^1_{RR} & \\ & \boldsymbol{m}^1_{\theta\theta} \end{bmatrix} \tag{155}$$

Mass matrices of the second and third bodies:

The second and third bodies are considered to be slender rods. The center of masses of the bodies are located in their geometrical center. See figure 26.

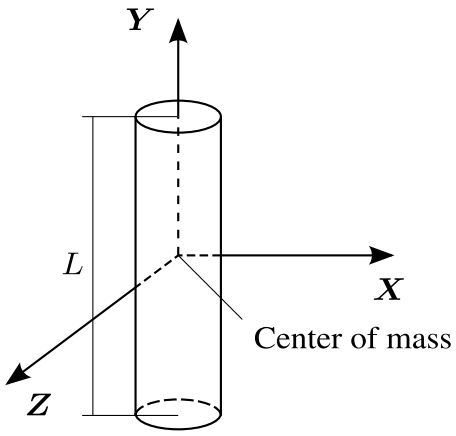

Figure 26. *Description of moments of inertia in the second and third body.*

The value of the moments of inertia for these two bodies is presented in the next equations. Similarly to the case presented for the first body, the axes are set in such a way that the products of inertia of both bodies become zero. Also, the procedure developed for the mass matrix of the first body is used for the remaining cases.

The second body equations are

$$i_{xx}^2 = i_{yy}^2 = \frac{m^2}{12}(L_2)^2 \tag{156}$$

$$i_{zz}^2 = 0 \tag{157}$$

And the third body equations are

$$i_{xx}^3 = i_{yy}^3 = \frac{m^3}{12}(L_3)^2 \tag{158}$$

$$i_{zz}^3 = 0 \tag{159}$$

Then, the $\bar{\boldsymbol{G}}^2$ and $\bar{\boldsymbol{G}}^3$ matrices are

$$\bar{\boldsymbol{G}}^2 = \begin{bmatrix} \sin\theta^2 \sin\psi^2 & \cos\psi^2 & 0 \\ \sin\theta^2 \cos\psi^2 & -\sin\psi^2 & 0 \\ \cos\theta^2 & 0 & 1 \end{bmatrix} \tag{160}$$

$$\bar{\boldsymbol{G}}^3 = \begin{bmatrix} \sin\theta^3 \sin\psi^3 & \cos\psi^3 & 0 \\ \sin\theta^3 \cos\psi^3 & -\sin\psi^3 & 0 \\ \cos\theta^3 & 0 & 1 \end{bmatrix} \tag{161}$$

The component related to the rotation of the body mass matrix is

$$\boldsymbol{m}^2_{\theta\theta} = \begin{bmatrix} \sin\theta^2 \sin\psi^2 & \sin\theta^2 \cos\psi^2 & \cos\theta^2 \\ \cos\psi^2 & -\sin\psi^2 & 0 \\ 0 & 0 & 1 \end{bmatrix} \begin{bmatrix} I^2_{xx} & & \\ & I^2_{yy} & \\ & & 0 \end{bmatrix} \begin{bmatrix} \sin\theta^2 \sin\psi^2 & \cos\psi^2 & 0 \\ \sin\theta^2 \cos\psi^2 & -\sin\psi^2 & 0 \\ \cos\theta^1 & 0 & 1 \end{bmatrix} \tag{162}$$

$$\boldsymbol{m}^3_{\theta\theta} = \begin{bmatrix} \sin\theta^3 \sin\psi^3 & \sin\theta^3 \cos\psi^3 & \cos\theta^3 \\ \cos\psi^3 & -\sin\psi^3 & 0 \\ 0 & 0 & 1 \end{bmatrix} \begin{bmatrix} I^3_{xx} & & \\ & I^3_{yy} & \\ & & 0 \end{bmatrix} \begin{bmatrix} \sin\theta^3 \sin\psi^3 & \cos\psi^3 & 0 \\ \sin\theta^3 \cos\psi^3 & -\sin\psi^3 & 0 \\ \cos\theta^3 & 0 & 1 \end{bmatrix} \tag{163}$$

The matrices related to the translation of the bodies and the individual mass matrices are

$$\boldsymbol{m}^2_{RR} = \begin{bmatrix} m^2 & & \\ & m^2 & \\ & & m^2 \end{bmatrix} \tag{164}$$

$$\boldsymbol{m}^3_{RR} = \begin{bmatrix} m^3 & & \\ & m^3 & \\ & & m^3 \end{bmatrix} \tag{165}$$

$$\boldsymbol{M}^2 = \begin{bmatrix} \boldsymbol{m}^2_{RR} & \\ & \boldsymbol{m}^2_{\theta\theta} \end{bmatrix} \tag{166}$$

$$\boldsymbol{M}^3 = \begin{bmatrix} \boldsymbol{m}^3_{RR} & \\ & \boldsymbol{m}^3_{\theta\theta} \end{bmatrix} \tag{167}$$

The mass matrix of the model can be then presented as in equation (168):

$$\boldsymbol{M} = \begin{bmatrix} \boldsymbol{M}^1 & & \\ & \boldsymbol{M}^2 & \\ & & \boldsymbol{M}^3 \end{bmatrix} \tag{168}$$

4.6 Vector of Lagrange multipliers of the skier model

When one takes into account that the number of constraint equations applied to the model is 17 (13 scleronomic constraints and four rheonomic constraints), the vector of Lagrange multipliers applicable to the case may be formulated as

$$\boldsymbol{\lambda} = \begin{bmatrix} \lambda_1 & \lambda_2 & \lambda_3 & \lambda_4 & \lambda_5 & \lambda_6 & \lambda_7 & \lambda_8 & \lambda_9 & \lambda_{10} \\ \lambda_{11} & \lambda_{12} & \lambda_{13} & \lambda_{14} & \lambda_{15} & \lambda_{16} & \lambda_{17} & & & \end{bmatrix}^{\mathrm{T}} \tag{169}$$

where each Lagrange multiplier corresponds to its equivalent constraint in the order presented in the vector of constraint equations.

4.7 Vector of generalized forces of applied to the model

The forces originating from the work performed by the leg during the push-off phase are shown in figure 27. These forces act during a period of the gliding time of the opposite leg. They are considered to be applied to the center of mass (CM) of the skier and are located in both the third body and the first body (in the case of the friction force) of the model.

With the expansion of equation (83) for the multibody system applied to the skier, where the number of bodies is 3, the form of the vector of generalized forces due to the pushing force, air drag, and friction force can be formulated as follows below.

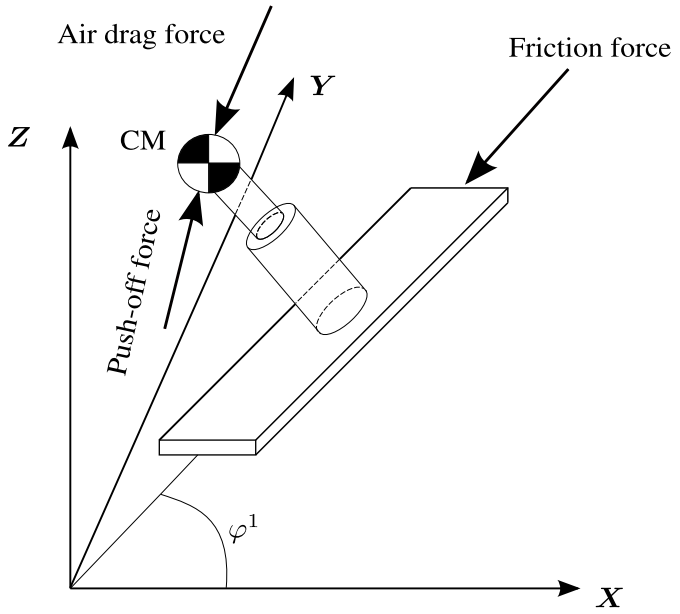

Figure 27. *External forces applied to the system.*

For the first body (representing the ski), the only force applied is the friction force generated by the contact between the snow and the ski. One important characteristic of this force is that it is oriented at all moments along the axis $\boldsymbol{Y}^1$. The virtual work produced by this force on the first body is

$$\delta W_e^1 = \left(\boldsymbol{Q}_e^1\right)_R^T \delta \boldsymbol{R} + \left(\boldsymbol{Q}_e^1\right)_\theta^T \delta \boldsymbol{\theta} \tag{170}$$

The force presented during the formulation of the procedure to determine the virtual work has already been defined in the absolute frame of reference. In the case of the skier, it is convenient to present this force in the local reference system, which means that the additional transformation $\boldsymbol{F}_{friction} = \boldsymbol{A}^1 \bar{\boldsymbol{F}}^1_{friction}$ must be applied. It is possible to find the value of $\boldsymbol{A}^1$ from the previous sections.

$$\boldsymbol{F}_{friction} = \boldsymbol{A}^1 \bar{\boldsymbol{F}}^1_{friction} \tag{171}$$

$$\boldsymbol{F}_{friction} = \begin{bmatrix} \cos\phi^1 & \sin\phi^1 & 0 \\ -\sin\phi^1 & \cos\phi^1 & 0 \\ 0 & 0 & 1 \end{bmatrix} \begin{bmatrix} 0 \\ -F^1_{friction} \\ 0 \end{bmatrix} \tag{172}$$

$$\boldsymbol{F}_{friction} = \begin{bmatrix} -F^1_{friction} \sin\phi^1 \\ -F^1_{friction} \cos\phi^1 \\ 0 \end{bmatrix} \tag{173}$$

$$\left(\mathbf{Q}^1_e\right)_R = - \begin{bmatrix} F^1_{friction} \sin\phi^1 \\ F^1_{friction} \cos\phi^1 \\ 0 \end{bmatrix} \tag{174}$$

The moment caused by this force may be written as

$$\left(\boldsymbol{Q}^1_e\right)_\theta = \boldsymbol{G}^{1^T} \left[\boldsymbol{u}_{friction} \times \boldsymbol{F}^1_{friction}\right] \tag{175}$$

in which, after the substitution of each one of the terms,

$$\left(\boldsymbol{Q}^1_e\right)_\theta = \begin{bmatrix} 0 & 0 & 1 \\ \cos\phi^1 & \sin\phi^1 & 0 \\ \sin\phi^1 \sin\theta^1 & -\cos\phi^1 \sin\theta^1 & \cos\theta^1 \end{bmatrix} \left[\begin{bmatrix} \begin{bmatrix} \cos\phi^1 & \sin\phi^1 & 0 \\ -\sin\phi^1 & \cos\phi^1 & 0 \\ 0 & 0 & 1 \end{bmatrix} \begin{bmatrix} 0 \\ 0 \\ 0 \end{bmatrix} \\ \times \begin{bmatrix} -F^1_{friction} \sin\phi^1 \\ -F^1_{friction} \cos\phi^1 \\ 0 \end{bmatrix} \end{bmatrix} \right] \tag{176}$$

It can be noticed in equation (176) that the point of application of the force on the ski is considered to be at the origin of this body. Then, the value of the moment produced by this force can be presented as in the next equation.

$$\left(\boldsymbol{Q}^1_e\right)_\theta = \begin{bmatrix} 0 & 0 & 1 \\ \cos\phi^1 & \sin\phi^1 & 0 \\ 0 & 0 & 1 \end{bmatrix} \begin{bmatrix} 0 \\ 0 \\ 0 \end{bmatrix} = \begin{bmatrix} 0 \\ 0 \\ 0 \end{bmatrix} \tag{177}$$

The vector of generalized forces corresponding to the friction force can be presented in its final form as

$$\boldsymbol{Q}^{1^T}_e = \begin{bmatrix} -F^1_{friction} \sin\phi^1 & -F^1_{friction} \cos\phi^1 & 0 & 0 & 0 & 0 \end{bmatrix} \tag{178}$$

The third body is the next body where forces can be found in the skier model. These forces, as mentioned before, originate from the action of the pushing of the leg and the air drag. The formulation of the generalized force due to these forces is shown next; it follows the procedure applied to the first body.

The push-off force and the air drag force are considered to be applied in the origin of the local reference system of the third body. This consideration is important in order to formulate the moment produced by these forces. The next equation shows the generalized forces related to the translation produced by the forces.

$$\left(\boldsymbol{Q}_e^3\right)_R = \sum_{j=1}^{2} \boldsymbol{F}_j^3 = \boldsymbol{F}_{push}^3 + \boldsymbol{F}_{air}^3 \tag{179}$$

$$\left(\boldsymbol{Q}_e^3\right)_R = \boldsymbol{A}^3 \left(\bar{\boldsymbol{F}}_{push}^3 + \bar{\boldsymbol{F}}_{air}^3\right) \tag{180}$$

The orientation of the force due to air drag is considered to be aligned with the axis $\boldsymbol{Y}^3$ in the third body. The push-off force, is considered to have components in the $\boldsymbol{X}^3$, $\boldsymbol{Y}^3$ and $\boldsymbol{Z}^3$ axis.

The orientation of the force due to the air drag is considered to be aligned with the axis $\boldsymbol{Y}^3$ in the third body and for the case of the push off force, the consideration made is that this force has components in the $\boldsymbol{X}^3$, $\boldsymbol{Y}^3$ and $\boldsymbol{Z}^3$ axis.

In the case of the component $\left(\boldsymbol{Q}_e^3\right)_\theta$

$$\left(\boldsymbol{Q}_e^3\right)_\theta = \begin{bmatrix} 0 \\ 0 \\ 0 \end{bmatrix} \tag{181}$$

This result is similar to that of the first body because of the selection of origin of the local reference system as an application point for the forces.

The total vector of generalized forces consists of the following form:

$$\boldsymbol{Q}_e = \begin{bmatrix} \boldsymbol{Q}_e^1 & \boldsymbol{Q}_e^2 & \boldsymbol{Q}_e^3 \end{bmatrix}^T \tag{182}$$

where the vector $\boldsymbol{Q}_e^2$ is equal to **zero** because no forces are applied to this body.

4.8 Vector absorbing the terms that are quadratic in the velocities.

The following body velocity vectors are found through the application of the previous definitions to each one of the bodies forming the model.

In the case of the quadratic velocity vector of the ski (first body), the origin of the body reference system coincides with the center of mass, yielding the following form of the quadratic velocity vector.

$$\boldsymbol{Q}_v^1 = \begin{bmatrix} \mathbf{0} \\ \left(\boldsymbol{Q}_v^1\right)_\theta \end{bmatrix} = \begin{bmatrix} \mathbf{0} \\ \bar{\boldsymbol{G}}^{1^T}\left[\bar{\boldsymbol{\omega}}^1 \times \left(\bar{\boldsymbol{I}}_{\theta\theta}^1 \bar{\boldsymbol{\omega}}^1\right) + \bar{\boldsymbol{I}}_{\theta\theta}^1 \dot{\bar{\boldsymbol{G}}}^1 \dot{\boldsymbol{\theta}}^1\right] \end{bmatrix} \tag{183}$$

The coincidence of the origin of the local reference body with the center of mass also serves to simplify the form of the quadratic velocity vector of the second and third bodies.

$$\boldsymbol{Q}_v^2 = \begin{bmatrix} \mathbf{0} \\ \left(\boldsymbol{Q}_v^2\right)_\theta \end{bmatrix} = \begin{bmatrix} \mathbf{0} \\ \bar{\boldsymbol{G}}^{2^T}\left[\bar{\boldsymbol{\omega}}^2 \times \left(\bar{\boldsymbol{I}}_{\theta\theta}^2 \bar{\boldsymbol{\omega}}^2\right) + \bar{\boldsymbol{I}}_{\theta\theta}^2 \dot{\bar{\boldsymbol{G}}}^2 \dot{\boldsymbol{\theta}}^2\right] \end{bmatrix} \tag{184}$$

$$\boldsymbol{Q}_v^3 = \begin{bmatrix} \mathbf{0} \\ \left(\boldsymbol{Q}_v^3\right)_\theta \end{bmatrix} = \begin{bmatrix} \mathbf{0} \\ \bar{\boldsymbol{G}}^{3^T}\left[\bar{\boldsymbol{\omega}}^3 \times \left(\bar{\boldsymbol{I}}_{\theta\theta}^3 \bar{\boldsymbol{\omega}}^3\right) + \bar{\boldsymbol{I}}_{\theta\theta}^3 \dot{\bar{\boldsymbol{G}}}^3 \dot{\boldsymbol{\theta}}^3\right] \end{bmatrix} \tag{185}$$

Finally, the quadratic velocity vector may be written in its complete form as

$$\boldsymbol{Q}_v = \begin{bmatrix} \boldsymbol{Q}_v^1 & \boldsymbol{Q}_v^2 & \boldsymbol{Q}_v^3 \end{bmatrix}^T \tag{186}$$

5 MODELING RESULTS

In this section, the results of the integration of the equation of motion (EOM) of the skier will be presented along with graphs showing the fulfillment of the rheonomic and scleronomic constraints respectively imposed on defined trajectories and joints in the model.

As previously mentioned in the introduction, after the EOM of the skier was defined, the resulting equation was coded into Matlab (Moler, 2004). The resultant positions and velocities were obtained by performing the integration of the set of ODE and were then plotted in order to visualize the influence of some key variables on the execution of the skating technique by the skier. However, before some of these results can be produced, the values must be defined of certain physiological variables and dimensional characteristics needed as inputs for the model. These variables include the following.

- Limits of the phase time length and skating angle
- Leg retraction and extension vs. time
- Push-off force function vs. time, friction force and air drag
- Movement of the origin of the local reference system of the second body

Part of the set of variables presented define the rheonomic constraints needed to completely formulate the movement of the skier. For example, the movement of the leg during the active phase will establish the path followed by it. This path is needed as an input in the constraint equations $C9$, $C10$ and $C11$.

Other types of parameters, such as variables representing the mass of the skier and the measurement of the parts of the lower and upper leg, need to be included in the equations formulated for the skier. These three variables are shown in the next table.

Table 6. Mass and leg dimension of the skate skier

Variable	Value
Mass (Kg)	75
Upper leg (m)	0.5
Lower leg (m)	0.4

5.1 Definition of the cases to be analyzed in terms of phase time and skating angle.

In this section, a group of cases will be formulated in order to simulate the effect that the change in the phase time and skating angle have on the velocity of the skier. To

accomplish this, the following values for these variables are proposed. See table 7.

Table 7. Definition of the changing variables

Phase Time (sec)	Skating angle (deg)
0.5	70
1	50
2	30

For example, in the first case, the skier has phase times of 0.5 seconds with a skating angle of 70 degrees. Although this combination is not usually found when a skier executes the technique on leveled planes, it will help one to understand the results of the model.

5.2 Leg retraction and extension versus time.

During the active phase of the leg, it is neither fully retracted at the beginning of the phase nor fully extended when applying the push-off force for the next phase. The leg extension vs. time will thus be assumed to increase linearly from a value of 50% to ultimately 90% of the total length at the moment before changing to the other leg. In figure 28, this movement is described with the CM of the skier located vertically in line with the center of the ski.

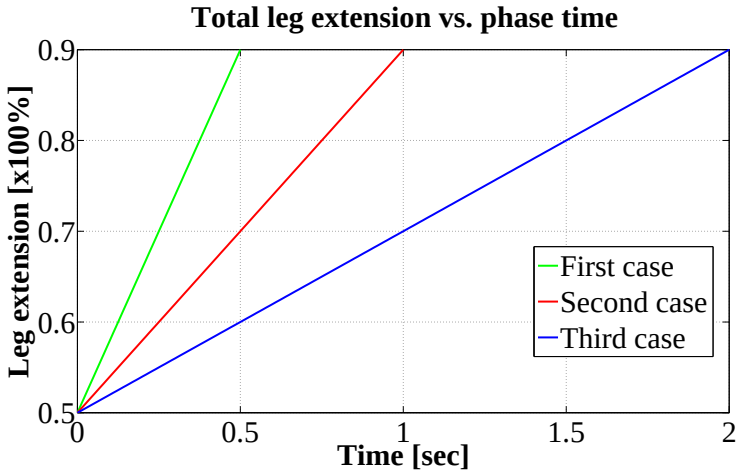

Figure 28. *Leg extension of the skier in function of phase time.*

It can be seen that for a smaller phase time value, the prescribed extension will be achieved faster than for larger phase time values. This is indeed the case when the skier skis on steeper hills and has to increase the skating angle to compensate for the backward pulling effect of the gravity.

Although in this research the condition of steep hills is not considered, a similar action on a leveled plane was modeled in the first trial run.

The time functions that describe these three lines are shown in the next equations. These time functions are incorporated directly into the constraint equation $C14$.

$$Leg_{ext} = Ini_{ext} + C_{extension}.t \tag{187}$$

where Leg_{ext} is the value of the leg extension in function of time in meters; Ini_{ext} is the initial leg extension at the beginning of the push-off phase; $C_{extension} = 0.8$, 0.4, 0.2 is a constant that depends on the simulation time for the first, second, and third trial, respectively; and t is the time in seconds.

5.3 Push-off force function versus time, friction force, and air drag

The push-off force produced by the skier in each of the active phases was taken from the data collected from the measurements taken in Vuokatti in December, 2011. The specifications of the equipment used to obtain these data can be summarized as follows:

- Two custom-made small and lightweight (1070 g) force plate pairs built by the Neuromuscular Research Center, University of Jyväskylä
- 12 channel ski force amplifier built by the Neuromuscular Research Center, University of Jyväskylä
- A/D converter with sampling rate of 1 kHz, model NI 9205; National Instruments; Austin, Texas, USA
- Wireless transmitter WLS-9163; National Instruments; Austin, Texas, USA
- PC-laptop with wireless receiver card and data collection software LabVIEW 8.5; National Instruments; Austin, Texas, USA

As mentioned previously in the section dedicated to the development of the constraint equations of the system, this force is considered to be applied to the center of mass of the skier and is directed along a unit vector formed between the origins of the first and third body of the modeled leg exerting the push-off.

Figures 29 and 30 show the complete arrangement of the equipment carried by the skier and a general view of the construction of the ski binding with the installed force plates.

Figure 31 shows the cyclic behavior of the force exerted by the skier while performing the skating technique. Only a representative portion of these data of one phase is taken into

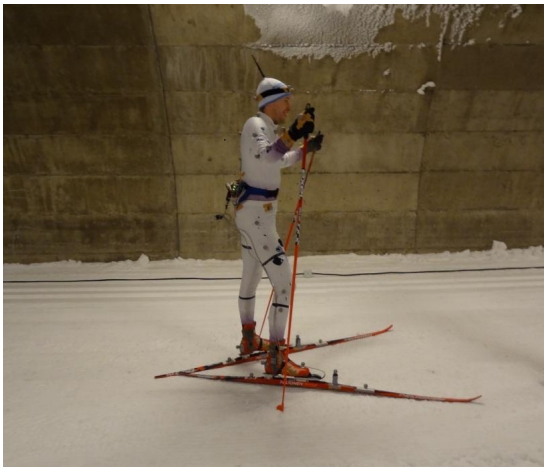

Figure 29. *Force measurement set up at Vuokatti ski tunnel facility.*

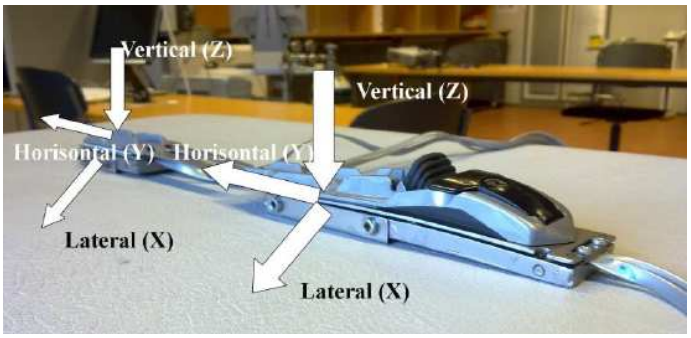

Figure 30. *Force plates installed in the ski bindings (Ohtonen, 2010, p. 9).*

account for simulating the push-off of the skier during a phase. Refer to figure 32, which shows the portion used in all the trial runs and adapted to the simulation time proposed. In this figure, the fitted curve used to input the value of the force related to time is plotted. It can be seen that the applied fitting process seems to conveniently model the behavior of the discrete data. The value of the Pearson coefficient obtained for this particular fitting process is 0.9976.

With the data obtained from the measurements, it is possible to determine the value of the friction force produced at the time of the experiment. Figure 33 shows the behavior of this friction force during the execution of the experiment.

The researcher's use of an average value to take into account the force acting in opposition to the movement of the skier might seem misappropriated. However, this use is due to the complex characteristics of the ski-snow mechanics in which the coefficient of friction produced in this contact depends on different factors not easily obtained. Figure 34 shows the different values that this coefficient of friction can have in the relative movement of the ski with respect to the the snow.

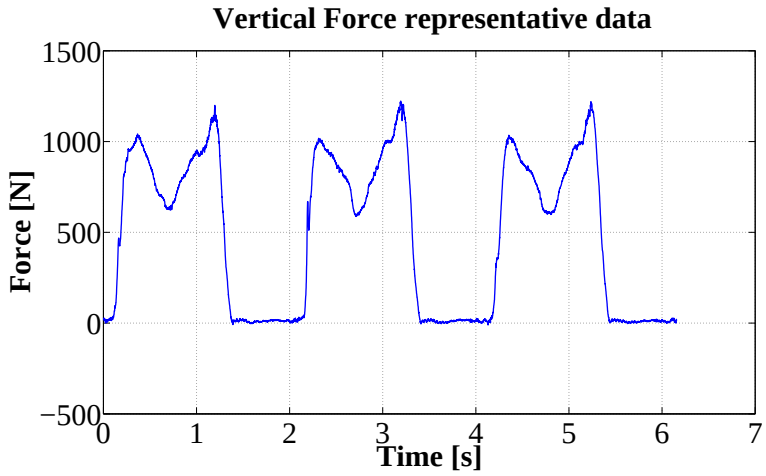

Figure 31. *Total force exerted by the skier.*

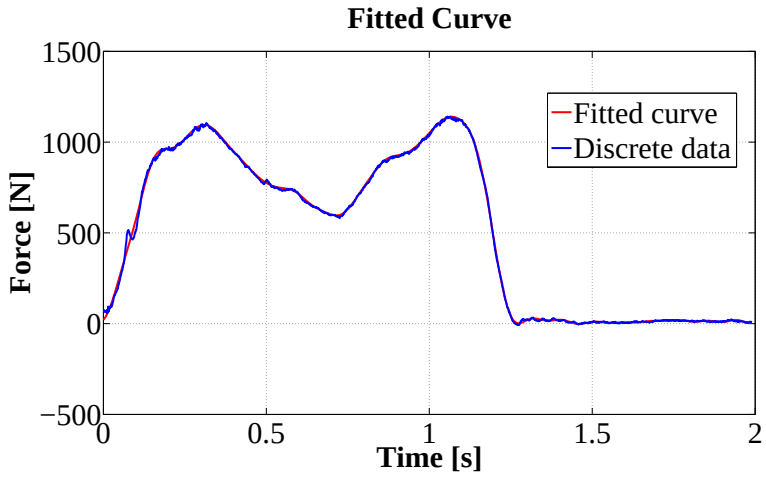

Figure 32. *Force representative data of one active phase.*

In figure 34, f is the total friction coefficient, f_d is the dry friction coefficient produced by the solid-solid contact between the ski and the snow, f_w is the lubricated friction coefficient due to the hydrodynamic effect of the ski, and f_s is the water capillary coefficient of friction that appears due to the adherence of the water beneath the ski to both surfaces with relative movement. The complex combination of these three friction mechanisms dictates the friction laws applied to skiing.

The average value can be calculated from the discrete measurement data. This set of values can be seen in table 8 for the trial selected.

It can be noticed that the friction force is small when compared with the value of the actual push-off force in this short trial. Although it might be considered as not having been taken into account in the analysis presented in this report, it is still important to notice that these values of friction force depend on the specific characteristics of the experiment facilities,

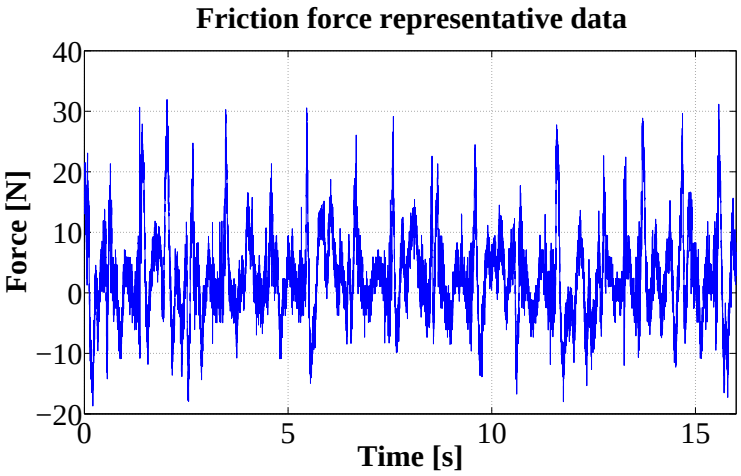

Figure 33. *Friction force produced during the execution of the trial run.*

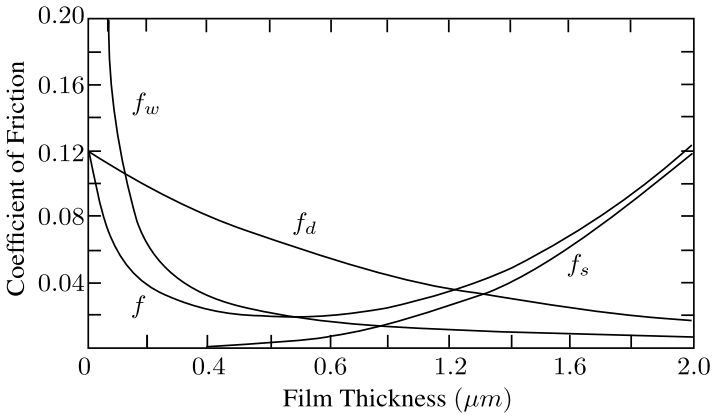

Figure 34. *Variation of the total coefficient of friction in the ski-snow contact (Colbeck, 1988, p. 83).*

and they must be included for further analysis when the value of the coefficient of friction reaches higher values because of the different combination of factors that generate this.

The air drag will not be considered in this analysis because of the short length of the experiment. The air drag can be included at any moment into the model; however, further studies must first be conducted regarding the values that the air drag can adopt in function of the apparent restrictive area created by both the upper body position of the skier and the characteristics of the gear being worn.

Table 8. Key values of the measured friction force

Friction force	$[N]$
Maximum	31.894
Average	5.305
Minimum	-18.7134

5.4 Movement of the origin of the local reference system of the second body

To constrain the movement of the origin of the local reference system of the second body, it is only necessary to estimate the orientation of this system during the simulation phase. No additional constraints or path prescriptions need be made pertaining to the distance between this point and the origin of the local reference system of the first body because of the conditions imposed by the spherical joint.

For simulation purposes, and according to the on-site observations, it is assumed that the angle θ^2 specifying the rotation about the local $\boldsymbol{X}^2$ axis changes as indicated in figure 35. The orientation of the reference system attached to the upper leg follows the same movement because of the constraints imposed by the prismatic joint between the two bodies. The change in this angle simulates the rotation of the leg of the skier when producing the pushing-off and shift to the other leg.

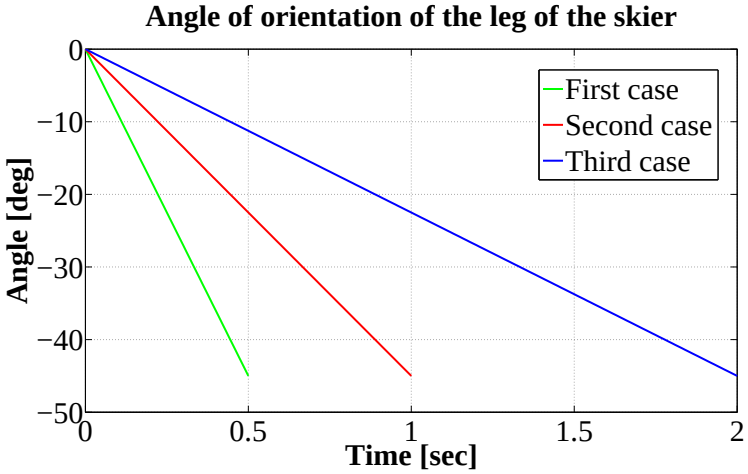

Figure 35. *Rotation of the leg in function of the phase duration.*

These variations can be written as a function of the simulation time, such as in the case of the prescription of the leg extension. See equation (188).

$$Leg_{rot} = Ini_{rot} + C_{rotation}t \tag{188}$$

in which Leg_{rot} is the angle that the skier has rotated the leg in time t; Ini_{rot} is the initial rotation angle the skier uses to begin the gliding phase; and $C_{rotation} = 90$, 45, 22.5 consists of the respective values of the constant indicating how the rotation is being performed, depending on the selected case. The rotation starts at the beginning of the active phase, as represented in figure 35.

The definition of the rotation angles of the leg is important because it also affects how the force is transmitted to the other leg when the skate skier shifts between phases.

5.5 Set of simulation results

After one inputs all the required variables into the model, one obtains the following set of simulation results presented immediately below. An analysis of each item follows (with the exception of the last item, for which results are presented in appendix C).

- Vertical movement of the CM of the skier
- Fulfillment of the prescribed orientation of the leg of the skier during the gliding phase
- Movement in X-Y plane of the CM of the skier and the center of the ski
- Travel velocity of the CM of the skier
- Fulfillment of the constraints imposed on the model (these results are presented in appendix C)

In this section of the paper, the analysis of single phase simulations will be conducted in order to explain the details involving the development of the movement of the skier. In section 5.6, a simulation of a combination of phases will be described in order to analyze the convenient use of this code to model longer distances involving several strides.

Results from the first set of initial values of the skating angle and phase time

The following results are obtained from the set of parameters for the trials. Figure 36 shows the previously proposed leg extension in function of the phase time. The change in the orientation of the leg of the skier modifies the linear function that defines the vertical

position of the center of mass, creating a parabolic trajectory in each case.

It can also be seen that in all cases, the prescribed condition of the beginning and ending of the movement of the leg is accomplished.

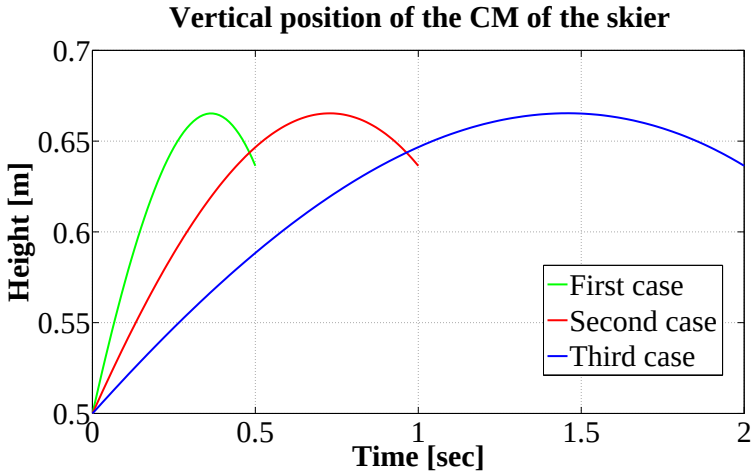

Figure 36. *Vertical movement of the CM of the skier. First trial.*

Figure 37 presents a top view of the movements of origin of the ski and the CM of the skier. Careful attention must be given to the trajectory followed by the CM, which breaks its vertical alignment with the ski to follow the physiological movement of the leg. In this figure, the segmented lines represent the travel trajectory of the ski for each one the cases.

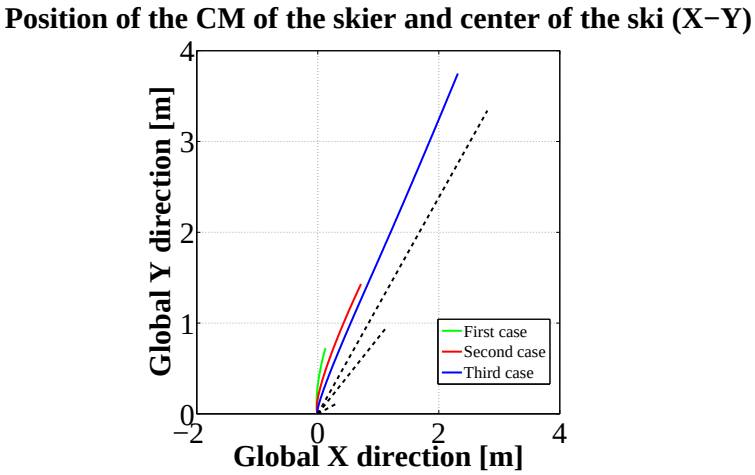

Figure 37. *Trajectory of the CM of the skier and the center of the ski in the X-Y plane.*

Figure 38 shows how the center of mass of the skier displaces along the travel direction (Global X direction) with respect to the phase time.

The effect of the friction force opposing the skier displacement can also be observed. This is depicted by the change in slope in the third case. If the simulation time is increased,

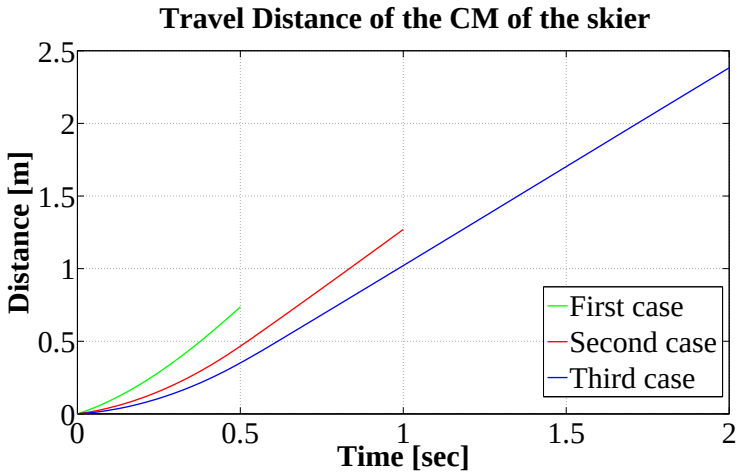

Figure 38. *Distance covered by the CM of the skier in the active phase.*

this effect can be greatly noticed and the velocity will start decreasing because of the lack of propulsion force.

5.6 Simulation of a long ski run.

In this section, a new aspect of the model will be explored. The continuous movement of the skier will be presented with several sets of strokes. This is so that one may observe the behavior of the increase of the velocity of the skier because of the effects of the imposed forces until the absolute magnitude of the velocity reaches an equilibrium. In this case, the input parameters used to accomplish this task are mentioned in table 9.

Table 9. Long ski run simulation parameters

Input parameter	Value
Mass (Kg)	75
Phase time (s)	1
Clength	0.2
Crotation	22.5
Strokes	10
Skating angle (deg)	50
Init. velocity (m/s)	0

The trajectory of the CM of the skier and the local body reference system located on the ski during each stroke are depicted in figure 39. In this trial, the global X direction is taken as the main travel direction. This will be the main consideration for the long run simulation cases. It is noticeable how the trajectory of the CM of the skier follows a periodic function quite close to a sin or cos functions.

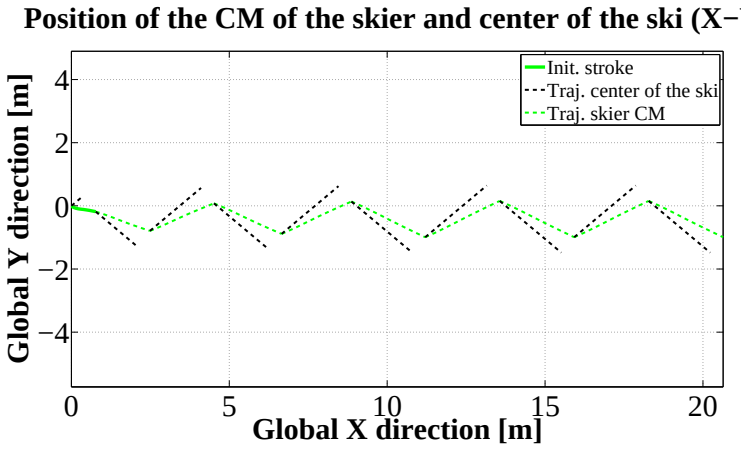

Figure 39. *Description of the continuous strokes.*

In figure 40, it is possible to distinguish some important characteristics pertaining to the velocities of the CM of the skier. Firstly, figure 40 shows the effect of the applied push-off force at the beginning of each stroke. This is clearly noted from the crescent slope of the velocity curve of each phase.

Secondly, the figure displays the effect of the stride or change of active phase, which is a decrease in the absolute velocity of the skier during the shift, followed by the recovery of the level of velocity in consonance with the applied force.

Figure 41 depicts how the equilibrium between the forces applied is found after the sixth stroke. This equilibrium is described by the convergence of the value of the velocity of the CM of the skier to a constant value. The average total velocity found for this movement is about $2.47\ m/s$.

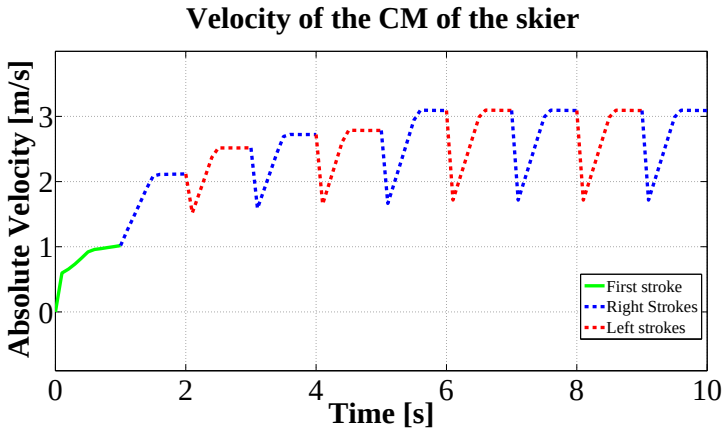

Figure 40. *Velocity of the CM of the skier during the long ski run simulation.*

The large influence of the selected skating angle φ^1 when the technique is performed

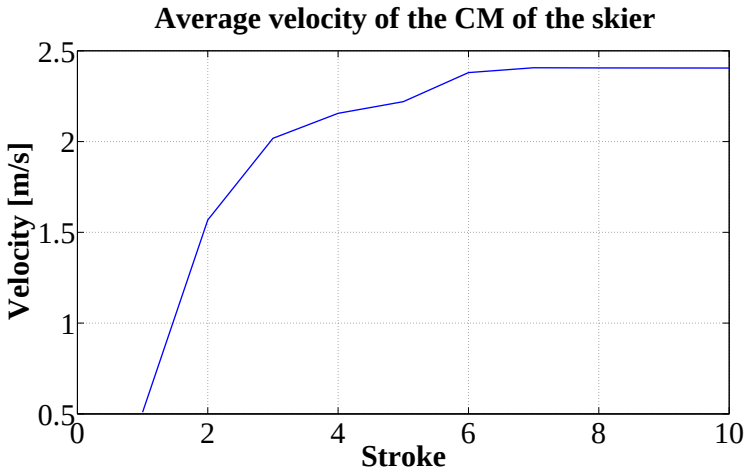

Figure 41. *Average velocity of the CM of the skier in each stroke.*

should be noted. Figure 42 shows that if the long run trial is set as a base case for the comparison, a second skier will be able to acquire a slightly superior average velocity by reducing the skating angle 10 degrees, with the added benefit of using only half of the force employed in the base case.

It is also observed that when a skier retains a skating angle of 50 degrees and employs half of the baseline force, the resultant average velocity is reduced by approximately 32 % and not by 50 %, as intuitively might be thought. Further studies of this issue may lead to the discovery of the optimum relationship between the skating angle, power of the skier, and stride rate in specific cases.

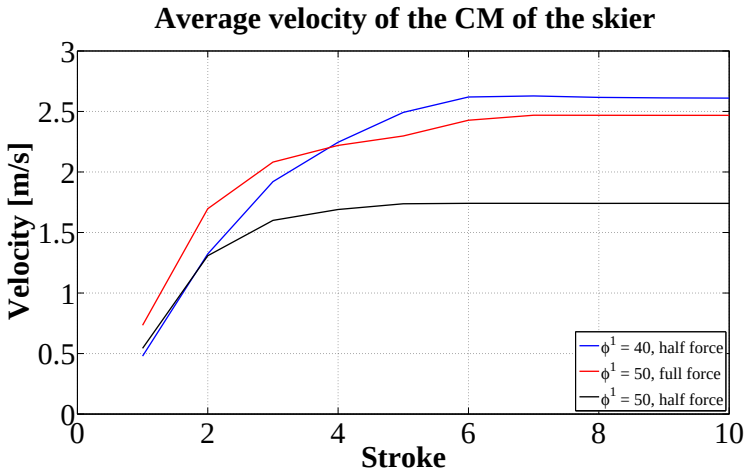

Figure 42. *Comparison of average velocity with modified skating angles and push-off forces.*

Figure 43 presents the different components of the velocity of the skier in the X-Y plane. It can be noted that in spite of the fact that the Y component of the skier velocity is almost twice larger than the correspondent in the X direction, the absolute value of the skier

travel velocity is mainly influenced by the last one.

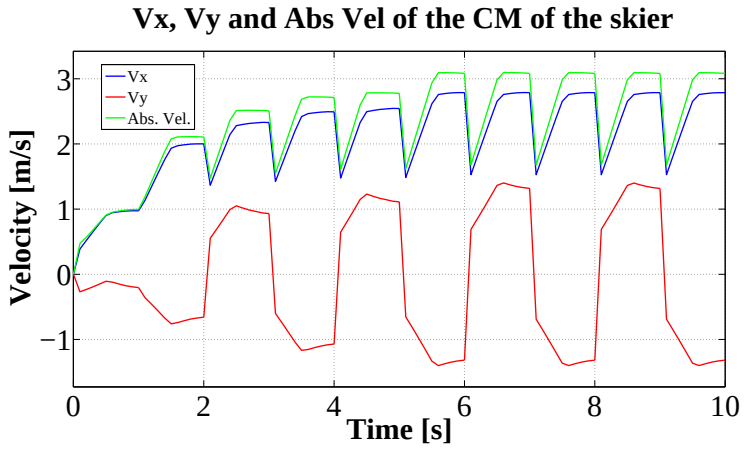

Figure 43. *Value of the velocity components and absolute value.*

Taking into account the previous comment regarding the importance of the skier velocity in the X axes, figure 44 present the obtained simulated power exerted by the skier. Under the afore stated skier run conditions. From the model it is obtained an average power around $300\ W$ when the stable conditions are reached.

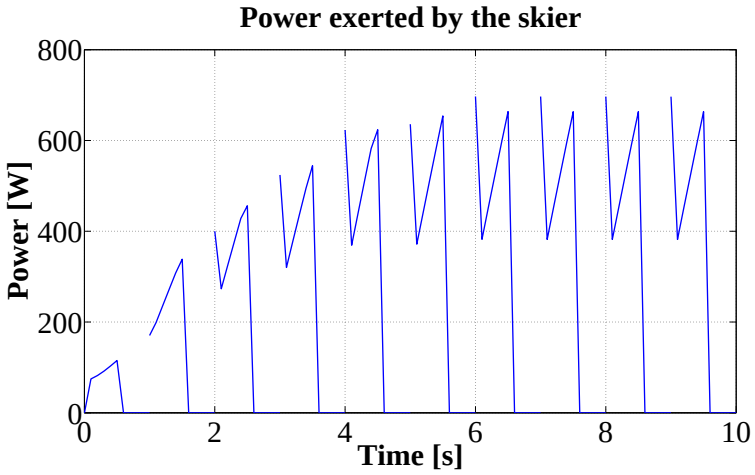

Figure 44. *Power exerted by the skier during the long ski run.*

6 CONCLUSIONS

In this thesis, a multibody dynamic model of a cross-country skier executing the skating technique without poles has been formulated and presented. This thesis has also presented the related required theory, description of fundamental concepts, and application of these to solve a real physical problem.

The formulation of this model has retained the generality of the shape of the equation of motions (with no simplifications applied), thus allowing the implementation of necessary changes to include any of the variations left out during the postulation of the assumptions.

The flexibility of the model has facilitated the path for generating the Matlab code to obtain the numerical results needed for every simulation study case. Furthermore, it was noticed that the change in the CPU simulation time was not important, nor was it considered as a relevant variable to control.

The effect of several forces can be easily added to the systems as well as any specific trajectory of the leg of the skier. In addition, a skating plane other than leveled can be modeled by easily changing the corresponding constraints. This versatility makes the code flexible and adaptable to new conditions, which may be imposed with little effort on the part of the researcher.

To obtain the first set of results from the skier model, three cases were analyzed. The skating angles and the gliding time were varied, and the push-off force was kept as an invariant external force. With these variations, several physical conditions are imposed on the model, and the coherent results can be studied and compared to the reality of the skier situation.

When skiers skate with high skating angles and short stride rates, their velocity is lower than when they skate with smaller skating angles and longer stride rates. This result is generated because of the apparent sensitivity of the technique to the skating angle. With this approach, it is possible to find the optimal combination of parameters, skating angle, and gliding length, which would allow a skate skier to obtain maximum speed according to the determined force availability of the athlete.

One illustration of the conclusion mentioned in the previous paragraph is the result presented in figure 42. It can be observed that two different athletes who do not have the same leg power might still achieve the same average velocity by varying the skating angle. This demonstrates one of the advantages of using a multibody model in sports, the discovery of optimum combinations.

The final simulation trial points to the possibility of analysis of the dependence of the average velocity on the applied push-off force. These are directly related, but not in a linear form. This is demonstrated by the variation of the push-off force with the retention of the same skating angle, as also shown in figure 42 The intuitive assumption is that when the push-off force is reduced by half, the resultant average velocity will also be reduced by half; however, it was demonstrated that this is not the case.

From the last simulation trial, it might be also possible to analyze the dependency of the average velocity and the applied push off force. They are directly related however not in a linear form. This is demonstrated by the variation of the push off force keeping the same skating angle as shown also in figure 42.

Much needs to be refined to reasonably match the model to several real conditions, such as irregular travel planes, skis, air drag consideration, and specific movement of the legs of the athletes. The research conducted for this thesis can conveniently contribute to future work because of its flexibility and its adaptability to real external and internal prescribed parameters.

REFERENCES

Allen, J. 2007. The Culture and Sport of Skiing: From Antiquity to World War II. Massachusetts: University of Massachusetts.

Allen, J. 2008. Skiing [online document]. [Accessed 15 January 2012]. Available at http://www.britannica.com/EBchecked/topic/547535/skiing

Bauchau, O. 2011. Solid Mechanics And Its Applications, vol. 176. Flexible Multibody Dynamics. New York: Springer.

Blikom, A. & Molde, E. 2010. Sondre Norheim [online document]. [Accessed 15 September 2011]. Available at http://www.sondrenorheim.com/history

Chaudhary, H. & Saha, S. 2009. Lecture Notes in Applied and Computational Mechanics, vol. 37. Dynamics and balancing of multibody systems. Berlin / Heidelberg: Springer.

Cline, M. & Dinesh, K. 2003. Post-stabilization for rigid body simulation with contact and constraints. IEEE Internations Conference on Robotics and Automation. Taiwan, 14-19 September 2003. The IEEE Robotics and Automation Society, National Science Council, Taiwan, R.O.C., Ministry of Education, Taiwan, R.O.C. vol. 3, pp. 3744-3751.

Colbeck, S. 1988. The kinetic friction of snow. Journal of Glaciology, vol. 34, no. 116, pp. 78-86.

Duoos-Asche, B. 1984. Fatigue and the diagonal stride in cross-country skiing. 2 International Symposium on Biomechanics in Sports. Colorado Springs, 1984. International Society of Biomechanics in Sport, pp. 219-226.

Fintelman, D., Den Braver, O. & Schwab, A. 2011. A simple 2-dimensional model of speed skating which mimics observed forces and motions. Multibody Dynamics 2011, ECCOMAS Thematic Conference, Brussels, Belgium. 4-7 July 2011. Université Catholique de Louvain, pp. 1-20.

Flores, P., Pereira, R., Machado, M. & Seabra, E. 2009. Proceedings of EUCOMES 08: Investigation on the Baumgarte Stabilization Method for Dynamic Analysis of Constrained Multibody Systems. Netherlands: Springer.

Garcia, J. & Bayo, E. 1994. Kinematic and Dynamic Simulation of Multibody Systems. New york: Springer-Verlag.

Grassia, F. 1998. Practical parameterization of rotations using the exponential map. The Journal of Graphics Tools, vol. 3, no. 3, pp. 1-13.

Hindman, S. 2005. Cross-Country Skiing: building skills for fun and fitness. 1st ed. Seattle: The mountaineers Books.

Huston, R. 1990. Multibody Dynamics. USA: Butterworth-Heinemann.

Knightson, S. 2010. Telemark technique in short [online document]. [Accessed 15 September 2011]. Available at http://www.squidoo.com/telemark_skiing?utm_source=google

Korkealaako, P. 2009. Real-time Simulation of Mobile and Industrial Machines Using The Multibody Simulation Approach. Doctoral dissertation. Lappeenranta University of Technology.

Lind, D. & Sanders, S. 2010.The Physics of Skiing: Skiing at the Triple Point. 2nd ed. Michigan: American Institute of Physics.

Moher, D., Liberati, A., Tetzlaff J., Altman D. & The PRISMA Group. 2009. Preferred Reporting Items for Systematic Reviews and Meta-Analyses: The Prisma Statement. PLoS med., vol. 6, no. 7, pp. 1-6.

Moler, C. 2004. Numerical Computing with MATLAB [online ducument]. [Accessed 18 October 2011]. Available at http://www.mathworks.se/moler

Ohtonen, O. 2010. The effect of ski gliding properties on the force production of v2-technique. Master's thesis, University of Jyväskylä.

Rusko, H. 2003. Cross Country Skiing. Oxford: Blackwell Science Ltd.

Shabana, A. 1998. Dynamics of multibody systems. 2nd. ed. Cambridge: The Press Syndicate of the University of Cambridge.

Shabana, A. 2001. Computational dynamics. 2nd. ed. New York: John Wiley & Sons, INC.

Skating technique basics [online document]. [Accessed 15 September 2011]. Available at http://www.xcskiworld.com/training/Technique/skating.htm

Soellner, E. & Führer, C. 2008. Numerical Methods in Multibody Dynamics. Stuttgart: Teubner-Verlag.

The Nordic Ski Project. Nordic ski technique. 2006. DVD. Ontario, xczone.tv.

Wittenburg, J. 2008. Dynamics of multibody systems. 2nd. ed. Berlin: Springer-Verlag.

APPENDICES

APPENDIX A

In table 10, the list of articles found per database searched is presented.

Table 10. Number of articles obtained by database.

DATABASE NAME	RESULTS
WILIMA	10
ABI/INFORM GLOBA (PROQUEST)	47
DOAJ Directory of open access journals	0
EBSCO Academic search elite	56
EBSCO Business source complete	0
Elsevier (Science direct)	99
Emerald Journals (Emerald)	4
Springer Journals	372
SCOPUS - V.4 (Elsevier)	716
ARTO	0
Conference Papers Index (CSA)	Not available
METADEX (CSA)	Not available
TALI	5
VTT:n julkasuja	4
Web of Science	3
Lappeenranta Maakuntakirjasto	0
WebStat	0
LUTPub - Doria	0
INSSI - TKK	5
PROLA - American Physical Society	Not available
TKKDOC - Teknillinsen korkeakoulun elektroninen julkaisuarkisto	0
Knovel	0
TOTAL	**1311**

APPENDIX B

Developed terms of the equation of motion of the model

Vector of generalized coordinates

$$\boldsymbol{q} = \begin{bmatrix} R_1^1 & R_2^1 & R_3^1 & \varphi^1 & \theta^1 & \psi^1 & R_1^2 & R_2^2 & R_3^2 & \varphi^2 \\ \theta^2 & \psi^2 & R_1^3 & R_2^3 & R_3^3 & \varphi^3 & \theta^3 & \psi^3 & & \end{bmatrix}^T$$

Vector of constraints

$$\boldsymbol{C} = \begin{bmatrix} R_3^1 - c_3^1 \\ R_1^1 \sin\phi^1 - R_2^1 \cos\phi^1 \\ \phi^1 - c_{\phi^1} \\ \theta^1 - c_{\theta^1} \\ \psi^1 - c_{\psi^1} \\ R_1^1 - R_1^2 - l_1.A_{13}^2 \\ R_2^1 - R_2^2 - l_1.A_{23}^2 \\ R_3^1 - R_3^2 - l_1.A_{33}^2 \\ A_{11}^2 A_{13}^3 + A_{21}^2 A_{23}^3 + A_{31}^2 A_{33}^3 \\ A_{12}^2 A_{13}^3 + A_{22}^2 A_{23}^3 + A_{32}^2 A_{33}^3 \\ A_{11}^2 \left(R_1^2 - R_1^3\right) + A_{21}^2 \left(R_2^2 - R_2^3\right) + A_{31}^2 \left(R_3^2 - R_3^3\right) \\ A_{12}^2 \left(R_1^2 - R_1^3\right) + A_{22}^2 \left(R_2^2 - R_2^3\right) + A_{32}^2 \left(R_3^2 - R_3^3\right) \\ A_{12}^2 A_{11}^3 + A_{22}^2 A_{21}^3 + A_{32}^2 A_{31}^3 \\ \sqrt{\left(R_1^3 - R_1^1\right)^2 + \left(R_2^3 - R_2^1\right)^2 + \left(R_3^3 - R_3^1\right)^2} - lex\left(t\right) \\ R_1^2 - f_1\left(t\right) \\ R_2^2 - f_2\left(t\right) \\ R_3^2 - f_3\left(t\right) \end{bmatrix}$$

Jacobian matrix of the system

$$
\mathbf{C}_q = \begin{bmatrix}
0 & 0 & 1 & 0 & 0 & 0 & 0 & 0 & 0 & 0 & 0 & 0 & 0 & 0 & 0 & 0 & 0 & 0 & 0 \\
C_{q2,1} & C_{q2,2} & 0 & C_{q2,4} & 0 & 0 & 0 & 0 & 0 & 0 & 0 & 0 & 0 & 0 & 0 & 0 & 0 & 0 & 0 \\
0 & 0 & 0 & 1 & 0 & 0 & 0 & 0 & 0 & 0 & 0 & 0 & 0 & 0 & 0 & 0 & 0 & 0 & 0 \\
0 & 0 & 0 & 0 & 1 & 0 & 0 & 0 & 0 & 0 & 0 & 0 & 0 & 0 & 0 & 0 & 0 & 0 & 0 \\
0 & 0 & 0 & 0 & 0 & 1 & 0 & 0 & 0 & 0 & 0 & 0 & 0 & 0 & 0 & 0 & 0 & 0 & 0 \\
1 & 0 & 0 & 0 & 0 & 0 & -1 & 0 & 0 & $C_{q6,10}$ & $C_{q6,11}$ & 0 & 0 & 0 & 0 & 0 & 0 & 0 & 0 \\
0 & 1 & 0 & 0 & 0 & 0 & 0 & -1 & 0 & $C_{q7,10}$ & $C_{q7,11}$ & 0 & 0 & 0 & 0 & 0 & 0 & 0 & 0 \\
0 & 0 & 1 & 0 & 0 & 0 & 0 & 0 & -1 & 0 & $C_{q8,11}$ & 0 & 0 & 0 & 0 & 0 & 0 & 0 & 0 \\
0 & 0 & 0 & 0 & 0 & 0 & 0 & 0 & 0 & $C_{q9,10}$ & $C_{q9,11}$ & $C_{q9,12}$ & 0 & 0 & 0 & $C_{q9,16}$ & $C_{q9,17}$ & 0 & 0 \\
0 & 0 & 0 & 0 & 0 & 0 & 0 & 0 & 0 & $C_{q10,10}$ & $C_{q10,11}$ & $C_{q10,12}$ & 0 & 0 & 0 & $C_{q10,16}$ & $C_{q10,17}$ & 0 & 0 \\
0 & 0 & 0 & 0 & 0 & 0 & $C_{q11,7}$ & $C_{q11,8}$ & $C_{q11,9}$ & $C_{q11,10}$ & $C_{q11,11}$ & $C_{q11,12}$ & $C_{q11,13}$ & $C_{q11,14}$ & $C_{q11,15}$ & 0 & 0 & 0 & 0 \\
0 & 0 & 0 & 0 & 0 & 0 & $C_{q12,7}$ & $C_{q12,8}$ & $C_{q12,9}$ & $C_{q12,10}$ & $C_{q12,11}$ & $C_{q12,12}$ & $C_{q12,13}$ & $C_{q12,14}$ & $C_{q12,15}$ & 0 & 0 & 0 & 0 \\
0 & 0 & 0 & 0 & 0 & 0 & 0 & 0 & 0 & $C_{q13,10}$ & $C_{q13,11}$ & $C_{q13,12}$ & 0 & 0 & 0 & $C_{q13,16}$ & $C_{q13,17}$ & $C_{q13,18}$ \\
$C_{q14,1}$ & $C_{q14,2}$ & $C_{q14,3}$ & 0 & 0 & 0 & 0 & 0 & 0 & 0 & 0 & 0 & $C_{q14,13}$ & $C_{q14,14}$ & $C_{q14,15}$ & 0 & 0 & 0 & 0 \\
0 & 0 & 0 & 0 & 0 & 0 & 1 & 0 & 0 & 0 & 0 & 0 & 0 & 0 & 0 & 0 & 0 & 0 & 0 \\
0 & 0 & 0 & 0 & 0 & 0 & 0 & 1 & 0 & 0 & 0 & 0 & 0 & 0 & 0 & 0 & 0 & 0 & 0 \\
0 & 0 & 0 & 0 & 0 & 0 & 0 & 0 & 1 & 0 & 0 & 0 & 0 & 0 & 0 & 0 & 0 & 0 & 0
\end{bmatrix}
$$

Where the terms of the Jacobian matrix are

$$C_{q2,1} = \sin\varphi^1$$

$$C_{q2,2} = -\cos\varphi^1$$

$$C_{q2,4} = R_1^1\cos\varphi^1 + R_2^1\sin\varphi^1$$

$$C_{q6,10} = -l1\cos\varphi^2\sin\theta^2$$

$$C_{q6,11} = -l1\sin\varphi^2\cos\theta^2$$

$$C_{q7,10} = -l1\sin\varphi^2\sin\theta^2$$

$$C_{q7,11} = l1\cos\varphi^2\cos\theta^2$$

$$C_{q8,11} = l1\sin\theta^2$$

$$\begin{aligned} C_{q9,10} = &-\sin\theta^3(\sin\varphi^3\sin\varphi^2\cos\psi^2 + \sin\theta^3\cos\varphi^2\cos\theta^2\sin\psi^2 \\ &+\cos\varphi^3\cos\varphi^2\cos\psi^2 - \cos\varphi^3\sin\varphi^2\cos\theta^2\sin\psi^2) \end{aligned}$$

$$C_{q9,11} = \sin\psi^2(\sin\varphi^2\sin\theta^2\sin\varphi^3\sin\theta^3 + \cos\varphi^2\sin\theta^2\cos\varphi^3\sin\theta^3 + \cos\theta^2\cos\theta^3)$$

$$\begin{aligned} C_{q9,12} = &-\sin\varphi^3\sin\theta^3\cos\varphi^2\sin\psi^2 - \sin\varphi^3\sin\theta^3\sin\varphi^2\cos\theta^2\cos\psi^2 \\ &+\cos\varphi^3\sin\theta^3\sin\varphi^2\sin\psi^2 - \cos\varphi^3\sin\theta^3\cos\varphi^2\cos\theta^2\cos\psi^2 \\ &+\sin\theta^2\cos\psi^2\cos\theta^3 \end{aligned}$$

$$\begin{aligned} C_{q9,16} = &\sin\theta^3(\sin\varphi^3\sin\varphi^2\cos\psi^2 + \sin\varphi^3\cos\varphi^2\cos\theta^2\sin\psi^2 + \cos\varphi^3\cos\varphi^2\cos\psi^2 \\ &-\cos(\varphi^3\sin\varphi^2\cos\theta^2\sin\psi^2) \end{aligned}$$

$$\begin{aligned} C_{q9,17} = &\sin\varphi^3\cos\theta^3\cos\varphi^2\cos\psi^2 - \sin\varphi^3\cos\theta^3\sin\varphi^2\cos\theta^2\sin\psi^2 \\ &-\cos\varphi^3\cos\theta^3\sin\varphi^2\cos\psi^2 - \cos\varphi^3\cos\theta^3\cos\varphi^2\cos\theta^2\sin\psi^2 \\ &-\sin\theta^2\sin\psi^2\sin\theta^3 \end{aligned}$$

$$\begin{aligned} C_{q10,10} = &\sin\theta^3(\sin\varphi^3\sin\varphi^2\sin(psi2) - \sin\varphi^3\cos\varphi^2\cos\theta^2\cos\psi^2 \\ &+\cos\varphi^3\cos\varphi^2\sin\psi^2 + \cos\varphi^3\sin\varphi^2\cos\theta^2\cos\psi^2) \end{aligned}$$

$$C_{q10,11} = \cos\psi^2(\sin\varphi^2\sin\theta^2\sin\varphi^3\sin\theta^3 + \cos\varphi^2\sin\theta^2\cos\varphi^3\sin\theta^3 + \cos\theta^2\cos\theta^3)$$

$$\begin{aligned} C_{q10,12} = &-\sin\varphi^3\sin\theta^3\cos\varphi^2\cos\psi^2 + \sin\varphi^3\sin\theta^3\sin\varphi^2\cos\theta^2\sin\psi^2 \\ &+\cos\varphi^3\sin\theta^3\sin\varphi^2\cos\psi^2 + \cos\varphi^3\sin\theta^3\cos\varphi^2\cos\theta^2\sin\psi^2 \\ &-\sin\theta^2\sin\psi^2\cos\theta^3 \end{aligned}$$

$$C_{q10,16} = -\sin\theta^3(\sin\varphi^3\sin\varphi^2\sin\psi^2 - \sin\varphi^3\cos\varphi^2\cos\theta^2\cos\psi^2 + \cos\varphi^3\cos\varphi^2\sin\psi^2 + \cos\varphi^3\sin\varphi^2\cos\theta^2\cos\psi^2)$$

$$C_{q10,17} = -\sin\varphi^3\cos\theta^3\cos\varphi^2\sin\psi^2 - \sin\varphi^3\cos\theta^3\sin\varphi^2\cos\theta^2\cos\psi^2 + \cos\varphi^3\cos\theta^3\sin\varphi^2\sin\psi^2 - \cos\varphi^3\cos\theta^3\cos\varphi^2\cos\theta^2\cos\psi^2 - \sin\theta^2\cos\psi^2\sin\theta^3$$

$$C_{q11,7} = \cos\varphi^2\cos\psi^2 - \sin\varphi^2\cos\theta^2\sin\psi^2$$

$$C_{q11,8} = \sin\varphi^2\cos\psi^2 + \cos\varphi^2\cos\theta^2\sin\psi^2$$

$$C_{q11,9} = \sin\theta^2\sin\psi^2$$

$$C_{q11,10} = -\sin\varphi^2\cos\psi^2R_1^2 + \sin\varphi^2\cos\psi^2R_1^3 - \cos\varphi^2\cos\theta^2\sin\psi^2R_1^2 + \cos\varphi^2\cos\theta^2\sin\psi^2R_1^3 + \cos\varphi^2\cos\psi^2R_2^2 - \cos\varphi^2\cos\psi^2R_2^3 - \sin\varphi^2\cos\theta^2\sin\psi^2R_2^2 + \sin\varphi^2\cos\theta^2\sin\psi^2R_2^3$$

$$C_{q11,11} = \sin\psi^2(\sin\varphi^2\sin\theta^2R_1^2 - \sin\varphi^2\sin\theta^2R_1^3 - \cos\varphi^2\sin\theta^2R_2^2 + \cos\varphi^2\sin\theta^2R_2^3 + \cos\theta^2R_3^2 - \cos\theta^2R_3^3)$$

$$C_{q11,12} = -\cos\varphi^2\sin\psi^2R_1^2 + \cos\varphi^2\sin\psi^2R_1^3 - \sin\varphi^2\cos\theta^2\cos\psi^2R_1^2 + \sin\varphi^2\cos\theta^2\cos\psi^2R_1^3 - \sin\varphi^2\sin\psi^2R_2^2 + \sin\varphi^2\sin\psi^2R_2^3 + \cos\varphi^2\cos\theta^2\cos\psi^2R_2^2 - \cos\varphi^2\cos\theta^2\cos\psi^2R_2^3 + \sin\theta^2\cos\psi^2R_3^2 - \sin\theta^2\cos\psi^2R_3^3$$

$$C_{q11,13} = -\cos\varphi^2\cos\psi^2 + \sin\varphi^2\cos\theta^2\sin\psi^2$$

$$C_{q11,14} = -\sin\varphi^2\cos\psi^2 - \cos\varphi^2\cos\theta^2\sin\psi^2$$

$$C_{q11,15} = -\sin\theta^2\sin\psi^2$$

$$C_{q12,7} = -\cos\varphi^2\sin\psi^2 - \sin\varphi^2\cos\theta^2\cos\psi^2$$

$$C_{q12,8} = -\sin\varphi^2\sin\psi^2 - \cos\varphi^2\cos\theta^2\cos\psi^2$$

$$C_{q12,9} = \sin\theta^2\cos\psi^2$$

$$C_{q12,10} = \sin\varphi^2\sin\psi^2R_1^2 - \sin\varphi^2\sin\psi^2R_1^3 - \cos\varphi^2\cos\theta^2\cos\psi^2R_1^2 + \cos\varphi^2\cos\theta^2\cos\psi^2R_1^3 - \cos\varphi^2\sin\psi^2R_2^2 + \cos\varphi^2\sin\psi^2R_2^3 - \sin\varphi^2\cos\theta^2\cos\psi^2R_2^2 + \sin\varphi^2\cos\theta^2\cos\psi^2R_2^3$$

$$C_{q12,11} = \cos\psi^2(\sin\varphi^2\sin\theta^2R_1^2 - \sin\varphi^2\sin\theta^2R_1^3 - \cos\varphi^2\sin\theta^2R_2^2 + \cos\varphi^2\sin\theta^2R_2^3 + \cos\theta^2R_3^2 - \cos\theta^2R_3^3)$$

$$
\begin{aligned}
C_{q12,12} = &- \cos\varphi^2 \cos\psi^2 R_1^2 + \cos\varphi^2 \cos\psi^2 R_1^3 + \sin\varphi^2 \cos\theta^2 \sin\psi^2 R_1^2 \\
&- \sin\varphi^2 \cos\theta^2 \sin\psi^2 R_1^3 - \sin\varphi^2 \cos\psi^2 R_2^2 + \sin\varphi^2 \cos\psi^2 R_2^3 \\
&- \cos\varphi^2 \cos\theta^2 \sin\psi^2 R_2^2 + \cos\varphi^2 \cos\theta^2 \sin\psi^2 R_2^3 - \sin\theta^2 \sin\psi^2 R_3^2 \\
&+ \sin\theta^2 \sin\psi^2 R_3^3
\end{aligned}
$$

$$
C_{q12,13} = \cos\varphi^2 \sin\psi^2 - \sin\varphi^2 \cos\theta^2 \cos\psi^2
$$

$$
C_{q12,14} = \sin\varphi^2 \sin\psi^2 - \cos\varphi^2 \cos\theta^2 \cos\psi^2
$$

$$
C_{q12,15} = - \sin\theta^2 \cos\psi^2
$$

$$
\begin{aligned}
C_{q13,10} = &\ \sin\varphi^2 \sin\psi^2 \cos\varphi^3 \cos\psi^3 - \sin\varphi^2 \sin\psi^2 \sin\varphi^3 \cos\theta^3 \sin\psi^3 \\
&- \cos\varphi^2 \cos\theta^2 \cos\psi^2 \cos\varphi^3 \cos\psi^3 + \cos\varphi^2 \cos\theta^2 \cos\psi^2 \sin\varphi^3 \cos\theta^3 \sin\psi^3 \\
&- \cos\varphi^2 \sin\psi^2 \sin\varphi^3 \cos\psi^3 - \cos\varphi^2 \sin\psi^2 \cos\varphi^3 \cos\theta^3 \sin\psi^3 \\
&- \sin\varphi^2 \cos\theta^2 \cos\psi^2 \sin\varphi^3 \cos\psi^3 - \sin\varphi^2 \cos\theta^2 \cos\psi^2 \cos\varphi^3 \cos\theta^3 \sin\psi^3
\end{aligned}
$$

$$
\begin{aligned}
C_{q13,11} = &- \cos\psi^2(-\sin\varphi^2 \sin\theta^2 \cos\varphi^3 \cos\psi^3 + \sin\varphi^2 \sin\theta^2 \sin\varphi^3 \cos\theta^3 \sin\psi^3 \\
&+ \cos\varphi^2 \sin\theta^2 \sin\varphi^3 \cos\psi^3 + \cos\varphi^2 \sin\theta^2 \cos\varphi^3 \cos\theta^3 \sin\psi^3 \\
&- \cos\theta^2 \sin\theta^3 \sin\psi^3)
\end{aligned}
$$

$$
\begin{aligned}
C_{q13,12} = &- \cos\varphi^2 \cos\psi^2 \cos\varphi^3 \cos\psi^3 + \cos\varphi^2 \cos\psi^2 \sin\varphi^3 \cos\theta^3 \sin\psi^3 \\
&+ \sin\varphi^2 \cos\theta^2 \sin\psi^2 \cos\varphi^3 \cos\psi^3 - \sin\varphi^2 \cos\theta^2 \sin\psi^2 \sin\varphi^3 \cos\theta^3 \sin\psi^3 \\
&- \sin\varphi^2 \cos\psi^2 \sin\varphi^3 \cos\psi^3 - \sin\varphi^2 \cos\psi^2 \cos\varphi^3 \cos\theta^3 \sin\psi^3 \\
&- \cos\varphi^2 \cos\theta^2 \sin\psi^2 \sin\varphi^3 \cos\psi^3 - \cos\varphi^2 \cos\theta^2 \sin\psi^2 \cos\varphi^3 \cos\theta^3 \sin\psi^3 \\
&- \sin\theta^2 \sin\psi^2 \sin\theta^3 \sin\psi^3
\end{aligned}
$$

$$
\begin{aligned}
C_{q13,16} = &\cos\varphi^2 \sin\psi^2 \sin\varphi^3 \cos\psi^3 + \cos\varphi^2 \sin\psi^2 \cos\varphi^3 \cos\theta^3 \sin\psi^3 \\
&+ \sin\varphi^2 \cos\theta^2 \cos\psi^2 \sin\varphi^3 \cos\psi^3 + \sin\varphi^2 \cos\theta^2 \cos\psi^2 \cos\varphi^3 \cos\theta^3 \sin\psi^3 \\
&- \sin\varphi^2 \sin\psi^2 \cos\varphi^3 \cos\psi^3 + \sin\varphi^2 \sin\psi^2 \sin\varphi^3 \cos\theta^3 \sin\psi^3 \\
&+ \cos\varphi^2 \cos\theta^2 \cos\psi^2 \cos\varphi^3 \cos\psi^3 - \cos\varphi^2 \cos\theta^2 \cos\psi^2 \sin\varphi^3 \cos\theta^3 \sin\psi^3
\end{aligned}
$$

$$
\begin{aligned}
C_{q13,17} = &\sin\psi^3(-\sin\varphi^3 \sin\theta^3 \cos\varphi^2 \sin\psi^2 - \sin\varphi^3 \sin\theta^3 \sin\varphi^2 \cos\theta^2 \cos\psi^2 \\
&+ \cos\varphi^3 \sin\theta^3 \sin\varphi^2 \sin\psi^2 - \cos\varphi^3 \sin\theta^3 \cos\varphi^2 \cos\theta^2 \cos\psi^2 \\
&+ \sin\theta^2 \cos\psi^2 \cos\theta^3)
\end{aligned}
$$

$$
\begin{aligned}
C_{q13,18} = &\cos\varphi^2 \sin\psi^2 \cos\varphi^3 \sin\psi^3 + \cos\varphi^2 \sin\psi^2 \sin\varphi^3 \cos\theta^3 \cos\psi^3 \\
&+ \sin\varphi^2 \cos\theta^2 \cos\psi^2 \cos\varphi^3 \sin\psi^3 + \sin\varphi^2 \cos\theta^2 \cos\psi^2 \sin\varphi^3 \cos\theta^3 \cos\psi^3 \\
&+ \sin\varphi^2 \sin\psi^2 \sin\varphi^3 \sin\psi^3 - \sin\varphi^2 \sin\psi^2 \cos\varphi^3 \cos\theta^3 \cos\psi^3 \\
&- \cos\varphi^2 \cos\theta^2 \cos\psi^2 \sin\varphi^3 \sin\psi^3 + \cos\varphi^2 \cos\theta^2 \cos\psi^2 \cos\varphi^3 \cos\theta^3 \cos\psi^3 \\
&+ \sin\theta^2 \cos\psi^2 \sin\theta^3 \cos\psi^3
\end{aligned}
$$

$$C_{q14,1} = \frac{R_1^1 - R_1^3}{\sqrt{\left(R_1^3 - R_1^1\right)^2 + \left(R_2^3 - R_2^1\right)^2 + \left(R_3^3 - R_3^1\right)^2}}$$

$$C_{q14,2} = \frac{R_2^1 - R_2^3}{\sqrt{\left(R_1^3 - R_1^1\right)^2 + \left(R_2^3 - R_2^1\right)^2 + \left(R_3^3 - R_3^1\right)^2}}$$

$$C_{q14,3} = \frac{R_3^1 - R_3^3}{\sqrt{\left(R_1^3 - R_1^1\right)^2 + \left(R_2^3 - R_2^1\right)^2 + \left(R_3^3 - R_3^1\right)^2}}$$

$$C_{q14,13} = \frac{R_1^3 - R_1^1}{\sqrt{\left(R_1^3 - R_1^1\right)^2 + \left(R_2^3 - R_2^1\right)^2 + \left(R_3^3 - R_3^1\right)^2}}$$

$$C_{q14,14} = \frac{R_2^3 - R_2^1}{\sqrt{\left(R_1^3 - R_1^1\right)^2 + \left(R_2^3 - R_2^1\right)^2 + \left(R_3^3 - R_3^1\right)^2}}$$

$$C_{q14,15} = \frac{R_3^3 - R_3^1}{\sqrt{\left(R_1^3 - R_1^1\right)^2 + \left(R_2^3 - R_2^1\right)^2 + \left(R_3^3 - R_3^1\right)^2}}$$

Terms of the mass matrix of the system

$$
\boldsymbol{M}^1 = \begin{bmatrix}
m^1 & 0 & 0 & 0 & 0 & 0 & 0 \\
0 & m^1 & 0 & 0 & 0 & 0 & 0 \\
0 & 0 & m^1 & 0 & 0 & 0 & 0 \\
0 & 0 & 0 & I_x x^1 sin^2\theta^1 sin^2\psi^1 + I_y y^1 sin^2\theta^1 cos^2\psi^1 + I_z z^1 cos^2\theta^1 & I_x x^1 \sin\theta^1 \sin\psi^1 \cos\psi^1 - I_y y^1 \sin\theta^1 \cos\psi^1 \sin\psi^1 & I_x x^1 \sin\theta^1 \cos\psi^1 \sin\psi^1 - I_y y^1 \sin\theta^1 \cos\psi^1 \sin\psi^1 & I_z z^1 \cos\theta^1 \\
0 & 0 & 0 & I_x x^1 \sin\theta^1 \sin\psi^1 \cos\psi^1 - I_y y^1 \sin\theta^1 \cos\psi^1 \sin\psi^1 & I_x x^1 cos^2\psi^1 + I_y y^1 sin^2\psi^1 & 0 \\
0 & 0 & 0 & I_z z^1 \cos\theta^1 & 0 & I_z z^1
\end{bmatrix}
$$

$$
\boldsymbol{M}^2 = \begin{bmatrix}
m^2 & 0 & 0 & 0 & 0 & 0 \\
0 & m^2 & 0 & 0 & 0 & 0 \\
0 & 0 & m^2 & 0 & 0 & 0 \\
0 & 0 & 0 & I_x x^2 sin^2\theta^2 sin^2\psi^2 + I_y y^2 sin^2\theta^2 cos^2\psi^2 & I_x x^2 \sin\theta^2 \sin\psi^2 \cos\psi^2 - I_y y^2 \sin\theta^2 \cos\psi^2 \sin\psi^2 & 0 \\
0 & 0 & 0 & I_x x^2 \sin\theta^2 \sin\psi^2 \cos\psi^2 - I_y y^2 \sin\theta^2 \cos\psi^2 \sin\psi^2 & I_x x^2 cos^2\psi^2 + I_y y^2 sin^2\psi^2 & 0 \\
0 & 0 & 0 & 0 & 0 & 0
\end{bmatrix}
$$

$$
\boldsymbol{M}^3 = \begin{bmatrix}
m^3 & 0 & 0 & 0 & 0 & 0 \\
0 & m^3 & 0 & 0 & 0 & 0 \\
0 & 0 & m^3 & 0 & 0 & 0 \\
0 & 0 & 0 & I_x x^3 sin^2\theta^3 sin^2\psi^3 + I_y y^3 sin^2\theta^3 cos^2\psi^3 & I_x x^3 \sin\theta^3 \sin\psi^3 \cos\psi^3 - I_y y^3 \sin\theta^3 \cos\psi^3 \sin\psi^3 & 0 \\
0 & 0 & 0 & I_x x^3 \sin\theta^3 \sin\psi^3 \cos\psi^3 - I_y y^3 \sin\theta^3 \cos\psi^3 \sin\psi^3 & I_x x^3 cos^2\psi^3 + I_y y^3 sin^2\psi^3 & 0 \\
0 & 0 & 0 & 0 & 0 & 0
\end{bmatrix}
$$

Vector of external generalized forces

$$
\boldsymbol{Q}_e =
\begin{bmatrix}
-\left(-\cos\varphi^1 \sin\psi^1 - \sin\varphi^1 \cos\theta^1 \cos\psi^1\right) Ff \\
-\left(-\sin\varphi^1 \sin\psi^1 + \cos\varphi^1 \cos\theta^1 \cos\psi^1\right) Ff \\
-\sin\theta^1 \cos\psi^1 Ff \\
0 \\
0 \\
0 \\
0 \\
0 \\
0 \\
0 \\
0 \\
\left(\cos\varphi^3 \cos\psi^3 - \sin\varphi^3 \cos\theta^3 \sin\psi^3\right) Fpx + \left(-\cos\varphi^3 \sin\psi^3 - \sin\varphi^3 \cos\theta^3 \cos\psi^3\right) Fpy + \sin\varphi^3 \sin\theta^3 Fpz - \left(-\cos\varphi^1 \sin\psi^1 - \sin\varphi^1 \cos\theta^1 \cos\psi^1\right) Fa \\
\left(\sin\varphi^3 \cos\psi^3 + \cos\varphi^3 \cos\theta^3 \sin\psi^3\right) Fpx + \left(-\sin\varphi^3 \sin\psi^3 + \cos\varphi^3 \cos\theta^3 \cos\psi^3\right) Fpy - \cos\varphi^3 \sin\theta^3 Fpz - \left(-\sin\varphi^1 \sin\psi^1 + \cos\varphi^1 \cos\theta^1 \cos\psi^1\right) Fa \\
\sin\theta^3 \sin\psi^3 Fpx + \sin\theta^3 \cos\psi^3 Fpy + \cos\theta^3 Fpz - \sin\theta^1 \cos\psi^1 Fa \\
0 \\
0 \\
0
\end{bmatrix}
$$

vector absorbing the terms that are quadratic in the velocities

$$
\left(Q_v^1\right)_\theta = \left[\begin{array}{c}
\left(\begin{array}{c}
\sin\theta^1 \sin\psi^1 \left(\begin{array}{c}
\frac{1}{12} m^1 \left(b^2+c^2\right) \left(\dot{\phi}^1 \sin\theta^1 \cos\psi^1 - \dot{\theta}^1 \sin\psi^1\right) \left(\dot{\phi}^1 \cos\theta^1 + \dot{\psi}^1\right) - \frac{1}{12} m^1 \left(a^2+b^2\right) \left(\dot{\phi}^1 \cos\theta^1 + \dot{\psi}^1\right) \left(\dot{\phi}^1 \sin\theta^1 \cos\psi^1 - \dot{\theta}^1 \sin\psi^1\right) + \\
+\frac{1}{12} m^1 \left(a^2+c^2\right) \left(\left(\dot{\theta}^1 \cos\theta^1 \sin\psi^1 + \dot{\psi}^1 \sin\theta^1 \cos\psi^1\right) \dot{\phi}^1 - \dot{\psi}^1 \dot{\theta}^1 \sin\psi^1\right)
\end{array}\right) \\
\sin\theta^1 \cos\psi^1 \left(\begin{array}{c}
\frac{1}{12} m^1 \left(a^2+c^2\right) \left(\dot{\phi}^1 \cos\theta^1 + \dot{\psi}^1\right) \left(\dot{\phi}^1 \sin\theta^1 \sin\psi^1 + \dot{\theta}^1 \cos\psi^1\right) - \frac{1}{12} m^1 \left(b^2+c^2\right) \left(\dot{\phi}^1 \sin\theta^1 \sin\psi^1 + \dot{\theta}^1 \cos\psi^1\right) \left(\dot{\phi}^1 \cos\theta^1 + \dot{\psi}^1\right) + \\
+\frac{1}{12} m^1 \left(a^2+b^2\right) \left(\left(\dot{\theta}^1 \cos\theta^1 \cos\psi^1 - \dot{\psi}^1 \sin\theta^1 \sin\psi^1\right) \dot{\phi}^1 - \dot{\psi}^1 \dot{\theta}^1 \cos\psi^1\right)
\end{array}\right) \\
\cos\theta \left(\begin{array}{c}
\frac{1}{12} m^1 \left(a^2+b^2\right) \left(\dot{\phi}^1 \sin\theta^1 \sin\psi^1 + \dot{\theta}^1 \cos\psi^1\right) \left(\dot{\phi}^1 \sin\theta^1 \cos\psi^1 - \dot{\theta}^1 \sin\psi^1\right) - \frac{1}{12} m^1 \left(a^2+c^2\right) \left(\dot{\phi}^1 \sin\theta^1 \cos\psi^1 - \dot{\theta}^1 \sin\psi^1\right) \left(\dot{\phi}^1 \sin\theta^1 \sin\psi^1 + \dot{\theta}^1 \cos\psi^1\right) \\
-\frac{1}{12} m^1 \left(b^2+c^2\right) \left(\dot{\theta}^1 \dot{\phi}^1 \sin\theta^1\right)
\end{array}\right)
\end{array}\right] = \left[\begin{array}{c}
\left(\begin{array}{c}
\cos\psi \left(\begin{array}{c}
\frac{1}{12} m^1 \left(b^2+c^2\right) \left(\dot{\phi}^1 \sin\theta^1 \cos\psi^1 - \dot{\theta}^1 \sin\psi^1\right) \left(\dot{\phi}^1 \cos\theta^1 + \dot{\psi}^1\right) - \frac{1}{12} m^1 \left(a^2+b^2\right) \left(\dot{\phi}^1 \cos\theta^1 + \dot{\psi}^1\right) \left(\dot{\phi}^1 \sin\theta^1 \cos\psi^1 - \dot{\theta}^1 \sin\psi^1\right) \\
+\frac{1}{12} m^1 \left(a^2+c^2\right) \left(\left(\dot{\theta}^1 \cos\theta^1 \sin\psi^1 + \dot{\psi}^1 \sin\theta^1 \cos\psi^1\right) \dot{\phi}^1 - \dot{\psi}^1 \dot{\theta}^1 \sin\psi^1\right)
\end{array}\right) \\
-\sin\psi \left(\begin{array}{c}
\frac{1}{12} m^1 \left(a^2+c^2\right) \left(\dot{\phi}^1 \cos\theta^1 + \dot{\psi}^1\right) \left(\dot{\phi}^1 \sin\theta^1 \sin\psi^1 + \dot{\theta}^1 \cos\psi^1\right) - \frac{1}{12} m^1 \left(b^2+c^2\right) \left(\dot{\phi}^1 \sin\theta^1 \sin\psi^1 + \dot{\theta}^1 \cos\psi^1\right) \left(\dot{\phi}^1 \cos\theta^1 + \dot{\psi}^1\right) \\
+\frac{1}{12} m^1 \left(a^2+b^2\right) \left(\left(\dot{\theta}^1 \cos\theta^1 \cos\psi^1 - \dot{\psi}^1 \sin\theta^1 \sin\psi^1\right) \dot{\phi}^1 - \dot{\psi}^1 \dot{\theta}^1 \cos\psi^1\right) \\
-\frac{1}{12} m^1 \left(b^2+c^2\right) \left(\dot{\phi}^1 \sin\theta^1 \sin\psi^1 + \dot{\theta}^1 \cos\psi^1\right) \left(\dot{\phi}^1 \cos\theta^1 + \dot{\psi}^1\right) + \frac{1}{12} m^1 \left(a^2+b^2\right) \left(\left(\dot{\theta}^1 \cos\theta^1 \cos\psi^1 - \dot{\psi}^1 \sin\theta^1 \sin\psi^1\right) \dot{\phi}^1 - \dot{\psi}^1 \dot{\theta}^1 \cos\psi^1\right)
\end{array}\right) \\
\left(\begin{array}{c}
\frac{1}{12} m^1 \left(a^2+b^2\right) \left(\dot{\phi}^1 \sin\theta^1 \sin\psi^1 + \dot{\theta}^1 \cos\psi^1\right) \left(\dot{\phi}^1 \sin\theta^1 \cos\psi^1 - \dot{\theta}^1 \sin\psi^1\right) - \frac{1}{12} m^1 \left(a^2+c^2\right) \left(\dot{\phi}^1 \sin\theta^1 \cos\psi^1 - \dot{\theta}^1 \sin\psi^1\right) \left(\dot{\phi}^1 \sin\theta^1 \sin\psi^1 + \dot{\theta}^1 \cos\psi^1\right) \\
-\frac{1}{12} m^1 \left(b^2+c^2\right) \dot{\theta}^1 \dot{\phi}^1 \sin\theta^1
\end{array}\right)
\end{array}\right]
$$

$$
\left(\boldsymbol{Q}_v^2\right)_\theta = \left[\begin{array}{c}
\left(\begin{array}{l}
\sin\theta^2 \sin\psi^2 \left(\begin{array}{l} -\frac{1}{12} m^2 (L_2)^2 \left(\dot{\phi}^2 \cos\theta^2 + \dot{\psi}^2\right) \left(\dot{\phi}^2 \sin\theta^2 \cos\psi^2 - \dot{\theta}^2 \sin\psi^2\right) \\ +\frac{1}{12} m^2 (L_2)^2 \left(\left(\dot{\theta}^2 \cos\theta^2 \sin\psi^2 + \dot{\psi}^2 \sin\theta^2 \cos\psi^2\right) \dot{\phi}^2 - \dot{\psi}^2 \dot{\theta}^2 \sin\psi^2\right) \end{array}\right) + \\
\sin\theta^2 \cos\psi^2 \left(\begin{array}{l} \frac{1}{12} m^2 (L_2)^2 \left(\dot{\phi}^2 \cos\theta^2 + \dot{\psi}^2\right) \left(\dot{\phi}^2 \sin\theta^2 \sin\psi^2 + \dot{\theta}^2 \cos\psi^2\right) \\ +\frac{1}{12} m^2 (L_2)^2 \left(\left(\dot{\theta}^2 \cos\theta^2 \cos\psi^2 - \dot{\psi}^2 \sin\theta^2 \sin\psi^2\right) \dot{\phi}^2 - \dot{\psi}^2 \dot{\theta}^2 \cos\psi^2\right) \end{array}\right) + \\
\cos\theta^2 \left(\begin{array}{l} \frac{1}{12} m^2 (L_2)^2 \left(\dot{\phi}^2 \sin\theta^2 \sin\psi^2 + \dot{\theta}^2 \cos\psi^2\right) \left(\dot{\phi}^2 \sin\theta^2 \cos\psi^2 - \dot{\theta}^2 \sin\psi^2\right) \\ -\frac{1}{12} m^2 (L_2)^2 \left(\dot{\phi}^2 \sin\theta^2 \cos\psi^2 - \dot{\theta}^2 \sin\psi^2\right) \left(\dot{\phi}^2 \sin\theta^2 \sin\psi^2 + \dot{\theta}^2 \cos\psi^2\right) \end{array}\right)
\end{array}\right) \\
\left(\begin{array}{l}
\cos\psi^2 \left(\begin{array}{l} -\frac{1}{12} m^2 (L_2)^2 \left(\dot{\phi}^2 \cos\theta^2 + \dot{\psi}^2\right) \left(\dot{\phi}^2 \sin\theta^2 \cos\psi^2 - \dot{\theta}^2 \sin\psi^2\right) \\ +\frac{1}{12} m^2 (L_2)^2 \left(\left(\dot{\theta}^2 \cos\theta^2 \sin\psi^2 + \dot{\psi}^2 \sin\theta^2 \cos\psi^2\right) \dot{\phi}^2 - \dot{\psi}^2 \dot{\theta}^2 \sin\psi^2\right) \end{array}\right) \\
-\sin\psi^2 \left(\begin{array}{l} \frac{1}{12} m^2 (L_2)^2 \left(\dot{\phi}^2 \cos\theta^2 + \dot{\psi}^2\right) \left(\dot{\phi}^2 \sin\theta^2 \sin\psi^2 + \dot{\theta}^2 \cos\psi^2\right) \\ +\frac{1}{12} m^2 (L_2)^2 \left(\left(\dot{\theta}^2 \cos\theta^2 \cos\psi^2 - \dot{\psi}^2 \sin\theta^2 \sin\psi^2\right) \dot{\phi}^2 - \dot{\psi}^2 \dot{\theta}^2 \cos\psi^2\right) \\ +\frac{1}{12} m^2 (L_2)^2 \left(\left(\dot{\theta}^2 \cos\theta^2 \cos\psi^2 - \dot{\psi}^2 \sin\theta^2 \sin\psi^2\right) \dot{\phi}^2 - \dot{\psi}^2 \dot{\theta}^2 \cos\psi^2\right) \end{array}\right)
\end{array}\right) \\
\left(\begin{array}{c} \frac{1}{12} m^2 (L_2)^2 \left(\dot{\phi}^2 \sin\theta^2 \sin\psi^2 + \dot{\theta}^2 \cos\psi^2\right) \left(\dot{\phi}^2 \sin\theta^2 \cos\psi^2 - \dot{\theta}^2 \sin\psi^2\right) \\ -\frac{1}{12} m^2 (L_2)^2 \left(\dot{\phi}^2 \sin\theta^2 \cos\psi^2 - \dot{\theta}^2 \sin\psi^2\right) \left(\dot{\phi}^2 \sin\theta^2 \sin\psi^2 + \dot{\theta}^2 \cos\psi^2\right) \end{array}\right)
\end{array}\right]
$$

$$
\left(\boldsymbol{Q}_v^3\right)_\theta = \left[\begin{array}{c}
\left(\begin{array}{l}
\sin\theta^3 \sin\psi^3 \left(\begin{array}{l} -\frac{1}{12} m^3 (L_3)^2 \left(\dot{\phi}^3 \cos\theta^3 + \dot{\psi}^3\right) \left(\dot{\phi}^3 \sin\theta^3 \cos\psi^3 - \dot{\theta}^3 \sin\psi^3\right) \\ +\frac{1}{12} m^3 (L_3)^2 \left(\left(\dot{\theta}^3 \cos\theta^3 \sin\psi^3 + \dot{\psi}^3 \sin\theta^3 \cos\psi^3\right) \dot{\phi}^3 - \dot{\psi}^3 \dot{\theta}^3 \sin\psi^3\right) \end{array}\right) + \\
\sin\theta^3 \cos\psi^3 \left(\begin{array}{l} \frac{1}{12} m^3 (L_3)^2 \left(\dot{\phi}^3 \cos\theta^3 + \dot{\psi}^3\right) \left(\dot{\phi}^3 \sin\theta^3 \sin\psi^3 + \dot{\theta}^3 \cos\psi^3\right) \\ +\frac{1}{12} m^3 (L_3)^2 \left(\left(\dot{\theta}^3 \cos\theta^3 \cos\psi^3 - \dot{\psi}^3 \sin\theta^3 \sin\psi^3\right) \dot{\phi}^3 - \dot{\psi}^3 \dot{\theta}^3 \cos\psi^3\right) \end{array}\right) + \\
\cos\theta^3 \left(\begin{array}{l} \frac{1}{12} m^3 (L_3)^2 \left(\dot{\phi}^3 \sin\theta^3 \sin\psi^3 + \dot{\theta}^3 \cos\psi^3\right) \left(\dot{\phi}^3 \sin\theta^3 \cos\psi^3 - \dot{\theta}^3 \sin\psi^3\right) \\ -\frac{1}{12} m^3 (L_3)^2 \left(\dot{\phi}^3 \sin\theta^3 \cos\psi^3 - \dot{\theta}^3 \sin\psi^3\right) \left(\dot{\phi}^3 \sin\theta^3 \sin\psi^3 + \dot{\theta}^3 \cos\psi^3\right) \end{array}\right)
\end{array}\right) \\
\left(\begin{array}{l}
\cos\psi^3 \left(\begin{array}{l} -\frac{1}{12} m^3 (L_3)^2 \left(\dot{\phi}^3 \cos\theta^3 + \dot{\psi}^3\right) \left(\dot{\phi}^3 \sin\theta^3 \cos\psi^3 - \dot{\theta}^3 \sin\psi^3\right) \\ +\frac{1}{12} m^3 (L_3)^2 \left(\left(\dot{\theta}^3 \cos\theta^3 \sin\psi^3 + \dot{\psi}^3 \sin\theta^3 \cos\psi^3\right) \dot{\phi}^3 - \dot{\psi}^3 \dot{\theta}^3 \sin\psi^3\right) \end{array}\right) \\
-\sin\psi^3 \left(\begin{array}{l} \frac{1}{12} m^3 (L_3)^2 \left(\dot{\phi}^3 \cos\theta^3 + \dot{\psi}^3\right) \left(\dot{\phi}^3 \sin\theta^3 \sin\psi^3 + \dot{\theta}^3 \cos\psi^3\right) \\ +\frac{1}{12} m^3 (L_3)^2 \left(\left(\dot{\theta}^3 \cos\theta^3 \cos\psi^3 - \dot{\psi}^3 \sin\theta^3 \sin\psi^3\right) \dot{\phi}^3 - \dot{\psi}^3 \dot{\theta}^3 \cos\psi^3\right) \\ +\frac{1}{12} m^3 (L_3)^2 \left(\left(\dot{\theta}^3 \cos\theta^3 \cos\psi^3 - \dot{\psi}^3 \sin\theta^3 \sin\psi^3\right) \dot{\phi}^3 - \dot{\psi}^3 \dot{\theta}^3 \cos\psi^3\right) \end{array}\right)
\end{array}\right) \\
\left(\begin{array}{c} \frac{1}{12} m^3 (L_3)^2 \left(\dot{\phi}^3 \sin\theta^3 \sin\psi^3 + \dot{\theta}^3 \cos\psi^3\right) \left(\dot{\phi}^3 \sin\theta^3 \cos\psi^3 - \dot{\theta}^3 \sin\psi^3\right) \\ -\frac{1}{12} m^3 (L_3)^2 \left(\dot{\phi}^3 \sin\theta^3 \cos\psi^3 - \dot{\theta}^3 \sin\psi^3\right) \left(\dot{\phi}^3 \sin\theta^3 \sin\psi^3 + \dot{\theta}^3 \cos\psi^3\right) \end{array}\right)
\end{array}\right]
$$

APPENDIX C

Fulfillment of the constraints imposed on the model

In figures 45, 46, and 47, the graph of the constraints is shown in order to validate that the prescribed values imposed on the model are being achieved. These constraints appear in the same order as they were developed in the section dedicated to the Jacobian matrix. This form of presentation will help the reader to follow how the tolerances within the constraints are fulfilled.

Figure 45 shows the constraints related to the ski - ground contact. It can be seen that the constraints are kept within the target values because of the stabilization process applied during the integration of the equation of motion.

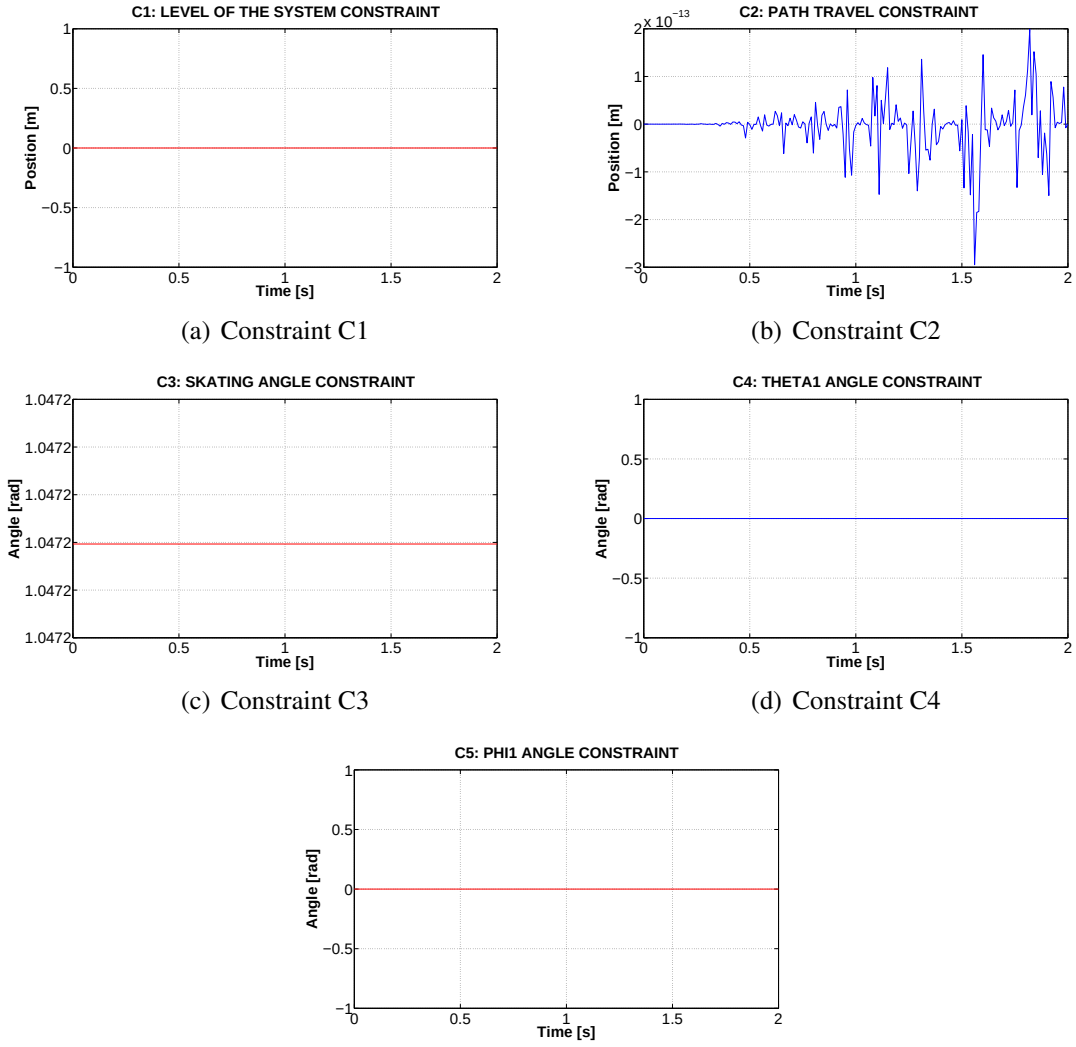

(a) Constraint C1

(b) Constraint C2

(c) Constraint C3

(d) Constraint C4

(e) Constraint C5

Figure 45. *Ski ground constraints.*

Figure 46 shows the constraints imposed on the contact between the ski and the second

body simulating the binding of the leg to the ski. It can also be observed that the joint constraints are fulfilled as well as the constraints related to the prescribed movement in the orientation of the leg about the ski travel line.

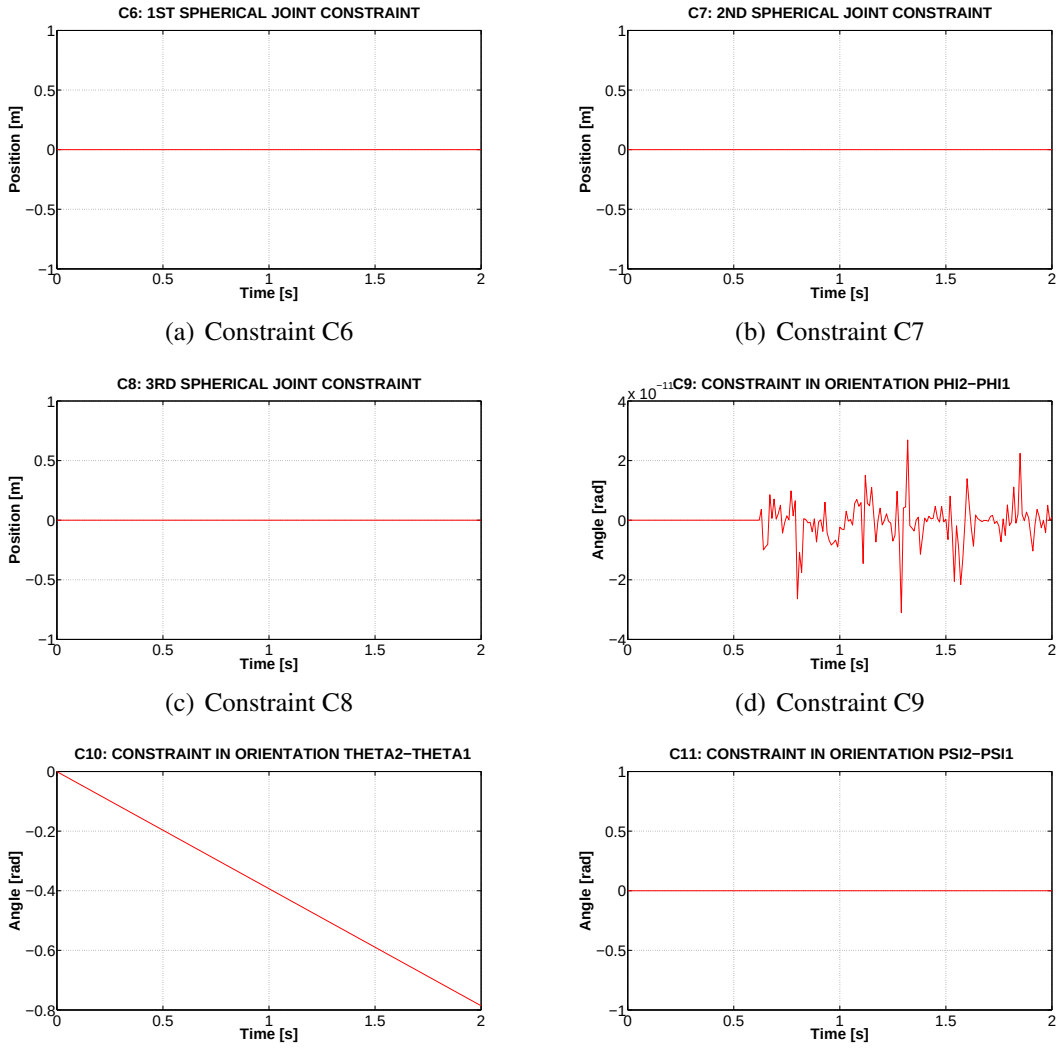

(a) Constraint C6

(b) Constraint C7

(c) Constraint C8

(d) Constraint C9

(e) Constraint C10

(f) Constraint C11

Figure 46. *Constraints between the first and second body.*

The last set of constraints shown are the ones related to the contact between the second and third body as well as the prescribed constraint for the leg extension. Also, it is possible to see how these constraints are nicely fulfilled. The results related to the second and third cases are similar to these already presented.

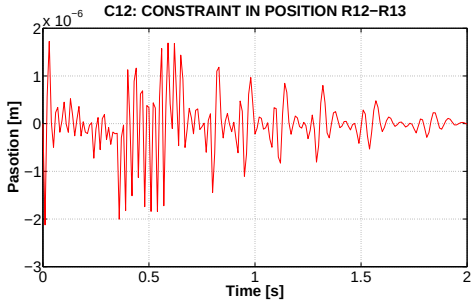

(a) Constraint C12

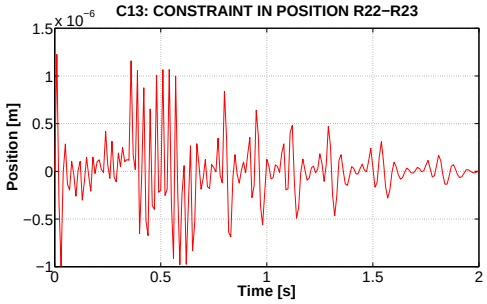

(b) Constraint C13

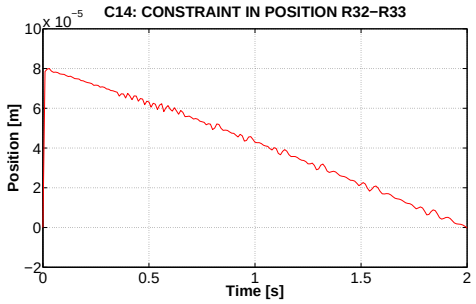

(c) Constraint C14

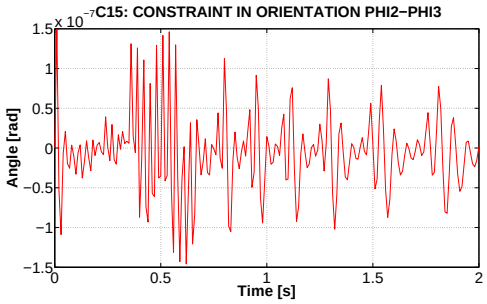

(d) Constraint C15

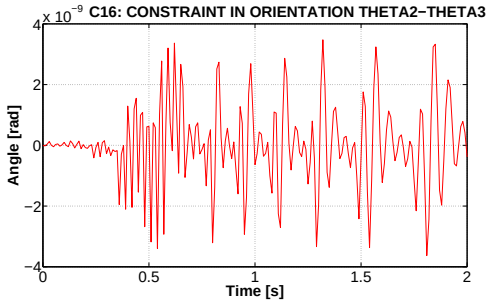

(e) Constraint C16

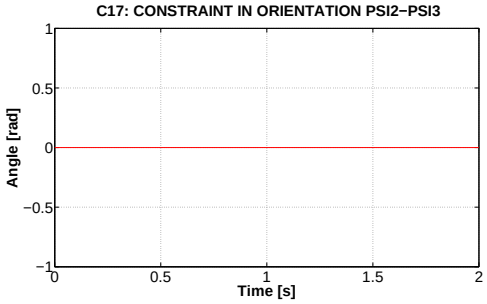

(f) Constraint C17

Figure 47. *Constraints between the second and third body.*